P-11-34

Investigation for identification of potential geological signatures for geophysical objects

Christin Döse, Seje Carlsten
Geosigma AB

September 2017

Svensk Kärnbränslehantering AB
Swedish Nuclear Fuel
and Waste Management Co

Box 250, SE-101 24 Stockholm
Phone +46 8 459 84 00

ISSN 1651-4416
SKB P-11-34
ID 1219971
September 2017

Investigation for identification of potential geological signatures for geophysical objects

Christin Döse, Seje Carlsten
Geosigma AB

This report concerns a study which was conducted for Svensk Kärnbränslehantering AB (SKB). The conclusions and viewpoints presented in the report are those of the authors. SKB may draw modified conclusions, based on additional literature sources and/or expert opinions.

Data in SKB's database can be changed for different reasons. Minor changes in SKB's database will not necessarily result in a revised report. Data revisions may also be presented as supplements, available at www.skb.se.

A pdf version of this document can be downloaded from www.skb.se.

Contents

1 Introduction

SKB conducts detailed investigations in Forsmark where the future deep repository for spent nuclear fuel is planned. A major issue when establishing the deep repository is to identify and avoid "long" fractures or fracture zones that can potentially be reactivated and thereby shear deposition holes.

These "long" fractures or fracture zones are believed to be identified by combining geological mapping of tunnel and borehole walls with geophysical measurements, for example radar measurements. Both geological mapping and geophysical measurements of boreholes were extensively carried out during the site investigation programmes in Forsmark and Oskarshamn. However, primary borehole data were not systematically processed with the aim to identify the geological character of the geophysical objects, for example radar reflectors.

Some special investigations have though been performed earlier where radar-reflectors have been correlated with geology. On the other hand, the previous investigations have not described the fractures and rock contacts causing radar reflector in detail. The earlier performed investigations are as follows:

- Borehole radar correlated with core mapping, Site Investigation Forsmark (Appendix in Stephens and Skagius 2007).
- Borehole radar correlated with core mapping, Site Investigation Oskarshamn (Carlsten 2004).
- Borehole radar correlated with tunnel mapping, Äspö HRL (Calsten et al. 1995, SKB 1994).
- GPR correlated with tunnel mapping, Äspö HRL (Stenberg and Forslund 1995, Olsson 1992).

The results from the earlier study of data from Forsmark can be concluded as follows. Of the oriented radar reflectors 45 % can be correlated with contacts between different rock types, 37 % with an open fracture, a crush or a breccia and only 10 % with sealed fracture or sealed fracture networks. It was hence concluded that the directional antenna is able to detect rock contacts more efficiently than open fractures, crush zones or breccias, while the method is not effective for the detection of sealed fractures, sealed networks, alteration and foliation.

The earlier GPR studies at Äspö HRL reveal that there is a generally good agreement between high magnitude radar reflectors and significant features observed in the tunnel, such as water bearing fractures, fracture zones, water inflow to the tunnel or boreholes or need of reinforcement. Some reflectors are correlated with dikes of fine-grained granite. Reflectors of low magnitude were uncertain and could be artifacts.

In this work extensive oriented radar reflectors were correlated with the corresponding geology. An attempt was made to identify the geological signatures of these reflectors with emphasis on fracture and fracture zone properties, i.e. mineralogy, width, aperture, alteration, roughness, surface, occurrence of kinematic indicators and water content. Data from the site investigations in Forsmark and Oskarshamn, as well as the SFR expansion-project and the Äspö HRL have been studied. At Äspö HRL also GPR reflectors have been studied.

2 Objective and scope

The work presented in this report is a follow-up to earlier performed studies of radar reflectors correlated with geology. The aim with this study is to identify which geological structures correlate with extensive radar reflectors and to assess whether or not there are specific geological attributes in the structures that correlate with extensive radar reflectors. The result will be used as input for establishing an experiment and writing a programme for development of methodology and technique for identification of "long" fractures and fracture zones.

The work was carried out in three main steps:

1) Correlation between extensive radar reflectors and geological structures.
2) Creation of Sicada tables and input of data to Sicada.
3) Evaluation of geological signatures of the reflectors.

The correlations between extensive radar reflectors and geology were based on three different methods:

1a) Correlation between borehole radar and core mapping (Forsmark and Oskarshamn site investigations, SFR extension).

1b) Correlation between borehole radar and tunnel mapping (Äspö HRL).

1c) Correlation between ground penetrating radar (GPR) and tunnel mapping (Äspö HRL).

The correlations with geological structures in boreholes have been performed irrespective of whether the structures occur along possible deformation zones (SHI) or not, while the correlations with geological structures in tunnels usually could be made with the deformation zone itself or with structures outside the deformation zone.

The boreholes investigated in 1a) above were:

- Site Investigation Forsmark: KFM04A, KFM05A, KFM06A, KFM06C, KFM07A, KFM08A, KFM08C, KFM09A, KFM09B, KFM11A, KFM12A.
- Site Investigation SFR expansion: KFR101, KFR102A, KFR104 and KFR27.
- Site Investigation Oskarshamn: KLX14A, KLX15A, KLX20A and KLX27A.

The boreholes investigated in 1b) above were: KA0575A, KA1061A, KA1131B, KA1754A, KA2048B, KA2162B, KA3191F, C2, C3 and C6 (later renamed to KXZC2, KXZC3 and KXZC6). The radar reflectors from loggings in these boreholes could be correlated to geological structures in the TASA-tunnel sections 619–752 m, 1 777–2 377 m and 3 193–3 364 m and in TASZ-tunnel section ~18.9–71.8 m.

The GPR-measurements in 1c) were performed on tunnel walls in the following tunnel sections: TASZ (~18.9–71.8 m) and TASA (~3 174.3–3 245 m).

The data to be investigated were chosen on the following criteria:

- The geological properties of the reflectors were believed to be site specific. Forsmark area was prioritized since SKB had decided to apply for a repository in this area. The boreholes chosen cover the planned deposition area and have well oriented mapping data (Döse et al. 2008).
- All boreholes where directional radar logging had been performed by summer 2009 within the project SFR expansion were selected.
- The number of boreholes from site Oskarshamn was decided to be four. These four boreholes were selected due to their well oriented mapping data and their diverging borehole directions.
- The boreholes at Äspö HRL were chosen because radar reflectors from loggings in these boreholes had already been correlated with tunnel mapping (Calsten et al. 1995, SKB 1994).
- The GPR-profiles at Äspö HRL were chosen due to their favourable position for correlation with tunnel mapping.

3 Terminology

Long fracture	At the current time, this term refers to a fracture with a radius exceeding 75 m. Definite minimum radius will be determined by SR-Site.
FPI-fracture	Full Perimeter Intersection Fracture, i.e. fractures that crosscuts the tunnel.
Possible deformation zone	Interpreted deformation zone in the single hole (SHI) and extended single hole (ESHI) interpretations.
Deformation zone	An essentially 2D structure along which there is a concentration of brittle, ductile or combined brittle and ductile deformation.
Fracture zone	A brittle deformation zone without any specification whether there has or has not been a shear sense of movement along the zone.
Reflector radius	The distance between the borehole and the point furthest away from the borehole where the reflector can still be observed. The radius is perpendicular to the borehole axis. The radius is interpreted from the radargram in the radar interpretation reports.
Extensive reflector	Reflector with a radius exceeding 18 m.
Alpha angle	Intersection angle to borehole/tunnel (0–90°).

4 Execution

4.1 In-data

Necessary in-data have been requested from Sicada, such as

- oriented borehole radar data (GP140),
- geological mapping of drill cores (GE041),
- correlation of pfl-anomalies with drill core-mapping (HY688),
- kinematic indications (GE303),
- interpreted (GE300 and GE302) and modeled deformation zones (GE306) (Stephens et al. 2007, Wahlgren et al. 2008).

The following Sicada deliveries have been used as in-data:

- 1216751 – Data Delivery SICADA_09_108
- 1217523 – Data Delivery SICADA_09_116
- 1218354 – Data Delivery SICADA_09_121
- 1219024 – Data Delivery SICADA_09_128
- 1220232 – Data Delivery SICADA_09_138
- 1220905 – Data Delivery SICADA_09_148

Since no images are stored in Sicada, the radar data in Sicada are complemented with the study of radar maps from P-reports produced during the Forsmark site investigation (Gustafsson and Gustafsson 2004a, b,c, 2005a, b, c, 2006a, b, c, 2007a, b), during the SFR site investigation (Gustafsson and Gustafsson 2008a, 2009) and during the Oskarshamn site investigation (Gustafsson and Gustafsson 2006d, e, 2007c, 2008b). From the radar maps, which are found in the Appendices of the mentioned P-reports, the detectable distance of the reflector from the borehole is registered.

The geological mapping of the Äspö HRL tunnel is not incorporated into the Sicada database, but exists separately in its own database: the TMS-database. Excel-files with tunnel mapping data from the investigated tunnel intervals were retrieved from Äspö HRL. Also pdf-files with tunnel mapping were retrieved as well as a dgn-file with tunnel mapping data from the GPR-intervals. Borehole radar data were mainly taken from reports Calsten et al. (1995) and SKB (1993, 1994).

The GPR-reflectors were retrieved from and a dgn-file (Figure 3-1 in the report).

4.2 Correlation of radar reflectors with geology

4.2.1 Correlation of oriented borehole radar with core mapping

The correlation of oriented borehole radar with core mapping was performed as follows. The radius of oriented radar reflectors were determined by inspection of radar maps (Gustafsson and Gustafsson 2004a, b,c, 2005a, b, c, 2006a, b, c, d, e, 2007a, b, c, 2008a, b, 2009). Reflectors with a radius exceeding ~18 m were considered to be extensive and analyzed further. In the investigated boreholes from Forsmark there were 122 extensive oriented radar reflectors having a radius ranging from 18 to 130 m (median radius was 20 m). In the investigated boreholes from SFR and Oskarshamn there were 18 and 27 extensive oriented radar reflectors, respectively. The span in radius was 18–54 m in SFR-boreholes (median 20 m) and 18–110 m in Oskarshamn-boreholes (median 30 m).

During the second stage, the extensive radar reflectors were correlated with core mapping. Geological structures with alpha angle (± 10°) and strike (± 20°) /dip (± 20°) similar to that of the radar reflector and within a span of ± 2 m borehole length (± 3 m if the alfa angle is ≤ 30°) from the radar reflector were considered confident candidates of the reflector. If the alpha angle was small (≤ 45°) the error in alpha was likely to be less than ± 7°, while if the alpha angle was great (≥ 70°) the error in alpha was likely to be as much as ± 10°. These accuracy spans are personal judgments and have been fine-tuned relative to previous works, Stephens and Skagius (2007) and Carlsten (2004). Another discrepancy from previous works is that the correlations are not performed by visual inspection of the BIPS-image in the software Boremap, but by looking at figures (mainly borehole lengths, alpha angles and strike/dip-values) in the database.

In the case were several possible geological candidates could be correlated with a reflector, a judgment was made regarding which of the candidates was the most reliable. For example, fractures not visible in BIPS or fractures only indicated by oxidized walls were excluded as confident candidates. Sometimes several candidates together were believed to cause the reflector, for example three parallel fractures.

When the correlation was carried out, a confidence was set for the correlation. Only correlations of high or medium confidence were investigated further, while correlations of low confidence were considered too unreliable for making any conclusions of the geological properties of the reflector.

Finally, the correlation data were imported to Sicada as a new activity (GP139).

4.2.2 Correlation of oriented borehole radar with tunnel mapping

The correlation of oriented borehole radar reflectors from tunnel boreholes with tunnel mapping was made as follows. In reports of borehole radar investigations in the different boreholes (Calsten et al. 1995, SKB 1994) a calculation of intersection with nearby tunnel sections is presented in form of tables and figures. The intersection is mainly presented as a value of the tunnel length where the oriented radar reflector is calculated to intersect. Since the calculations are based on the radar orientation values, there is an error which leaves some uncertainty about the exact intersection with tunnel. Also, the geometry between borehole and tunnel is important for the uncertainty of intersection. Therefore, a visual inspection of the tunnel maps was made at the calculated intersections and the closest surroundings, in order to find structures in the tunnel mapping having corresponding orientations as the borehole radar reflectors.

The tunnel section at KA3191F had to be reinterpreted when it was discovered that the orientation of candidates presented in Carlsten et al. (1995) no longer agreed with present tunnel data.

When finding the geological structure (fracture, zone or lithological contact) which was considered causing the radar reflector, the unique MSlink of the mapped structure was retrieved from the TMS-database. A confidence was also set for the correlation (high, medium or low) based on the agreement between the orientation of the reflector and the orientation of the geological structure as well as the position of the geological structure in the tunnel relative to the calculated intersection length of the reflector with the tunnel.

The radius of the oriented borehole radar reflectors that were correlated with tunnel mapping have not been evaluated as was the case for borehole radar reflectors that were correlated with core mapping. Hence, also reflectors that are not interpreted as extensive are included in this evaluation.

The correlations were documented in an Excel-file and imported to Sicada as a GP138 activity.

4.2.3 Correlation of ground penetrating radar with tunnel mapping

The correlation of ground penetrating radar with tunnel mapping was performed by visual inspection of two overlapping dgn-files: one displaying GPR-reflectors and one displaying the tunnel mapping (Figure 4-1). To make the correlation easy, only the horizontal GPR-profiles were investigated, since the strike of the reflector is almost equal to the strike of the geological structure. Hence the correlation could be performed in 2D.

In the dgn-file the strike of the reflector was compared with strikes of structures in the tunnel mapping in order to find similar strikes. The strikes of structures in the tunnel mapping are only displayed correctly in the tunnel mid-line. In order to make the visual comparison easier, GPR-reflectors were extended to tunnel mid-line. When finding one or more geological structures with similar strike, the position along the tunnel was also compared. The ones with best fit have the same position as the reflector in the tunnel wall.

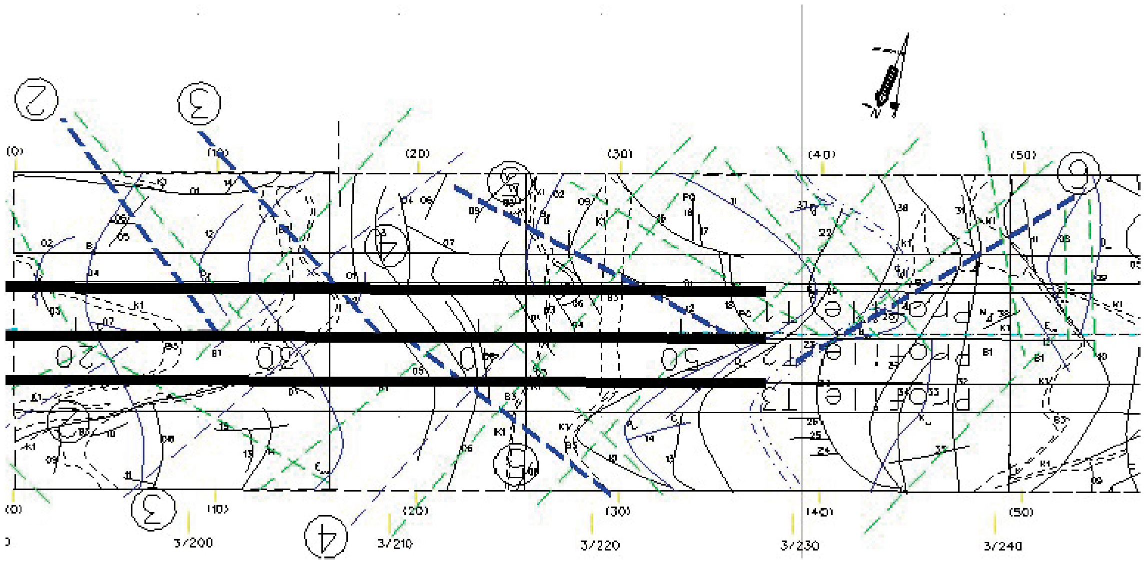

Figure 4-1. Example of 2D-image used for visual correlation of GPR-reflectors (blue and green dashed lines) with tunnel mapping data. TASA, Section 3 193–3 245.

When finding the geological structure (fracture, zone or lithological contact) which causes the reflector, the unique MSlink of the mapped structure was retrieved from the TMS-database. A confidence was also set for the correlation based on the agreement between strikes and position in tunnel.

The tunnel lengths, angles to tunnel wall and strikes of the GPR-reflectors were measured in the dgn-file and documented in an Excel-file, together with the correlations with tunnel mapping (MS-link) and were exported to Sicada as a GP350 activity. The GPR-reflectors had not been imported to Sicada previously.

4.3 Analysis of data

The core mapping or tunnel mapping data were compiled for the geological structures that were correlated with oriented borehole radar/GPR reflectors with medium or high confidence. The unique FeatureID of the core mapping data was used to find possible correlation with pfl-anomalies (HY688). Water content and type could be found in the tunnel mapping database (TMS). It was also noted if the correlated geological structure belongs to a possible deformation zone that has not been modeled deterministically or a deformation zone that has been modeled deterministically (Stephens et al. 2007, Wahlgren et al. 2008).

Mineralogy, alteration, width, aperture, roughness, surface, J_a-number and water content of the fractures or fracture zones, as well as rock contacts, which were identified with radar were compiled and compared with background data. Properties of fractures are mapped slightly differently in boreholes relative to tunnel. In the TMS-database fracture fillings are not only minerals but also rock types, whereas in the borehole data only minerals are denoted as fracture filling (with the exception of oxidized walls). Some of the compilation was based on weighted data, while others were based on non-weighted data (see chapter 4.3.1 below).

FPI-fractures are considered especially interesting. The properties of FPI-fractures correlated with a reflector relative to those with no correlation with a reflector have been compared.

4.3.1 Weighted and non-weighted data

Since many reflectors could be correlated with more than one possible candidate, and it was impossible to decide which one of the candidates caused the reflector or if they caused it together, data was weighted before the summary of correlations. The weighting was performed as follows:

- The sum of the weighted values for all candidates to one reflector was equal to 1.
- A candidate with confidence 3 was weighted twice as much as a candidate with confidence 2.
- A candidate with confidence 1 was weighted as 0, i.e. it was not considered as a confident candidate for the reflector and was therefore not included in the analysis of the properties of the reflectors.

An example of the above mentioned weighting follows. If a reflector had three candidates, one of high confidence and two of medium confidence, the one with high confidence was weighted as 0.5 while the two with medium confidence was weighted as 0.25 each, i.e. the weighted sum is 1.

Fracture mineralogy, alteration and roughness data were not weighted, as weighted data would have complicated the analysis unreasonably much. Up to four mapped minerals were encountered in the analysis for the core mapping data, and up to five mapped minerals/fracture fillings (in some cases rock types are mapped as fracture fillings) were encountered in the analysis of tunnel mapping data.

4.3.2 Background data

The properties of the geological structures (fractures, crushes and rock contacts) correlated with oriented radar reflectors were compared with corresponding background properties. For example, mineralogy of open fractures giving rise to a radar reflector was compared with mineralogy of all open fractures in the investigated boreholes/tunnel sections at the site in question. No differentiation has been made whether the fracture, crush or rock contact is situated within a deformation zone or not. The used background data are listed in Table 4-1.

Table 4-1. List of used background data to correlated reflectors.

Correlated data	Background data
Properties of geological structures correlated with oriented extensive borehole radar reflectors at Forsmark.	Properties of all corresponding geological structures in the following boreholes: KFM04A, KFM05A, KFM06A, KFM06C, KFM07A, KFM08A, KFM08C, KFM09A, KFM09B, KFM11A, KFM12A.
Properties of geological structures correlated with oriented extensive borehole radar reflectors at SFR.	Properties of all corresponding geological structures in the following boreholes: KFR101, KFR102A, KFR104 and KFR27.
Properties of geological structures correlated with oriented extensive borehole radar reflectors at Oskarshamn.	Properties of all corresponding geological structures in the following boreholes: KLX14A, KLX15A, KLX20A and KLX27A.
Properties of geological structures correlated with oriented borehole radar reflectors at Äspö HRL.	Properties of all corresponding geological structures at Äspö HRL in the following tunnel sections: TASZ-tunnel: whole TASA-tunnel, Section ID:s • 619–752, • 1777–2377 and • 3193–3364 (*only P & T mappings*).
Properties of geological structures correlated with GPR reflectors at Äspö HRL.	Properties of all corresponding geological structures at Äspö HRL in the following tunnel sections: TASZ-tunnel: whole TASA-tunnel, Section ID:s • 3191–3240 (*only P & T mappings*).

4.3.3 Analysis of deformation zones and crushes with no radar reflector

Possible deformation zones determined in the SHI or ESHI which have no radar reflector were identified. The radargrams from the intervals with possible deformation zones were studied. No further analysis was considered necessary.

Crush with no radar reflector were also identified and studied in more detail. Crush with no radar reflector were compared with background.

5 Data handling

This activity resulted in new Sicada-tables and parameters. The new tables and parameters are listed in Table 5-1.

Table 5-1. New Sicada tables and parameters created within this activity.

Activity	Table	Parameter	Reference in this report
GP139	radar_dir_feature_id	bhradar_boremap_feat	Section 4.2.1 and 6.1
GP138	radar_dir_mslink	bhradar_tms_fract bhradar_tms_contact bhradar_tms_fraczon1 bhradar_tms_rock	Section 4.2.2 and 6.2
GP351	tunnel_gpr_refl_tms	tungpr_tms_fract tungpr_tms_contact tungpr_tms_fractzon1 tungpr_tms_rock	Section 4.2.3 and 6.3

6 Results

6.1 Borehole radar versus core mapping

6.1.1 Forsmark Site Investigation

122 extensive oriented radar reflectors were investigated. Of these 96 (79 %) could be confidently correlated with a geological structure (Table 6-1). Most of the reflectors correspond to rock contacts (31 %), sealed fractures (27 %) or open fractures (15 %). Only 3 % of the reflectors can be correlated with crush and only 2 % to sealed networks. This means that more sealed fractures were correlated with oriented radar reflectors on behalf of open fractures, crush and rock contacts in comparison with an earlier performed investigation (see Stephens and Skagius 2007).

The extensive oriented radar reflectors have mostly intersection angles with the borehole of 30–60° (Figure 6-1). Extensive oriented radar reflectors correlated with geological structures seem to show some overrepresentation in the alpha-interval 40–50° (Figures A1-1 to A1-4).

Table 6-1. Summary of results from correlating oriented radar reflectors with borehole mapping in KFM-boreholes.

	Weighted correlations*		Non-weighted correlations*		Reflectors
	No	**% of all**	**No**	**% of all**	**TOT**
TOT no of reflectors					122
Correlated reflectors	96	79	96	79	
Non-correlated reflectors	26	21	26	21	
Structures correlated with reflectors:					
- open fracture(s)**	18.6	15	43	35	
- crush	3.8	3	6	5	
- sealed fracture(s)	32.4	27	80	66	
- sealed network	2.8	2	5	4	
- rock contact	37.8	31	75	61	
- other	0.6	0	2	2	
SUM	**96**	**79**	**211*** **	**173******	

* Correlations of medium or high confidence.
** Open and partly open fracture(s).
*** SUM can be greater than NO of correlated reflectors due to several candidates.
**** SUM can be greater than 100 due to several candidates.

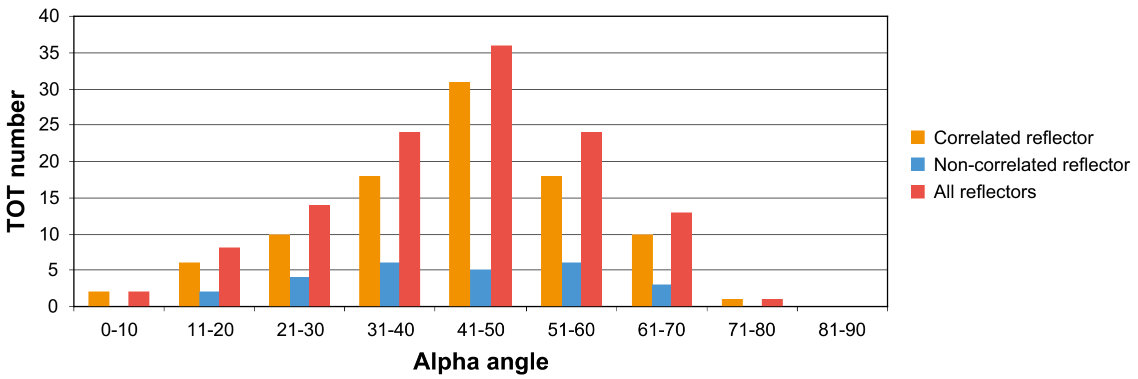

Figure 6-1. *Alpha angles of oriented extensive borehole radar reflectors, Forsmark site investigation.*

Most rock contacts, fractures, crushes or sealed networks which cause radar reflectors follow the orientation pattern in the background data from the Forsmark site (Appendix 2a).

The mineralogy of fractures causing a radar reflector is presented in Figure A3a-1 – A3a-4 as well as Table A3b-1. It can be tempting to draw the conclusion from the figures that calcite, chlorite, hematite and pyrite are overrepresented in fractures correlated with a reflector relative to background data, but the amount of data is rather small and the overrepresentation is only minor. Therefore overrepresentations should only be considered a hint.

Open fractures giving rise to a radar reflector are generally only slightly altered, while sealed fractures are generally fresh (Table A4-1), which are the general appearances of open and sealed fractures in Forsmark. The most altered fractures (highly altered, completely altered or gouges) do not result in extensive radar reflectors.

Fractures correlated with oriented radar reflectors are generally only 0.5 mm wide, planar or stepped with a rough surface (Table A5-1 & Table A5-6).

Table 6-2. The proportion of kinematic indicators and pfl-anomalies in fractures correlated with extensive oriented radar reflectors. Non-weighted data. Forsmark site investigation.

		Kinematic indicator			Pfl-anomaly		
Fracture type	TOT	Fracture with kinematic indicator	Fracture with no kinematic indicator*	No information**	Fracture with pfl-anomaly	Fracture with no pfl-anomaly	No information***
Open and partly open fractures correlated with extensive radar reflector	43	1	24	18	7	19	17
Sealed fractures correlated with extensive radar reflector	80	1	45	34	2	61	17

* Fractures within possible deformation zones that have no documented kinematic indicator.

** Kinematics in fractures outside possible deformation zones are generally not investigated. DZ5 in KFM04A and DZ5 in KFM06C are also lacking kinematical data.

*** No correlations between pfl-anomalies and fractures were retrieved from boreholes KFM06C, KFM09A, KFM09B and KFM12A.

Only two of the fractures that correlated with extensive oriented radar reflectors in Forsmark have a documented kinematic indicator, despite that as many as 431 fractures have documented kinematic indicators in the investigated boreholes (Table 6-2). Nine fractures correlated with extensive oriented radar reflectors have an interpreted pfl-anomaly. In total there are as many as 1 917 fractures with interpreted pfl-anomalies in the 11 boreholes studied at Forsmark.

Of the rock contacts giving rise to a radar reflector about 40 % are contacts between metagranite-granodiorite (101057) and pegmatite (101061) while about 20 % are contacts between metagranite-granodiorite (101057) and amphibolites (102017, Table 6-3). Pegmatite or amphibolite occur in ~75 % of the rock contacts that are confidently correlated with oriented radar reflectors. Other contacts giving rise to radar reflectors are subordinate.

Table 6-3. Character of rock contacts that were confidently correlated with extensive oriented radar reflectors in KFM-boreholes. Non-weighted values.

Rock 1	Rock 2	no	%		
Metagranite-granodiorite	Granodiorite	1	*1*		
Metagranite-granodiorite	Metadiorite-quarz diorite-gabbro	1	*1*		
Metagranite-granodiorite	Metagranite-granodiorite-tonalite	1	*1*		
Metagranite-granodiorite	Aplitic metagranite	2	*3*		
Metagranite-granodiorite	**Pegmatite**	**29**	***39***		
Aplitic metagranite	Pegmatite	3	*4*	**no**	**%**
Felsic to intermediate metavolcanic rock	Pegmatite	1	*1*	36	48
Pegmatite	Amphibolite	3	*4*		
Aplitic metagranite	Amphibolite	2	*3*	**no**	**%**
Metagranite-granodiorite	**Amphibolite**	**15**	***20***	24	32
Felsic to intermediate metavolcanic rock	Amphibolite	3	*4*		
Quartz diorite	Amphibolite	1	*1*		
Breccia	Granitic rock	4	*5*		
Quarz vein	Granitic rock	3	*4*		
Change in structure?		6	*8*		
Total amount of rock contacts correlated with extensive radar reflectors		**75**	**100**		

6.1.2 SFR Site Investigation

18 extensive oriented radar reflectors were investigated. Of these 15 reflectors (83 %) could be confidently correlated with a geological structure (Table 6-4). Two of the reflectors that could not be correlated with any geological structure were out of the geological mapping range. Most of the reflectors correspond to open fractures (43 %), rock contacts (20 %) and sealed fractures (18 %). Only one of the reflectors can be correlated with crush.

Table 6-4. Summary of results from correlating oriented radar reflectors with borehole mapping in KFR-boreholes. SFR Site Investigation.

	Weighted correlations*		High confidence correlations**		Reflectors
	No	**% of all**	**No**	**% of all**	**Total**
Total no of reflectors					18
Coupled reflectors	15	83	12	67	
Non-coupled reflectors	3	17	6	33	
Reflectors coupled to:					
- open fracture(s)* **	7.7	43	5	28	
- crush	0.5	3	1	6	
- sealed fracture(s)	3.3	18	3	17	
- sealed network	0	0	0	0	
- rock contact	3.6	20	3	17	
- other	0	0	0	0	
Sum	**15**		**12**		

* Coupling with medium to high confidence.
** No of reflectors with high confidence, not weighted.
*** Open and partly open fracture(s).

The intersection angles of the extensive oriented radar reflectors with the borehole vary (Figure 6-2). Diagrams showing alpha angles of reflectors correlated with open fractures, sealed fractures, crush and rock contacts are shown in Figures A1-5 to A1-8, but the data set is too small to make statistically valid conclusions. The same counts for the orientations of rock occurrences and open fractures correlated with oriented radar reflector relative to main contact and fracture orientations in SFR, which are shown in Appendix 2b, the mineralogy of fractures causing a radar reflector which is presented in Figure A3a-5 and A3a-6, as well as Table A3b-2 and finally also width, aperture, alteration and roughness of fractures correlated with extensive oriented radar reflectors (Table A4-2, Table A5-2 and Table A5-6).

Six rock contacts of different character have been identified as confident radar reflectors (Table 6-5). Four of the contacts are also correlated with parallel crush or fractures.

6.1.3 Site Investigation Oskarshamn

27 extensive oriented radar reflectors were investigated. The amount of the studied reflectors is too small to make any statistically valid conclusions. The figures that follow in this chapter are only for presentation of the results in this investigation, but they do not necessarily describe the real character of the extensive radar reflectors.

Of the 27 investigated extensive oriented radar reflectors, 22 (81 %) could be confidently correlated with a geological structure (Table 6-6). Most of the reflectors correspond to open fractures (35 %), rock contacts (22 %), or sealed fractures (16 %). Only 6 % of the reflectors can be correlated with crush and only 2 % to sealed fracture networks.

Most extensive oriented radar reflectors have intersection angles with the borehole of 20–50° (Figure 6-3). Diagrams showing alpha angles of reflectors correlated with open fractures, sealed fractures, crush and rock contacts are shown in Figures A1-9 to A1-12.

Table 6-5. Character of rock contacts that were confidently correlated with extensive oriented radar reflectors in KFR-boreholes. Non-weighted values. SFR site investigation.

Rock 1	Rock 2	no	%
Metagranite-granodiorite	Breccia	1	17
Pegmatite	Breccia	1	17
Pegmatite	Fine-grained granite	1	17
Pegmatite	Metagranite-granodiorite	2	33
Pegmatite	Amphibolite	1	17
Total amount of rock contacts correlated with extensive oriented radar reflectors		**6**	**100**

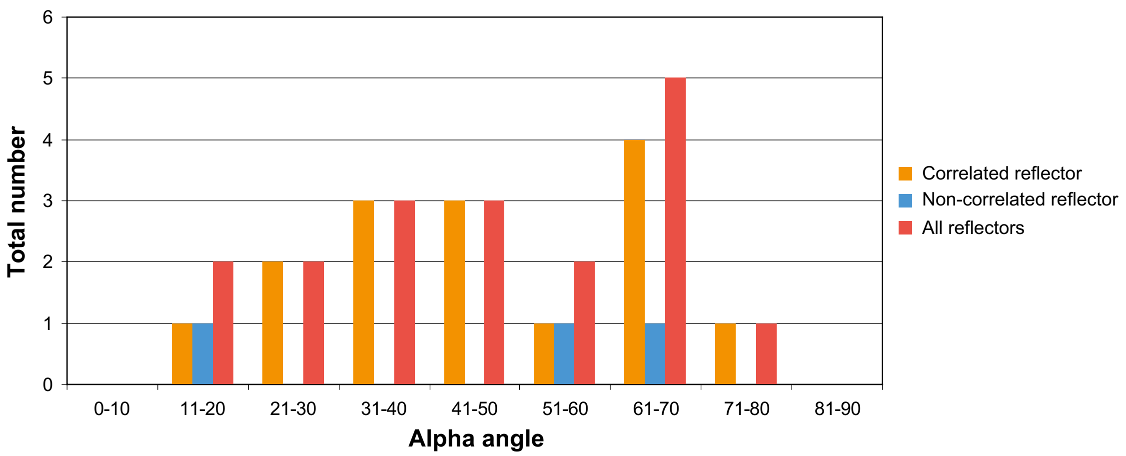

Figure 6-2. Alpha angles of extensive oriented borehole radar reflectors, SFR site investigation.

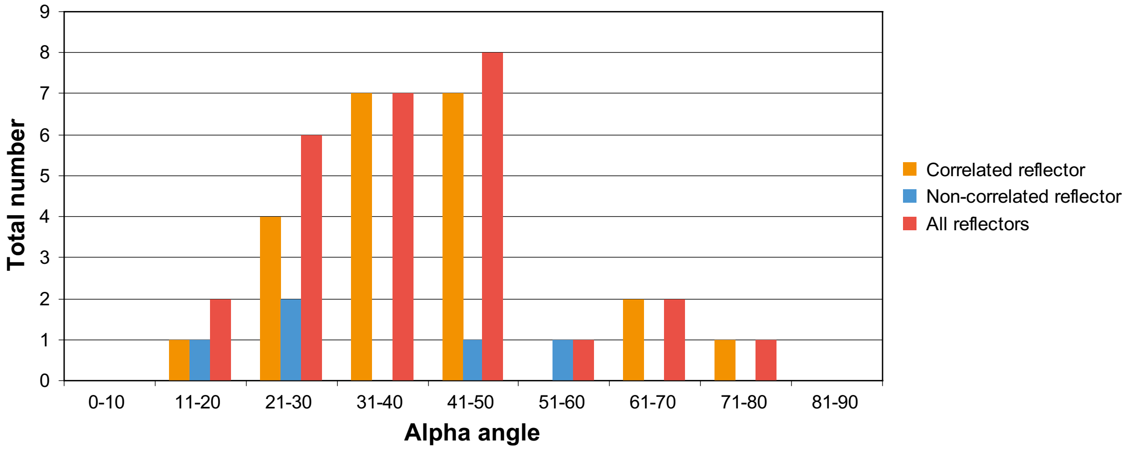

Figure 6-3. *Alpha angles of extensive oriented borehole radar reflectors, Oskarshamn site investigation.*

Table 6-6. Summary of results from correlating oriented radar reflectors with borehole mapping in KLX-boreholes. Oskarshamn site investigation.

	Weighted correlations*		Non-weighted correlations*		Reflectors
	No	% of all	No	% of all	Total (no)
Total No of reflectors					27
Correlated reflectors	22	81	22	81	
Non-correlated reflectors	5	19	5	19	
Structures correlated with reflectors:					
-open fracture(s)**	9.5	35	28	104	
-crush	1.7	6	5	19	
-sealed fracture(s)	4.4	16	16	59	
-sealed network	0.6	2	2	7	
-rock contact	5.9	22	16	59	
-other	0	0	0	0	
Sum	**22.0**	**81**	**67*****	**248******	

* Correlations of medium or high confidence.
** Open and partly open fracture(s).
*** SUM can be breater than NO of correlated reflectors due to several candidates.
**** SUM can be greater than 100 due to several candidates.

The orientation of open fractures, crush and rock contacts that correlate with extensive radar reflectors are in accordance with the most dominating orientations of the structure in question (Appendix 2c).

The mineralogy of fractures, fracture networks and crushes causing an extensive radar reflector are presented in Figures A3a-7 – A3a-10 and Table A3b-3. There is no clear difference between the mineralogy of fractures correlated with extensive radar reflectors compared to all fractures in the investigated boreholes.

The width, aperture, alteration, roughness and surface of fractures resulting in extensive radar reflectors are presented in Table A4-3, Table A5-3 and Table A5-6. There are no great differences in these properties between fractures with extensive reflectors and fractures as a whole in the investigated boreholes.

None of the fractures correlated with oriented radar reflectors has any kinematic indicator in Oskarshamn (Table 6-7). In the investigated boreholes from Oskarshamn 48 fractures with kinematic indicators have been documented (only results from KLX15A and KLX20A). 12 fractures correlated with extensive oriented radar reflectors in Oskarshamn have an interpreted pfl-anomaly. In total there are 723 fractures with interpreted pfl-anomalies in the four boreholes studied at Oskarshamn.

Table 6-7. Numbers of fractures with kinematic indicator and/or pfl-anomalies in fractures correlated with extensive oriented radar reflectors. Non-weighted data. Oskarshamn site investigation.

		Kinematic indicator			Pfl-anomaly	
Fracture type	TOT	Fracture with kinematic indicator	Fracture with no kinematic indicator*	No information**	Fracture with pfl-anomaly	Fracture with no pfl-anomaly
Open and partly open fractures correlated with extensive radar reflector	28	0	2	26	9	19
Sealed fractures correlated with extensive radar reflector	16	0	7	9	3	13

* Fractures within possible deformation zones that have no documented kinematic indicator.

** Kinematic indicators were not investigated in KLX14A and KLX27A. In KLX15A and KLX20A kinematics in fractures outside possible deformation zones were generally not investigated.

Only two highly confident correlations between an extensive radar reflector and a rock contact have been made. Both are contacts between quartz monzodiorite (501036) and fine-grained granite (511058). If correlations of medium confidence are included, 16 rock contacts are identified by radar. The amount is too small to make statistically valid conclusions about their character. Of the correlated rock contacts over 60 % are contacts between Quartz monzodiorite and Fine-grained granite (Table 6-8) while roughly 40 % can be explained by change in structure and not necessarily by contact between two different rock types.

Table 6-8. Character of rock contacts that were confidently correlated with extensive oriented radar reflectors in KLX-boreholes. Non-weighted values. Site Investigation Oskarshamn.

Rock 1	Rock 2	No	%		
Quartz monzodiorite	Fine-grained granite	8	50	no	%
Quartz monzodiorite	Fine-grained granite, cataclastic	2	13	10	63
Quartz monzodiorite	Quartz monzodiorite, brittle-ductile shear zone	3	19	7	44
Quartz monzodiorite	Mafic rock, brittle-ductile shear zone	1	6		
Mafic rock, fine-grained	Mafic rock, breccia	1	6		
Quartz monzodiorite	Dolerite	1	6		
Total amount of rock contacts correlated with extensive radar reflectors		**16**	**100**		

6.1.4 Crush and possible deformation zones with no radar reflector

Crushes that have no radar reflector have been studied in order to characterize the crushes that are not captured by radar. Crushes with possible short oriented radar reflector or non-oriented radar reflectors are excluded in this study. There are 44 crushes in Forsmark, 40 crushes in SFR and 23 crushes in Oskarshamn that have no radar reflector. These constitute about half of all mapped crushes in Forsmark and Oskarshamn, and most of the crushes in the SFR-area (Table 6-9).

The alpha angles of the crushes with no radar reflector relative to all mapped crushes in the investigated boreholes (background data) are presented in Figure 6-4. Alpha angles of crushes with no reflector are generally slightly underrepresented within the interval 50–70° relative to alpha angles of all crushes, while alpha angles of 80–90° are slightly overrepresented. The orientations of crushes with no reflector generally reflect the overall crush orientations in the sites Forsmark, SFR and Oskarshman (Figures A2a-7, A2b-7 and A2c-7, respectively).

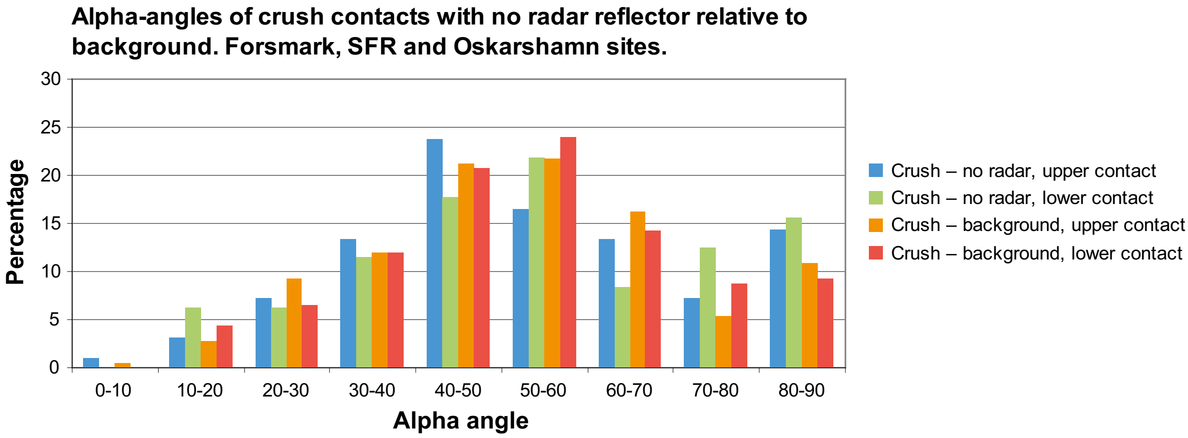

Figure 6-4. *Alpha angles of oriented crush contacts with no radar reflector relative to background. Number of data is:■=97, ■=96, ■=184 and ■=183. Not all crushes listed in Table 6-9 are oriented which explains the smaller number of crushes relative to Table 6-9.*

There is no clear difference in mineralogy between crushes not detected by borehole radar relative to all crushes in the investigated boreholes (Figure A6-1, A6-2 and A6-3, Table A6-1). The same is valid for alteration and width along borehole (Table A6-2 and A6-3).

Since the core mapping system does not reveal the character of the crush, i.e. if the fragments are rounded (a "real" crush), if there is outfall/aperture or if the crush is only a fractured section with no signs of greater displacement (but with crushed drill core), the crushes with no reflector have been divided into "crush" and "fractures mapped as crush" (Table A6-4). Quite a large number of the mapped crushes with no radar reflector are actually single fractures with aperture or a fractured section with no signs of rounded fragments. The parallelism of upper and lower contacts has also been looked at (Table A6-5), but with no valuable results.

Table 6-9. Number of crushes with possible radar reflectors and crushes with no radar.

Type of reflector/no reflector	Forsmark No	SFR No	Oskarshamn No
Crush with possible extensive oriented radar reflector*	12	4	9
Crush with possible short oriented radar reflector	14	0	3
Crush with possible non-oriented radar reflector	31	1	10
Crush with no radar reflector	44	40	23
TOT crushes	**101**	**45**	**45**

*Note! Also correlations of low confidence are included in this table.

Our task was also to look at borehole radar reflectors in relation to possible deformation zones. In Appendix 7a possible deformation zones with no extensive oriented radar reflector are listed, while in Appendix 7b possible deformation zones with no radar reflector at all are listed. Possible deformation zones with no radar reflector are not found in the investigated boreholes from Forsmark, while only two very minor possible deformation zones can be found in the boreholes from Oskarshamn. One of them has a radar reflector within 2 m away from the possible deformation zone (DZ 5 in KLX14). Most of the possible deformation zones with no radar reflector are found in Site Investigation SFR. One possible deformation zone, DZ6 in KFR104, is out of range of the radar logging, while DZ4 in KFR101, DZ3 in KFR102A, DZ3 and DZ4 in KFR27 are characterized by poor radar penetration (Gustafsson and Gustafsson 2008a, 2009). The remaining possible deformation zones seem to have short reflectors in the radargram in the report, although no reflector is documented in GP140.

Possible deformation zones with no extensive oriented radar reflector are not studied in detail in this work. Probable reasons for lacking extensive oriented radar reflectors are poor radar penetration or zones characterized by en echelon fracturing.

6.2 Borehole radar versus tunnel mapping

123 oriented reflectors from borehole radar have been investigated. These comprise not only extensive radar reflectors, but also shorter ones. 45 reflectors were confidently correlated with 59 geological structures in the tunnel mapping at Äspö HRL. Of the 59 correlated geological structures, 48 are fractures, 7 are fracture zones and 3 are rock contacts (Table 6-10). Attention has been paid on FPI-fractures and on fracture zones. 30 % of the FPI fractures and 83 % of the zones were detected by borehole radar (Table 6-11).

Table 6-10. Summary of results from correlating oriented borehole radar reflectors with tunnel mapping (TMS). Only correlations of high confidence are included.

	Reflectors (no)	Reflectors with no correlations* (no)	Correlations (no)	Fractures correlated with reflectors (no)	Fracture zones correlated with reflectors (no)	Rock contacts correlated with reflectors (no)
KA0575A	11	2	11	8	2	
KA1061A	19	19	0	0		
KA1131B	8	8	0	0		
KA1754A	13	13	0	0		
KA2048B	16	8	10	7	3	
KA2162B	16	4	15	14		1
KA3191F	10	5	11	9	2	
C2 (KXZC2)	8	5	3	2		1
C3 (KXZC3)	11	8	3	3		
C6 (KXZC6)	11	6	6	5		1
Total	**123**	**78**	**59****	**48**	**7**	**3**

* Note: reflectors having correlations of medium or low confidence are included.

** Number of correlations can be greater than the difference between reflectors and reflectors with no correlations if a reflector can be confidently correlated with several structures.

Table 6-11. Summary of FPI structures correlated/not correlated with oriented borehole radar reflectors.

	FPI detected by borehole radar (no)	FPI detected by borehole radar %	FPI not detected by borehole radar (no)	FPI not detected by borehole radar %	FPI total number
Fractures	25	30	58	70	83
Fracture zones	5	83	1	17	6

The distribution of alpha angles of the oriented reflectors is similar to the distribution of alpha angles of other borehole radar reflectors (Figure 6-5). An explanation to the very few correlated reflectors with low alpha angle is that most do not crosscut the tunnel.

There appears to be a dominance of steeply dipping fractures with dip directions to the NNE or SSW and a few gently dipping fractures that all conform to the background data (Appendix 2d). However, there is also an important group of steeply-dipping fractures that dip to the WNW and some moderately dipping fractures that are not prominent in the background data. Fracture zones correlated with a reflector are steeply dipping towards W or NW and the few rock contacts that are correlated with reflectors are also steeply dipping but towards NW or SE.

The occurrence of fracture fillings (as mapped in the TMS-database) have been studied for all fractures correlated with an oriented radar reflector showing no greater difference from other fractures in the area (Figure A3a-11). FPI-fractures seem to contain more often epidote, grout or mylonite relative to all fractures in the area (Figure A3a-12). Calcite and grout seem to be overrepresented among FPI-fractures captured by radar (n=25) relative to FPI-fractures not captured by radar (n=58), but in this group the number is too small for statistically valid conclusions.

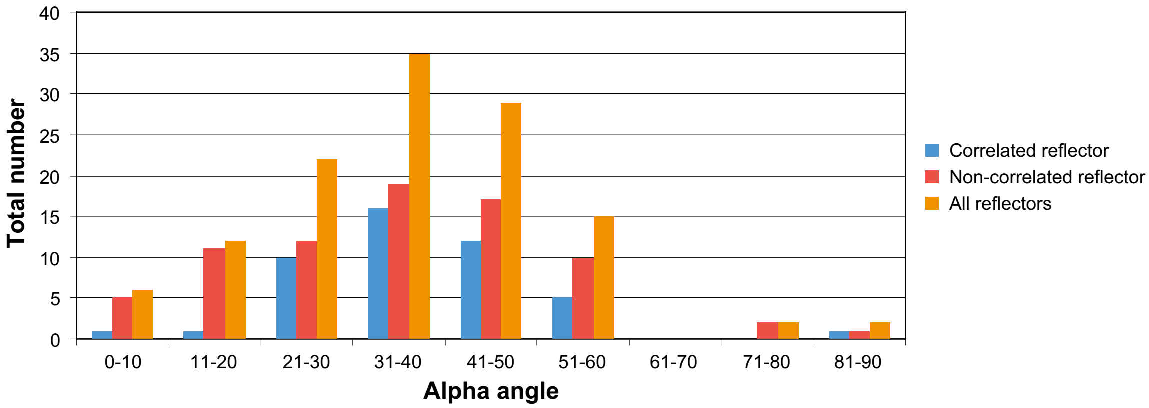

Figure 6-5. *Distribution of alpha angles of oriented borehole radar reflectors in boreholes at Äspö HRL. Number of data: ■=45, ■=78 ■=123.*

Fractures in the tunnel giving rise to oriented radar reflectors generally more often contain water compared to other fractures (Table A5-4, Figures A5-1 and A5-2), but the overrepresentation of water bearing fractures could also be explained by the captured FPI-fractures of which about one half are water bearing. Fractures correlated with borehole radar are generally planar with a rough surface.

6.3 GPR versus tunnel mapping

51 GPR reflectors were investigated. Of these 28 reflectors (55 %) could be confidently correlated with mapped geology (Table 6-12). Out of the 28 correlated reflectors, 22 were correlated with fractures; 5 with rock contacts and one single to a fracture zone, which is also the only fracture zone in the tunnel. The rock contacts were in all cases contact between Äspö diorite and fine-grained granite (Table 6-13).

Some GPR-reflectors that were not correlated with geology could actually reflect fractures in the opposite tunnel wall, since the GPR-antenna was unshielded. The reflectors TASA-V-T1-17, TASA-H-T3-4, TASA-H-T3-11 and TASA-H-T3-12 are suspected reflectors from the opposite tunnel wall.

Table 6-12. Summary of results from correlation of GPR reflectors with tunnel mapping (TMS). Only correlations with medium or high confidence are encountered. Äspö HRL.

	TASA 3174-3245 m		TASZ 25-76 m		SUM	
Reflector property	**No**	**% of all**	**No**	**% of all**	**No**	**% of all**
Reflectors	36		15		51	
Correlated reflectors	21	58	7	47	28	55
Non-correlated reflectors	15	42	8	53	23	45
Reflectors correlated with fractures	17	47	5	33	22	43
Reflectors correlated with fracture zones	1	3	0	0	1	2
Reflectors correlated with rock contacts	3	8	2	13	5	10

Table 6-13. Character of rock contacts with GPR reflector. Äspö HRL.

No	%	Rock contact Rock type 1	Rock type 2
5	100	Äspö-diorite	Fine-grained granite

The angle of the geological structure to the GPR profile is believed to be of importance for its visibility in the GPR-radargram. Figure A1-13 shows the distribution of alpha angles of the GPR reflectors that have been correlated with geology and those that have not been correlated with geology in relation to alpha angles of fractures in the area. The dataset is quite small but the preference for the GPR to catch structures lying at an angle of 30-50° to the profile is highlighted (see also Figure 6-6).

Due to the small data set no statistically valid conclusions can be made. The following statements do only count for the 22 fractures captured by GPR in this study. The fractures captured by GPR belong to the main fracture sets trending NW-SE or NE-SW with a dip of 70-90 (Appendix 2e). About half of the fractures captured by GPR are FPI-fractures. Horizontal fractures are absent, due to the fact that the GPR-profile is horizontal. The only fracture zone in the investigated area is oriented ~030/70 and it is also captured by GPR.

Calcite, epidote and grout seem to be overrepresented in fractures with GPR-reflector relative to background on behalf of chlorite (Figure A3a-13, Table A8-2) which supports the result from the study of borehole radar versus tunnel mapping.

Most fractures giving rise to a radar reflector are planar with a rough or smooth surface (Table A5-5). No difference between roughness of fractures with GPR-reflector relative to background have been noticed. Half of the fractures are water bearing, compared to only 12 % of background fractures. Of the 12 FPI fractures in the investigated tunnel interval, 9 were captured by GPR. The three FPI-fractures that were not captured by GPR are characterized by no water content (Table A5-5), while the mineralogy is quite similar to those that have been captured by radar.

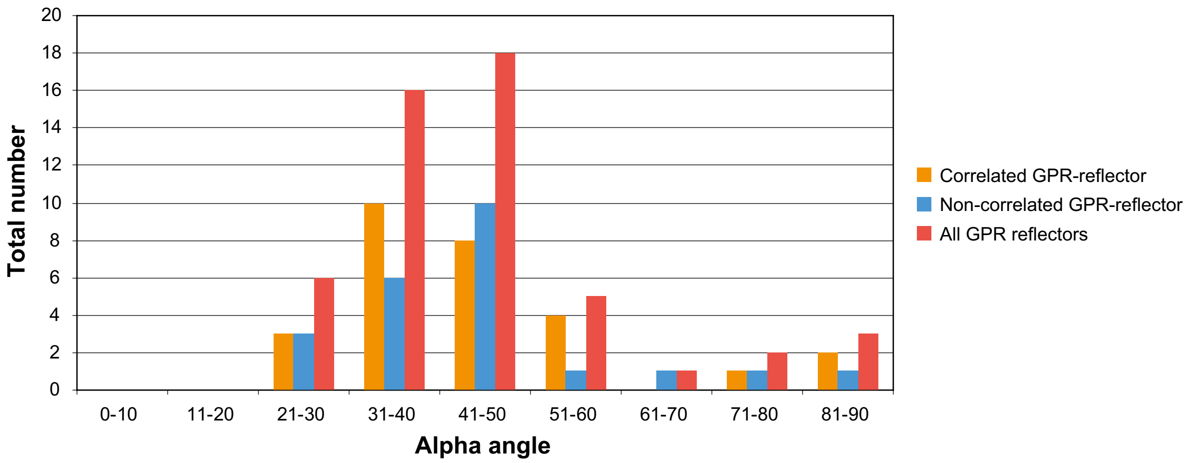

Figure 6-6. *Alpha angles of GPR-reflectors to tunnel wall, Oskarshamn site investigation.*

7 Conclusion

More than 80 % of the extensive oriented borehole radar reflectors could be confidently correlated with geology in the boreholes, while only 60 % of the oriented borehole radar and GPR reflectors could be confidently correlated with the tunnel mapping. Of the correlated reflectors in boreholes about 70 % are fractures (open fractures, sealed fractures, crushes or sealed fracture networks) and 30 % rock contacts, whereas of the correlated reflectors in the tunnel about 90 % are fractures or fracture zones and 10 % rock contacts. This means that only ~55 % of the oriented radar reflectors represent fractures, fracture zones or crushes in the bedrock.

Most possible deformation zones do have radar reflectors. Those which do not have any reflector are explained by poor radar penetration or no radar logging.

There is generally no outstanding property of fractures detected by radar, but the intersection angles of geological structures seem to be of importance whether this structure is registered by borehole radar or GPR or not. Fractures with intersection angles of 30-60° are generally slightly overrepresented in the radargrams relative to background.

The amount of data from each site was generally too small to make statistically valid conclusions about the properties of fractures giving rise to oriented radar reflectors. Looking at all sites together, the following can be stated:

- Fractures giving rise to a radar reflector was believed to belong to one of the main fracture sets. This study has not given any clear answer to this, since local fracture sets drown in the enormous amount of background data.
- Fracture mineralogy does not seem to be crucial for its visibility in the radargram.
- The most altered fractures are not captured by borehole radar. Fresh crushes are also not visible in radargrams, probably because they are actually artificial.
- The roughness of fractures with reflector is almost the same as for all fractures at the site in question. No clear preferred roughness is observed among fractures correlated with radar reflectors, except that irregular fractures are underrepresented. It should though be kept in mind that this straggling result may rather display differences in interpretation between mapping teams and not necessarily differences in properties (Gustafsson and Gustafsson 2007c, Section 4.3.4).
- Fractures and crushes giving rise to radar reflectors seem to be relatively thin. Many fractures correlated with reflectors are only about 0.5 mm wide. Crushes correlated with reflector are not the widest ones either (width only measured along borehole).
- In the correlation with tunnel mapping at Äspö HRL, water bearing fractures are overrepresented among fractures with borehole radar/GPR reflector. This overrepresentation of water bearing fractures is not observed in the correlations with borehole data (pfl-anomalies).
- Most fractures with kinematic indicators do not give rise to extensive radar reflectors.

8 Concluding remarks and recommendations

When planning the study and its delimitations, it seemed reasonable to concentrate on data from Forsmark, while the other sites served as a reference to observe which fracture properties related to radar reflectors may be site specific. Since the work with correlation is very time-consuming, the amount of data was also limited to extensive radar reflectors. This delimitation resulted in too few fracture data to make statistically valid conclusions about the fracture properties. However, this study has revealed that there is no outstanding property of fractures that matches radar reflectors. The study has also revealed that only ~55 % of the reflectors are explained by fractures, fracture zones or crush zones and that more than 20 % of the reflectors have no geological explanation.

Another feature in this study is the matter of scale and the difference in detail in the mapping of boreholes and tunnels. Several possible candidates were identified in the boreholes due to the very detailed borehole mapping. In the tunnel mapping, on the other hand, relatively few fractures are mapped and even fewer fractures are actually long enough to be probable candidates for the reflector. Approximately 5 sealed fractures/m are documented in the borehole mapping, while sealed fractures are generally not documented in the tunnel mapping. This explains why no sealed fractures in the Äspö HRL-tunnel are correlated with radar reflectors.

An important question concerns how the long fractures can be distinguished from all the other fractures in the pilot boreholes? It is clear that, if a fracture in the pilot borehole can be correlated with an extensive radar reflector, it is likely that the fracture is long. However there are quite often several possible candidates for one radar reflector and further studies are required to identify signatures for high confidence candidates. It can be concluded that 50-75 % of the long fractures (FPI) are captured by radar in the tunnel study at the Äspö HRL. Other methods need to be used to identify the remaining long fractures, for example, the modelling of long fractures between tunnels when the data assembly from tunnels has become sufficiently extensive.

The meaningless result from the study of mapped crush zones with no radar reflector reflects the need of defining crush better in the borehole mapping procedure. The mapped crush zones have very different character and the difference in character is not evident in the mapping data, as the mapping system is constructed today.

The oriented radar reflectors in the tunnel boreholes may, in some cases, have incorrect orientations which affect the correlation with geological structures negatively. The reason for this is that the borehole radar probe was not necessarily centralized in the boreholes during logging, and that the reflected incoming radar rays are diverging due to the amount of groundwater in the borehole surrounding the borehole radar probe. Technical developments that improve confidence in the orientation of radar reflectors are required.

9 Acknowledgements

The authors are very grateful to all who have contributed to this work: Isabelle Olofsson, Assen Simeonov, Michael Stephens, Stefan Sehlstedt, Leif Stenberg, Carljohan Hardenby, Oskar Sigurdsson, Johan Nissen, Elisabeth Djerf, Margareta Gerlach, and colleagues at our companies.

References

SKB's (Svensk Kärnbränslehantering AB) publications can be found at www.skb.com/publications.

Carlsten S, 2004. Oskarshamn site investigation. Geological interpretation of borehole radar reflectors in KSH01, HSH01–03, KAV01 and KSH02. SKB P-04-218, Svensk Kärnbränslehantering AB.

Carlsten S, Stanfors R, Askling P, Annertz K, 1995. Comparison between borehole radar data and geological parameters from tunnel mapping. SKB PR 25-95-22, Svensk Kärnbränslehantering AB.

Döse C, Stråhle A, Rauséus G, Samuelsson E, Olsson O, 2008. Revision of BIPS-orientations for geological objects in boreholes from Forsmark and Laxemar. SKB P-08-37, Svensk Kärnbränslehantering AB.

Gustafsson J, Gustafsson C, 2004a. Forsmark site investigation. RAMAC and BIPS logging in borehole KFM04A, KFM04B, HFM09 and HFM10. SKB P-04-67, Svensk Kärnbränslehantering AB.

Gustafsson J, Gustafsson C, 2004b. Forsmark site investigation. RAMAC and BIPS logging in borehole KFM06A, HFM16, HFM17 and HFM19. SKB P-04-69, Svensk Kärnbränslehantering AB.

Gustafsson J, Gustafsson C, 2004c. Forsmark site investigation. RAMAC and BIPS logging in borehole KFM05A. SKB P-04-152, Svensk Kärnbränslehantering AB.

Gustafsson J, Gustafsson C, 2005a. Forsmark site investigation. RAMAC and BIPS logging in borehole KFM07A. SKB P-05-52, Svensk Kärnbränslehantering AB.

Gustafsson J, Gustafsson C, 2005b. Forsmark site investigation. RAMAC and BIPS logging in borehole KFM08A. Revised April 2006. SKB P-05-158, Svensk Kärnbränslehantering AB.

Gustafsson J, Gustafsson C, 2005c. Forsmark site investigation. RAMAC and BIPS logging in borehole KFM06C. SKB P-05-242, Svensk Kärnbränslehantering AB.

Gustafsson J, Gustafsson C, 2006a. Forsmark site investigation. RAMAC and BIPS logging in boreholes KFM07B, KFM09A, HFM25 and HFM28. SKB P-06-44, Svensk Kärnbränslehantering AB.

Gustafsson J, Gustafsson C, 2006b. Forsmark site investigation. RAMAC and BIPS logging in boreholes KFM09B, HFM24, HFM26, HFM27, HFM29 and HFM32. SKB P-06-64, Svensk Kärnbränslehantering AB.

Gustafsson J, Gustafsson C, 2006c. Forsmark site investigation. RAMAC and BIPS logging in boreholes KFM08C, HFM30, HFM31, HFM33 and HFM34. SKB P-06-178, Svensk Kärnbränslehantering AB.

Gustafsson J, Gustafsson C, 2006d. Oskarshamn site investigation. RAMAC, BIPS and deviation logging in boreholes KLX11B, KLX11C, KLX11D, KLX11E, KLX11F, KLX18A, KLX20A, HLX28 and HLX40 and BIPS and deviation logging in KLX19A. SKB P-06-159, Svensk Kärnbränslehantering AB.

Gustafsson J, Gustafsson C, 2006e. Oskarshamn site investigation. RAMAC, BIPS and deviation logging in boreholes KLX13A, KLX14A, KLX22A, KLX22B, KLX23A, KLX23B, KLX24A, KLX25A, KLX26A, KLX26B, HLX39 and HLX41. SKB P-06-260, Svensk Kärnbränslehantering AB.

Gustafsson J, Gustafsson C, 2007a. Forsmark site investigation. RAMAC and BIPS logging in borehole KFM11A. SKB P-07-10, Svensk Kärnbränslehantering AB.

Gustafsson J, Gustafsson C, 2007b. Forsmark site investigation. RAMAC and BIPS logging in borehole KFM12A. SKB P-07-112, Svensk Kärnbränslehantering AB.

Gustafsson J, Gustafsson C, 2007c. Oskarshamn site investigation. Radar, BIPS and deviation logging in borehole KLX15A. SKB P-07-117, Svensk Kärnbränslehantering AB.

Gustafsson J, Gustafsson C, 2008a. Site investigation SFR. Radar and BIPS loggings in KFR101 and BIPS loggings in KFR27 (0–147 m), HFR101, HFR102 and HFR105. SKB P-08-71, Svensk Kärnbränslehantering AB.

Gustafsson J, Gustafsson C, 2008b. Oskarshamn site investigation. RAMAC, BIPS and deviation logging in borehole KLX27A. SKB P-08-30, Svensk Kärnbränslehantering AB.

Gustafsson J, Gustafsson C, 2009. Site investigation SFR. BIPS-logging in the core drilled boreholes KFR102A, KFR102B, KFR103, KFR104 and KFR27 (140–500 m) and radar logging in KFR27 (0–500 m), KFR102A and KFR104. SKB P-09-11, Svensk Kärnbränslehantering AB.

Olsson O, 1992. Characterization ahead of the tunnel front by radar and seismic methods – a case history from the Äspö Hard Rock Laboratory. SKB PR 25-92-01, Svensk Kärnbränslehantering AB.

SKB, 1994. Supplementary investigations of fracture zones in the tunnel, core mapping and radar measurement. Compilation of technical notes. Measurements performed during construction of section 1 475–2 265 m. SKB PR 25-94-01, Svensk Kärnbränslehantering AB.

Stephens M, Skagius K (eds), 2007. Geology – Background complementary studies. Forsmark stage modeling 2.2. SKB R-07-56, Svensk Kärnbränslehantering AB.

Stephens, M, Fox A, La Pointe P, Simeonov A, Isaksson H, Hermansson J, Öhman J, 2007. Geology Forsmark. Site descriptive modeling – Forsmark stage 2.2. SKB R-07-45, Svensk Kärnbränslehantering AB.

Wahlgren C-H, Curtis P, Hermanson J, Forssberg O, Öhman J, Fox A, La Pointe P, Drake H, Triumf C-A, Mattsson H, Thunehed H, Juhlin C, 2008. Geology Laxemar. Site descriptive modelling SDM-Site Laxemar. SKB R-08-54, Svensk Kärnbränslehantering AB.

Alpha angles of geological structures correlated with oriented extensive radar reflector relative to background

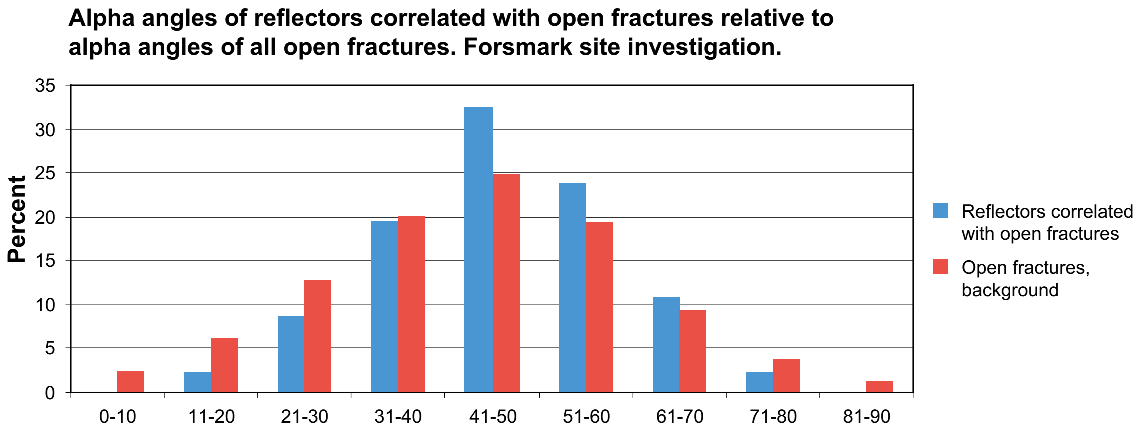

Figure A1-1. *Alpha angles of extensive oriented reflectors correlated with open fractures (n=46) relative to alpha angles of all open fractures in investigated boreholes at Forsmark (n=13 069) presented in %.*

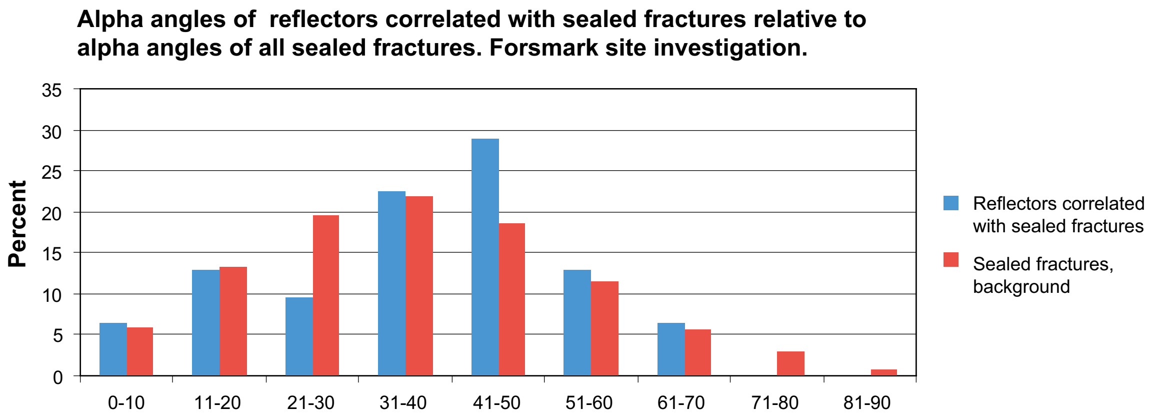

Figure A1-2. *Alpha angles of extensive oriented reflectors correlated with sealed fractures (n=31) relative to alpha angles of all sealed fractures in investigated boreholes at Forsmark (n=41 543) presented in %.*

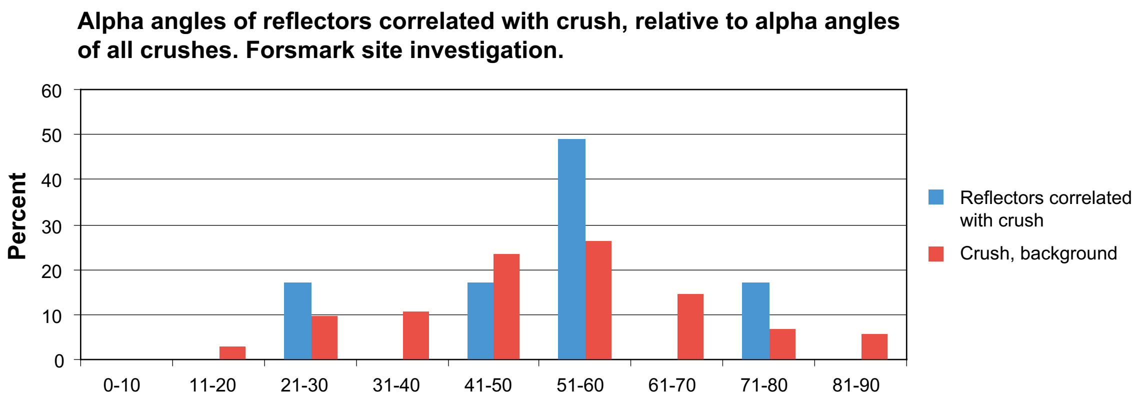

Figure A1-3. *Alpha angles of extensive oriented reflectors correlated with crush (n=6) relative to alpha angles of all crushes in investigated boreholes at Forsmark (n=103) presented in %.*

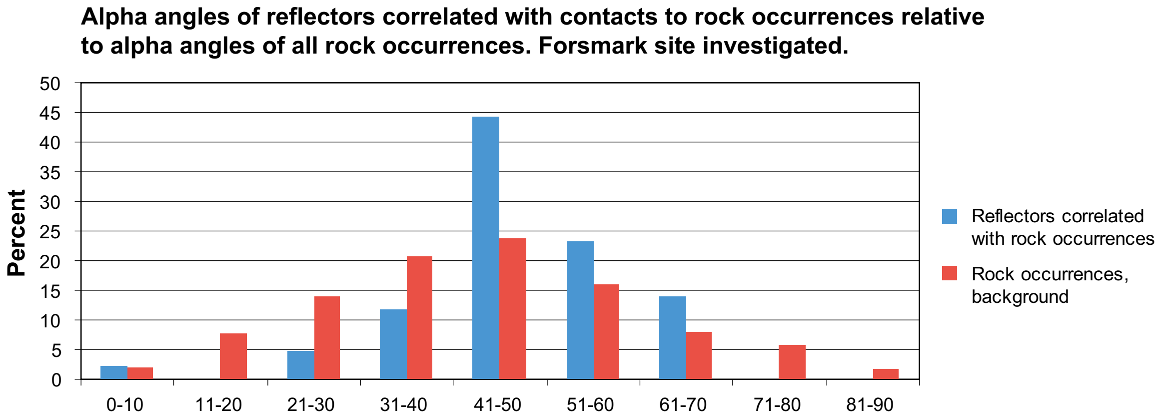

Figure A1-4. Alpha angles of extensive oriented reflectors correlated with contacts to rock occurrences (n=43) relative to alpha angles of all rock occurrences in investigated boreholes at Forsmark (n=16 676) presented in %.

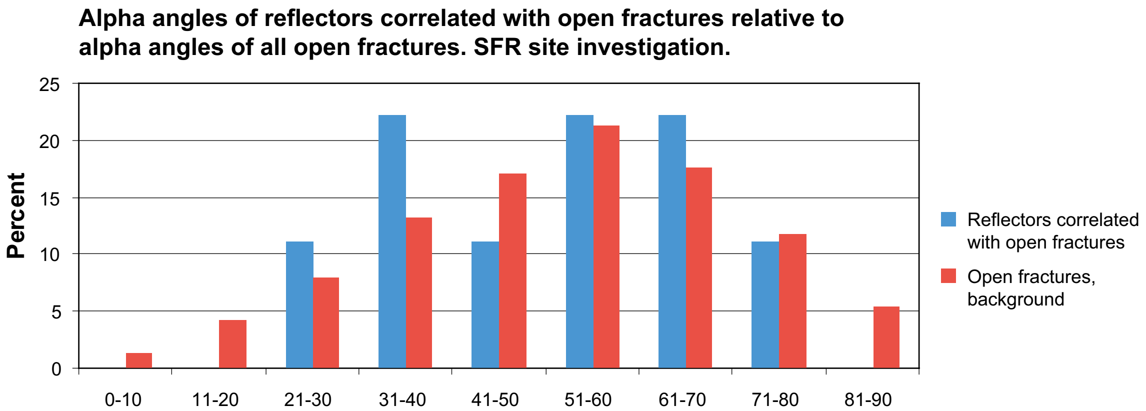

Figure A1-5. Alpha angles of extensive oriented reflectors correlated with open fractures (n=9) relative to alpha angles of all open fractures in investigated boreholes at SFR (n=6 375) presented in %.

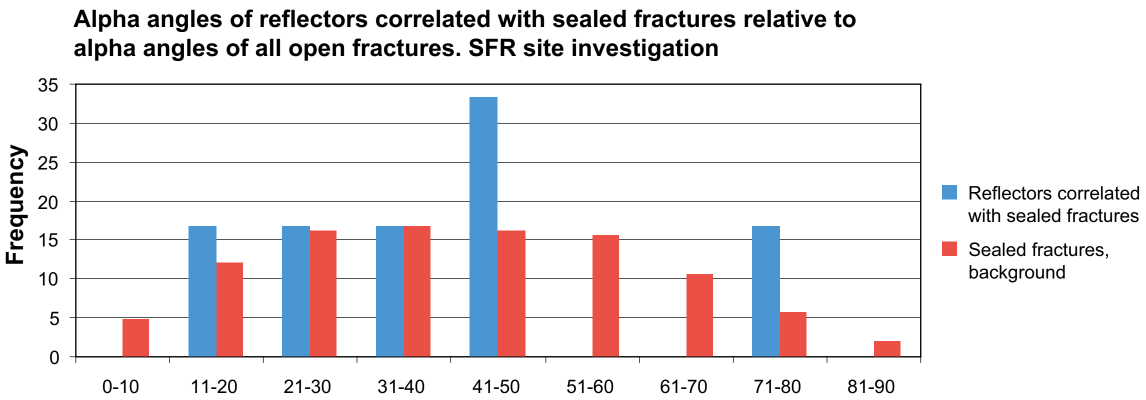

Figure A1-6. Alpha angles of extensive oriented reflectors correlated with sealed fractures (n=6) relative to alpha angles of all sealed fractures in investigated boreholes at SFR (n=11 948) presented in %.

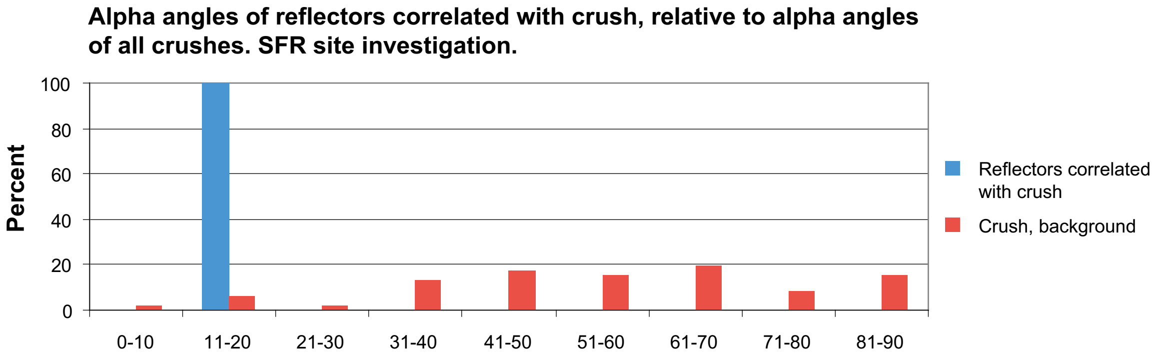

Figure A1-7. *Alpha angles of extensive oriented reflectors correlated with crush (n=1) relative to alpha angles of all crushes in investigated boreholes at SFR (n=100) presented in %.*

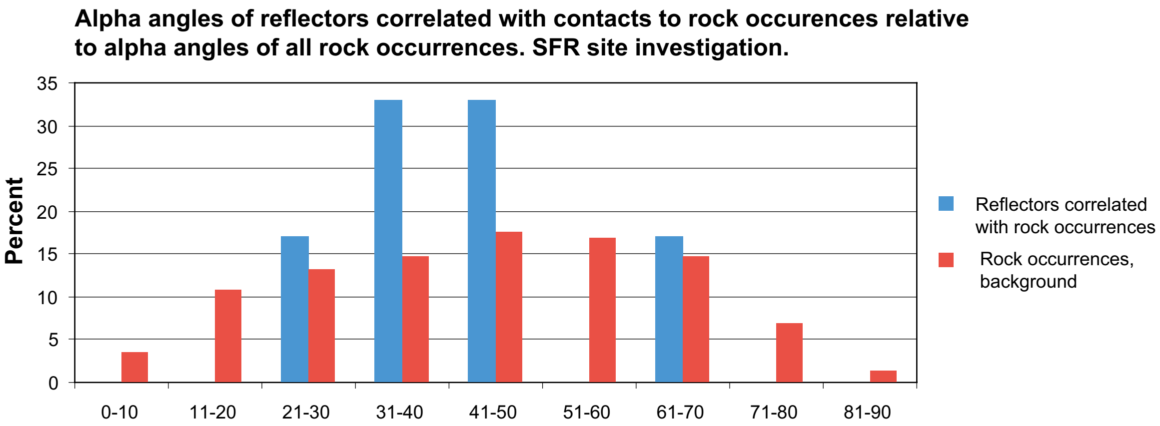

Figure A1-8. *Alpha angles of extensive oriented reflectors correlated with contacts to rock occurrences (n=6) relative to alpha angles of all rock occurrences in investigated boreholes at SFR (n=2 864) presented in %.*

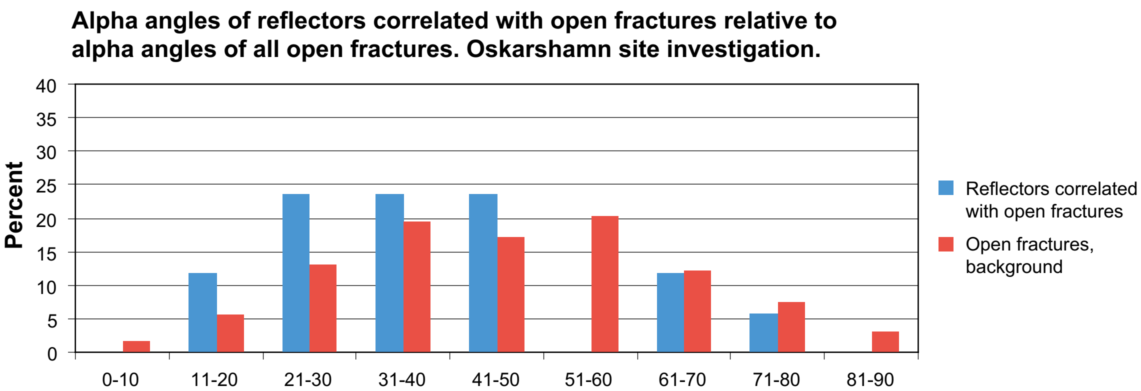

Figure A1-9. *Alpha angles of extensive oriented reflectors correlated with open fractures (n=17) relative to alpha angles of all open fractures in investigated boreholes at Oskarshamn (n=4 289) presented in %.*

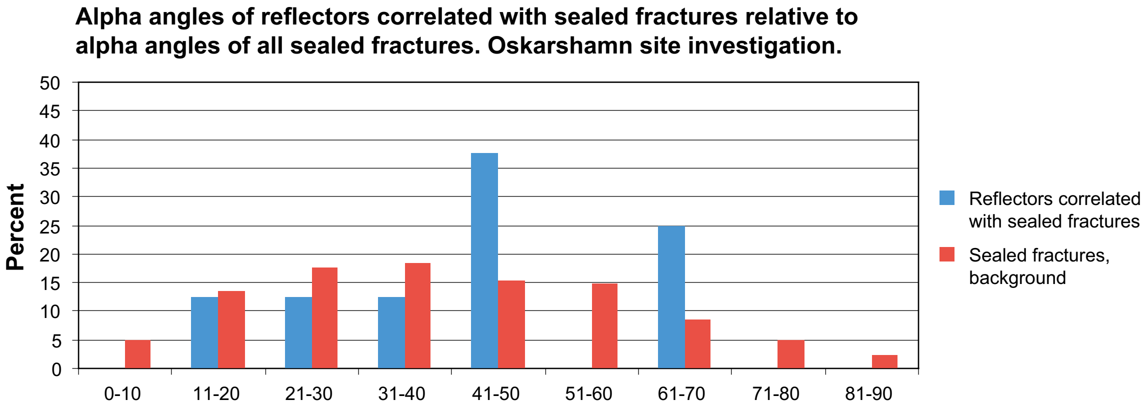

Figure A1-10. Alpha angles of extensive oriented reflectors correlated with sealed fractures (n=8) relative to alpha angles of all sealed fractures in investigated boreholes at Oskarshamn (n=7 573) presented in %.

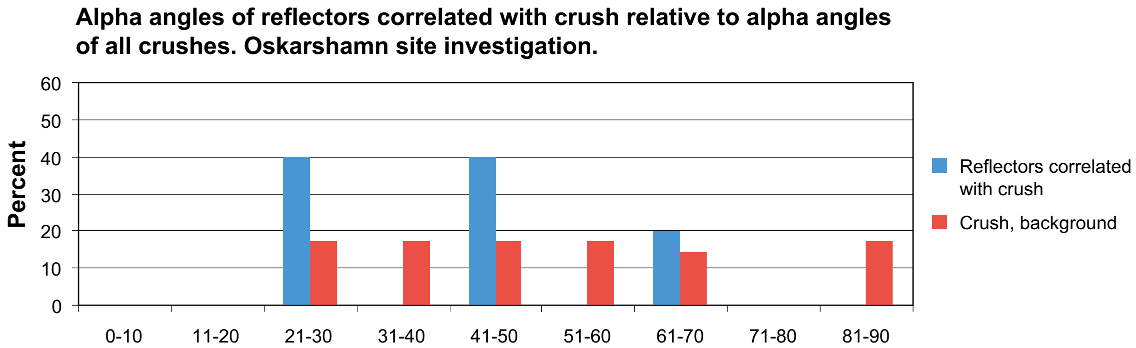

Figure A1-11. Alpha angles of extensive oriented reflectors correlated with crush (n=5) relative to alpha angles of crushes in investigated boreholes at Oskarshamn (n=35) presented in %.

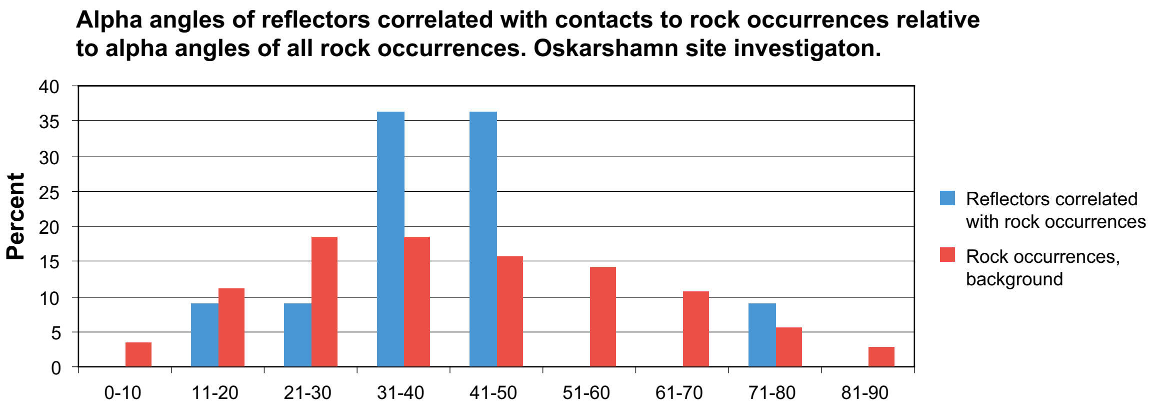

Figure A1-12. Alpha angles of extensive oriented reflectors correlated with contacts to rock occurrences (n=11) relative to alpha angles of all rock occurrences in investigated boreholes at Oskarshamn (n=1 288) presented in %.

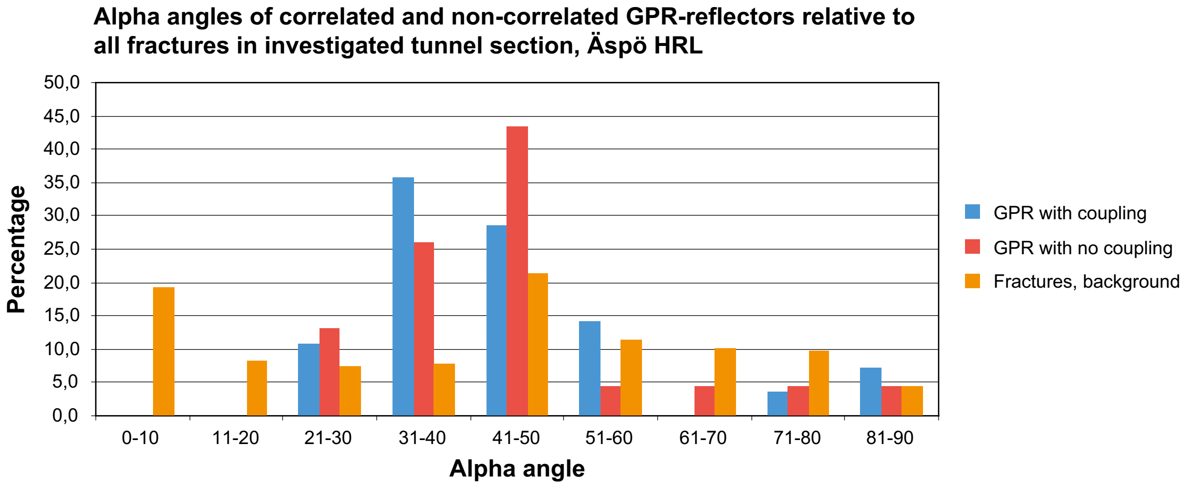

Figure A1-13. *Distribution of GPR alpha angles correlated with geology/not correlated with geology relative to alpha angles of fractures in the investigated tunnel sections (measured as angle to tunnel mid-line). Number of data with correlated GPR-reflectors is 28, non-correlated GPR-reflectors: 23, and all fractures in investigated tunnel section: 228.*

Stereographic projections showing oriented extensive radar reflectors in relation to main rock structures, Forsmark Site Investigation

Stereographic projections are on Schmidt net, lower hemisphere. Orientation data are poles to planes. Conventional contouring according to percentages. Non-weighted in-data.

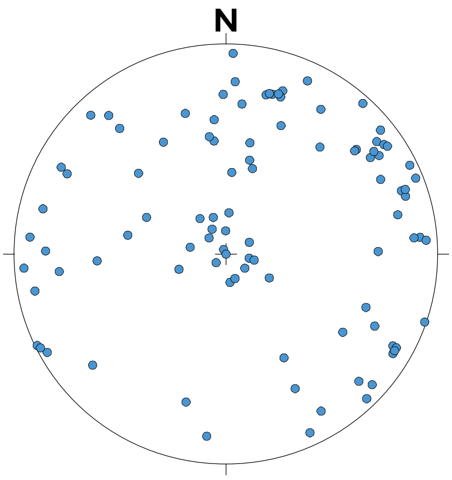

Figure A2a-1. *Oriented extensive radar reflectors that have been correlated confidently with mapped geology in KFM-boreholes (n=96, of which 1* may have two possible directions).*

* All poles to extensive radar reflector planes which are confidently correlated with geological structures are plotted.

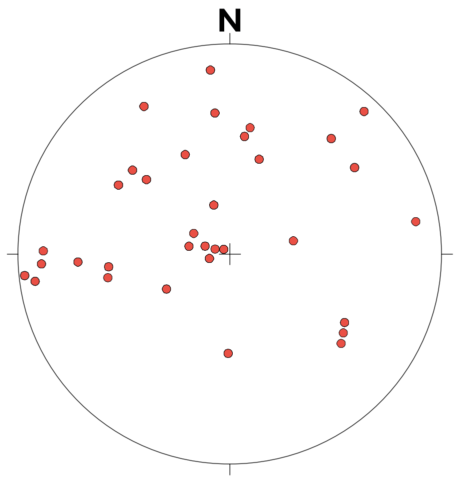

Figure A2a-2. *Oriented extensive radar reflectors that have not been confidently correlated with mapped geology in KFM-boreholes (n=26, of which 8** have two possible directions).*

** All poles to extensive radar reflector planes which are not confidently correlated with geological structures are plotted.

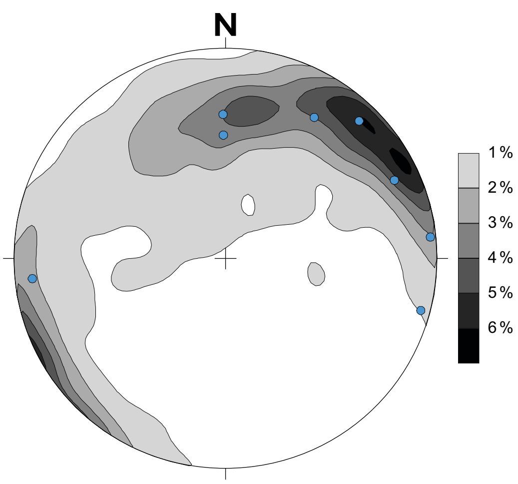

Figure A2a-3. *Contoured orientations of rock contacts (n=1 619) in KFM-boreholes. ● =Rock contacts correlated with oriented extensive radar reflector (n=8)*

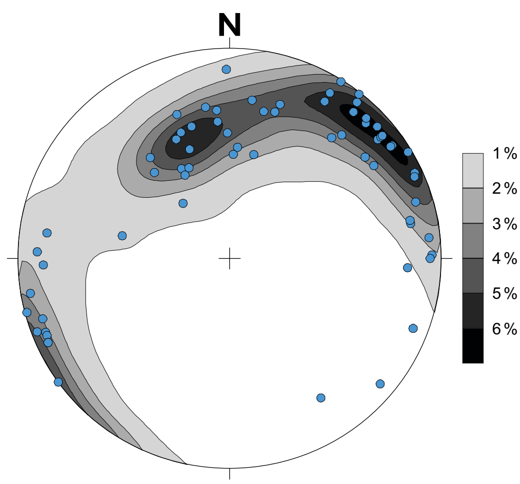

Figure A2a-4. *Contoured orientations of minor rock occurrences (n=16 676, upper contacts) in KFM-boreholes. ● =upper contacts to rock occurrences correlated with oriented extensive radar reflector (n=67).*

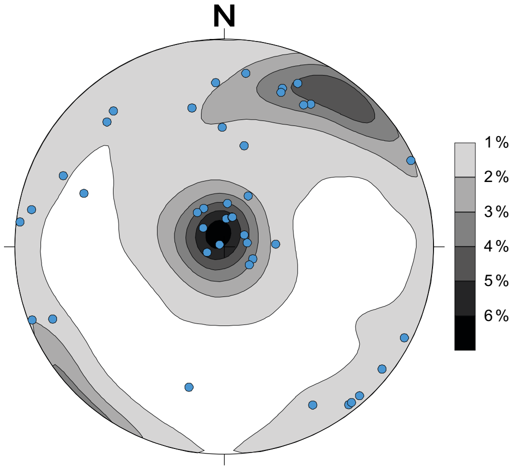

Figure A2a-5. *Contoured orientations of open fractures (n=13 069) in KFM-boreholes.* ● *=Open fractures correlated with oriented extensive radar reflectors (n=43).*

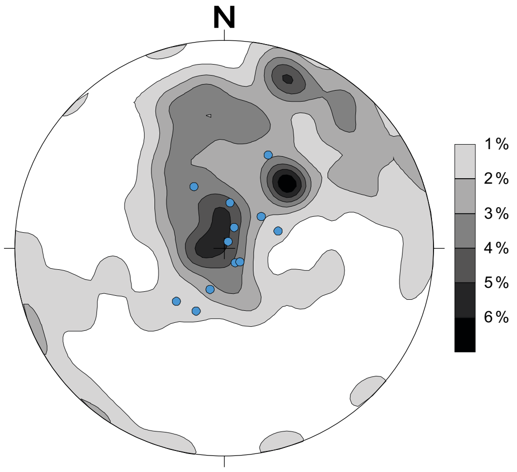

Figure A2a-6. *Contoured orientations of crushes in KFM-boreholes, both upper and lower contacts (n=204).* ● *=Crushes correlated with oriented extensive radar reflector (n=6, both upper and lower contacts).*

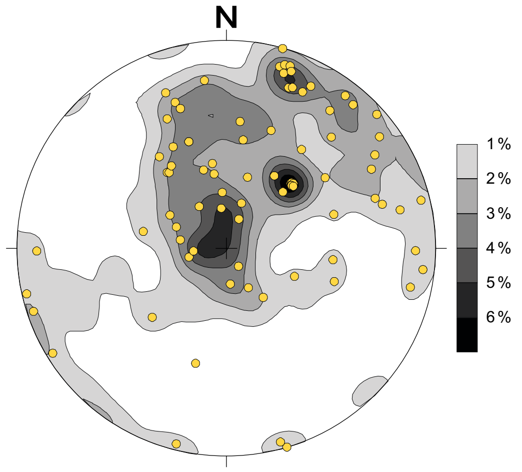

Figure A2a-7. *Contoured orientations of crushes in KFM-boreholes*, both upper and lower contacts (n=204).* ● *=crushes that have not been detected by borehole radar (n=44, both upper and lower contacts).*

* Crushes with possible long/short oriented radar reflectors or non-oriented radar reflectors are not encountered.

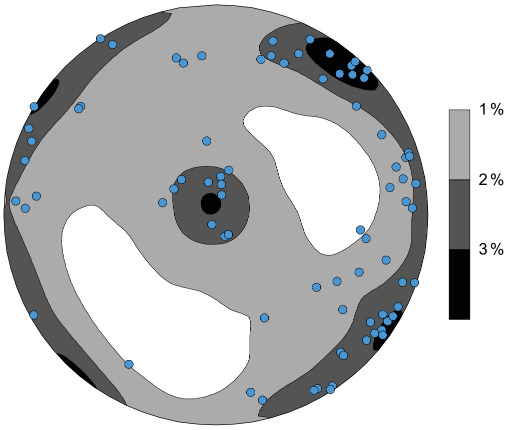

Figure A2a-8. *Contoured orientations of sealed fractures (n=41 543) in KFM-boreholes. ●=Sealed fractures correlated with oriented extensive radar reflector (n=80).*

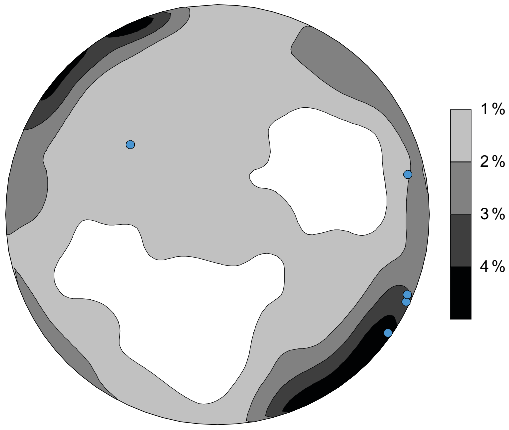

Figure A2a-9. *Contoured orientations of sealed fracture networks (n=1 740, Strike3Dip3-values) in KFM-boreholes. ●=Sealed fracture networks correlated with oriented extensive radar reflector (n=5).*

Stereographic projections showing oriented extensive radar reflectors in relation to main rock structures, SFR Site Investigation

Stereographic projections are on Schmidt net, lower hemisphere. Orientation data are poles to planes. Conventional contouring according to percentages. Non-weighted in-data.

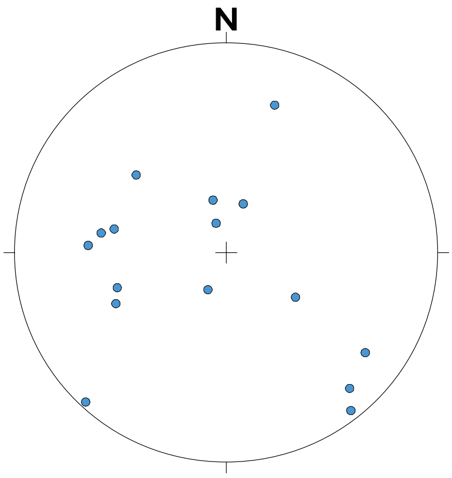

Figure A2b-1. Oriented extensive radar reflectors that have been confidently correlated with mapped geology in KFR-boreholes (n=15, of which one have two possible orientations).*

* All poles to extensive radar reflector planes which are confidently correlated with geological structures are plotted.

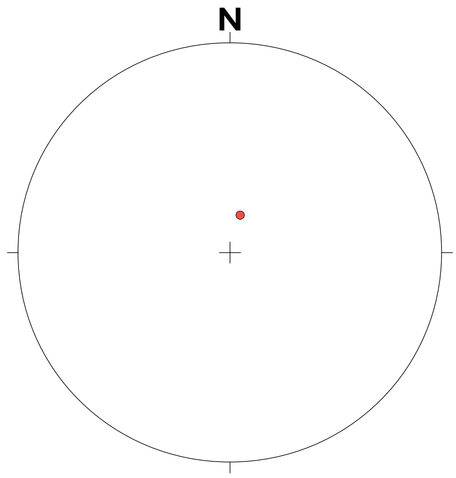

Figure A2b-2. Oriented extensive radar reflectors that have not been confidently correlated with mapped geology in KFR-boreholes (n=1). Reflectors outside range of core mapping are excluded.

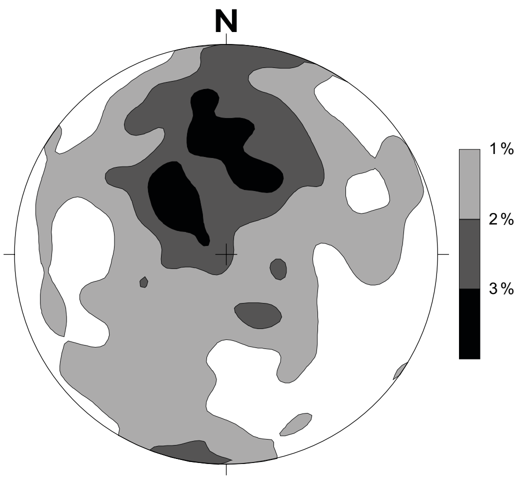

Figure A2b-3. Contoured orientations of rock contacts (n=331) in KFR-boreholes. No major rock contact is confidently correlated with any extensive radar reflector.

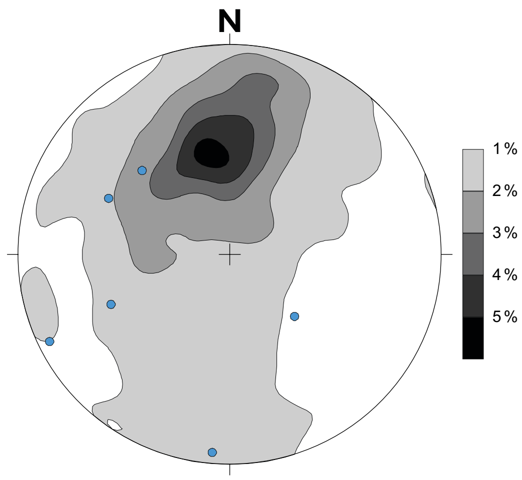

Figure A2b-4. Contoured orientations of minor rock occurrences in KFR-boreholes (n=2 860, upper contacts). ●=Minor rock contacts correlated with oriented extensive radar reflector (n=6).

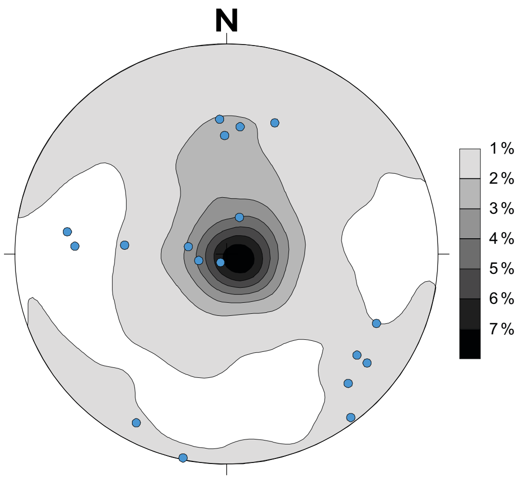

Figure A2b-5. *Contoured orientations of open fractures (n=6 831) in KFR-boreholes. ●=Open fractures and partly open fractures correlated with extensive oriented radar reflectors (n=18).*

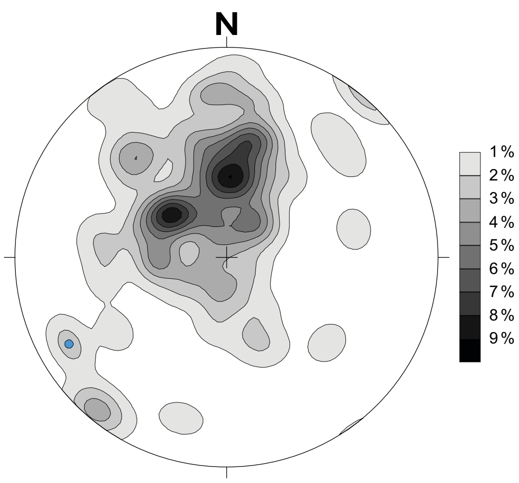

Figure A2b-6. *Contoured orientations of crushes in KFR-boreholes, both upper and lower contacts (n=92). ●=Crush correlated with extensive oriented radar reflector (n=1).*

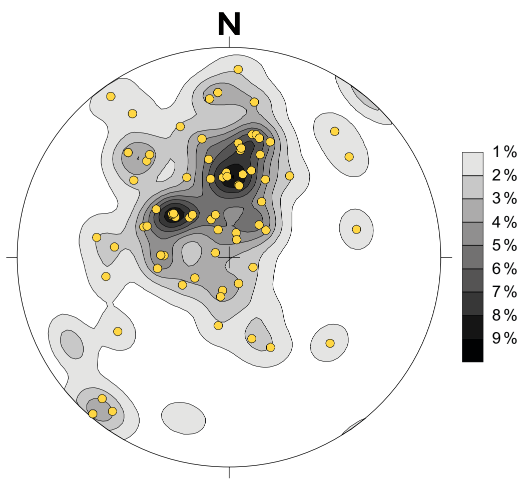

Figure A2b-7. *Contoured orientations of crushes in KFR-boreholes, both upper and lower contacs (n=92). ●=crushes that have not been detected by borehole radar* (n=40, both upper and lower contacts).*

* Crushes with possible long/short oriented radar reflectors or non-oriented radar reflectors are not encountered.

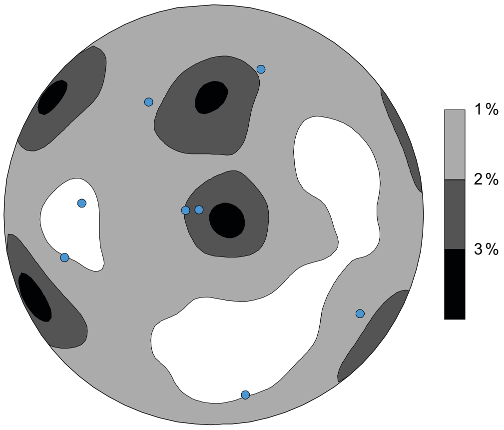

Figure A2b-8. Contoured orientations of sealed fractures (n=11 483) in KFR-boreholes. ●=Sealed fractures correlated with extensive oriented radar reflector (n=8).

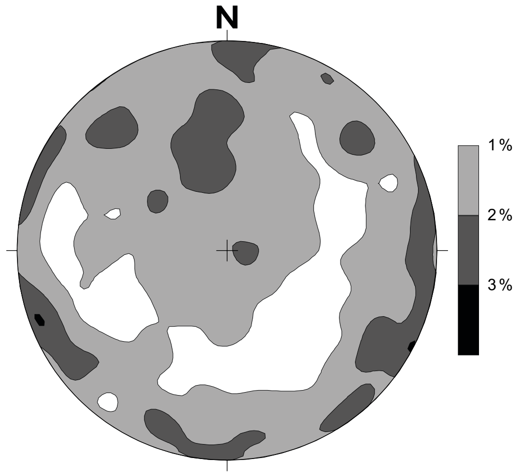

Figure A2b-9. Contoured orientations of sealed fracture networks (n=393, Strike3Dip3-values) in KFR-boreholes. No sealed fracture network is confidently correlated with any extensive radar reflector.

Stereographic projections showing oriented extensive radar reflectors in relation to main rock structures, Oskarshamn Site Investigation

Stereographic projections are on Schmidt net, lower hemisphere. Orientation data are poles to planes. Conventional contouring according to percentages. Non-weighted in-data.

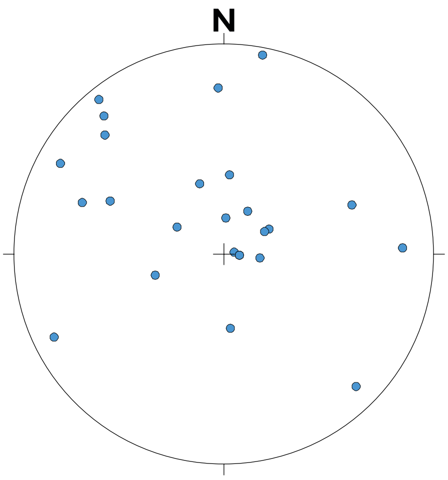

***Figure A2c-1.** Oriented extensive radar reflectors that have been confidently correlated with mapped geology in KLX-boreholes (n=22, of which 3 have two possible orientations*)*

* All poles to extensive radar reflector planes which are confidently correlated with geological structures are plotted.

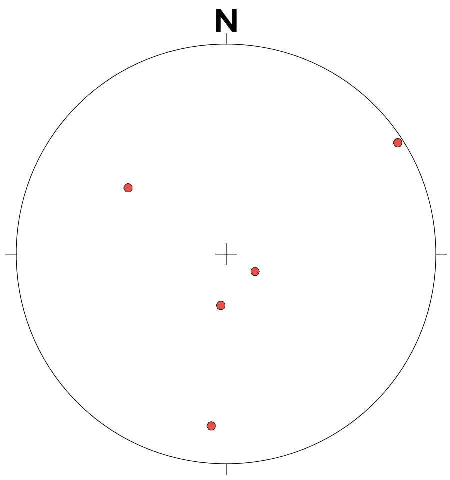

Figure A2c-2.** Oriented extensive radar reflectors that have not been confidently correlated with mapped geology in KLX-boreholes (n=5).

** If one of the interpreted reflector orientations is confidently correlated with a geological structure the other interpreted orientation is not encountered in this diagram.

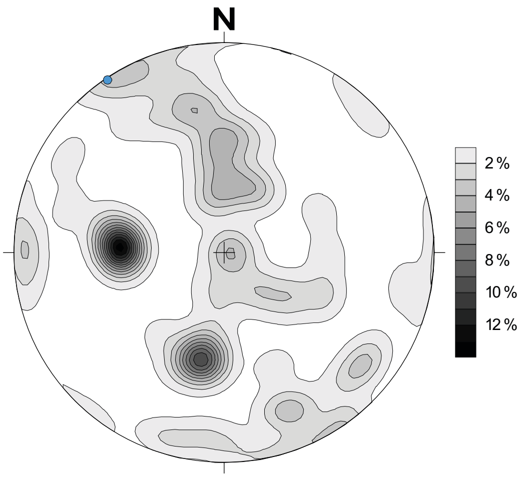

***Figure A2c-3.** Contoured orientations of rock contacts (n=99) in KLX-boreholes. ●=Rock contact correlated with oriented extensive radar reflector (n=1).*

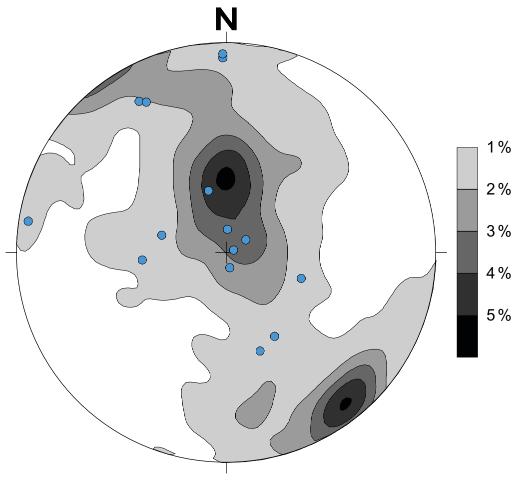

***Figure A2c-4.** Contoured orientations of minor rock occurrences in KLX-boreholes (n=1 288, upper contacts). ●=Minor rock occurrences correlated with extensive radar reflector (n=15).*

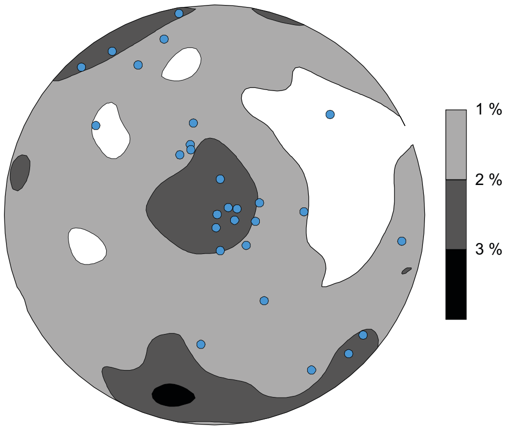

Figure A2c-5. *Contoured orientations of open fractures (n=4 129) in KLX-boreholes.* ● *=Open fractures correlated with oriented extensive radar reflector (n=28).*

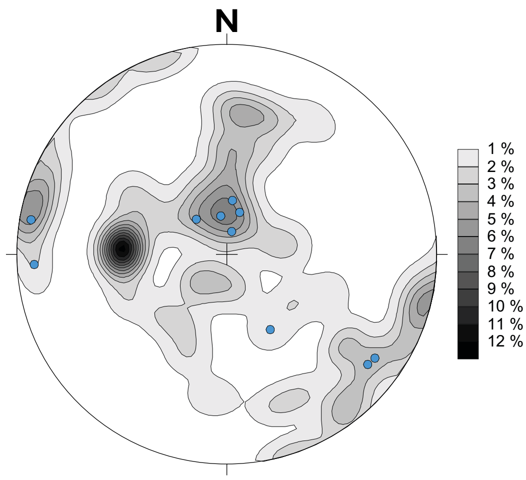

Figure A2c-6. *Contoured orientations of crushes in KLX-boreholes, both upper and lower contacts (n=71).* ● *=Crushes correlated with oriented extensive radar reflector (n=5, both upper and lower contacts plotted).*

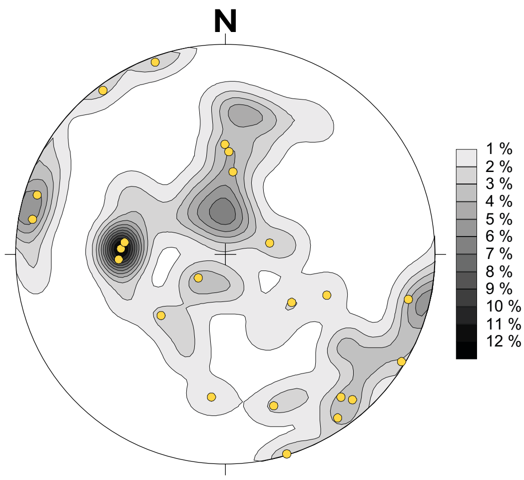

Figure A2c-7. *Contoured orientations of crushes in KLX-boreholes, both upper and lower contacs (n=71).* ● *=crushes that have not been detected by borehole radar* (n=23, of which 14 are oriented, both upper and lower contacts).*

* Crushes / open fractures with apertures ≥ 1 mm with possible long/short oriented radar reflectors or non-oriented radar reflectors are not encountered.

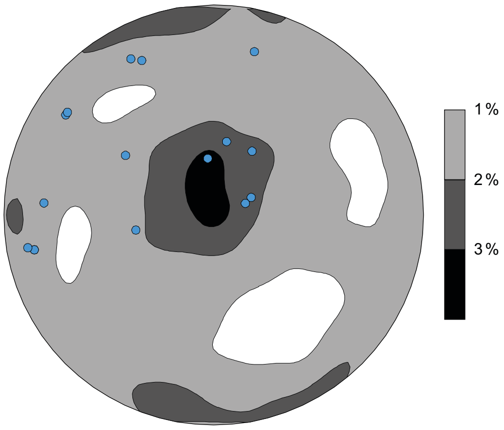

Figure A2c-8. *Contoured orientations of sealed fractures (n=7 733) in KLX-boreholes. ●=Sealed fractures correlated with oriented extensive radar reflector (n=16).*

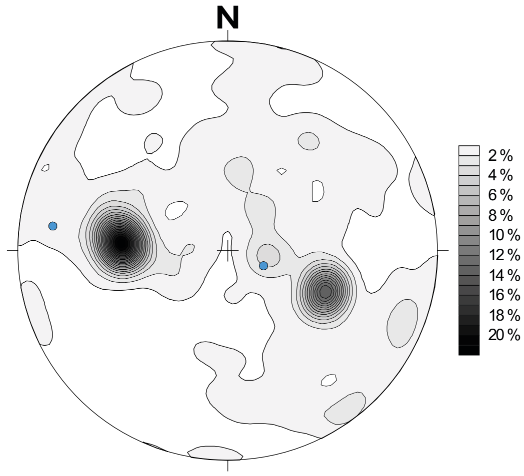

Figure A2c-9. *Contoured orientations of sealed fracture networks (n=175, Strike3Dip3-values) in KLX-boreholes. ●=Sealed fracture networks correlated with oriented extensive radar reflector (n=2).*

Stereographic projections showing oriented extensive borehole radar reflectors in relation to main rock structures, Äspö hard rock laboratory

Stereographic projections are on Schmidt net, lower hemisphere. Orientation data are poles to planes. Conventional contouring according to percentages. Non-weighted in-data.

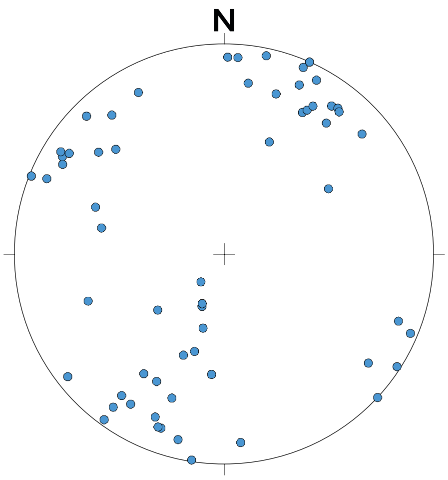

Figure A2d-1. *Oriented extensive borehole radar reflector which have been confidently correlated with tunnel mapping (n=63).*

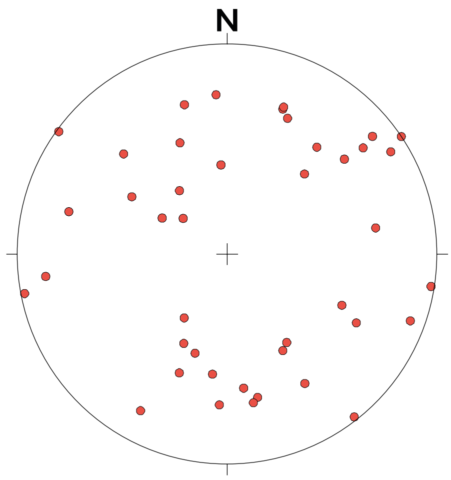

Figure A2d-2. *Oriented extensive borehole radar reflector which have not been confidently correlated with tunnel mapping (n=42)*

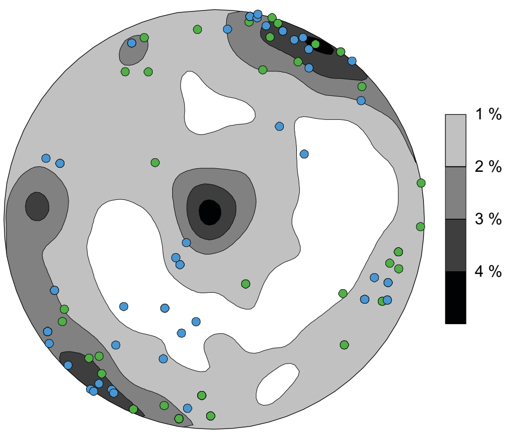

Figure A2d-3. *Contoured fracture orientations (n=2 919) in investigated tunnel sections, Äspö. Fractures correlated with oriented extensive borehole radar reflector with high confidence (●, n=48) and with medium confidence (●, n=57).*

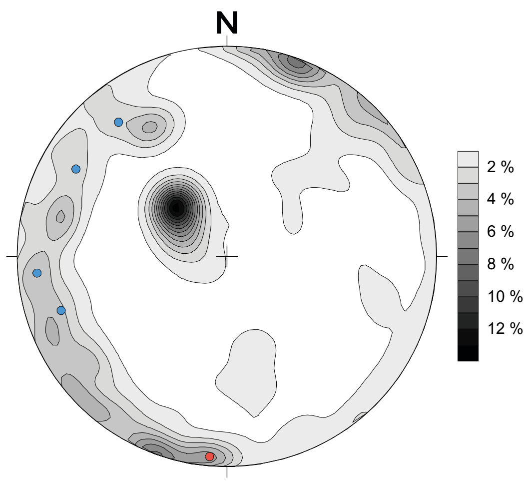

Figure A2d-4. *Contoured zone orientations* (n=228) in investigated tunnel sections. ●=Fracture zones correlated with oriented extensive borehole radar (n=4). ●=Fracture zones not correlated with oriented extensive borehole radar (n= 1).*

* Several orientation measurements from the same zone are encountered.

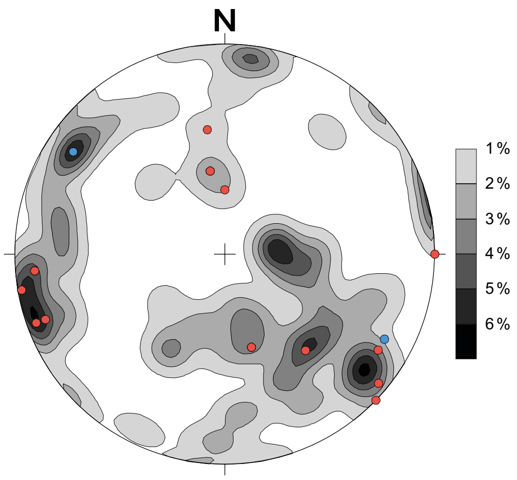

Figure A2d-5. *Contoured rock contact orientations (n=95) in investigated tunnel sections, Äspö. ●=Rock contacts correlated with oriented extensive borehole radar (n=2). ●=Rock contacts not correlated with borehole radar (n= 18).*

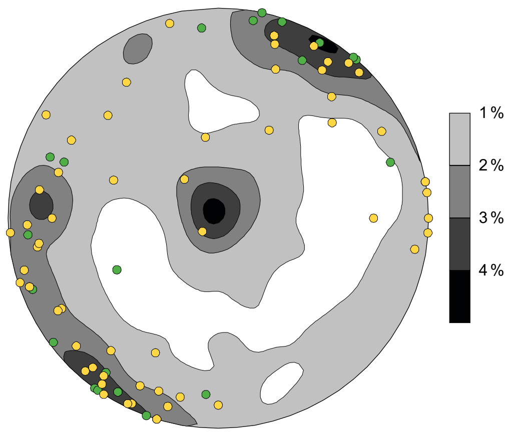

Figure A2d-6. *Contoured fracture orientations (n=2 919) in investigated tunnel sections, Äspö. ●=FPI- fractures (Full Perimeter Intersection) which have not been detected by extensive borehole radar (n=58). ●=FPI-fracture which have been detected by extensive oriented borehole radar (n=25).*

Stereographic projections showing GPR reflectors in relation to main rock structures, Äspö hard rock laboratory

Stereographic projections are on Schmidt net, lower hemisphere. Orientation data are poles to planes. Conventional contouring according to percentages. Non-weighted in-data.

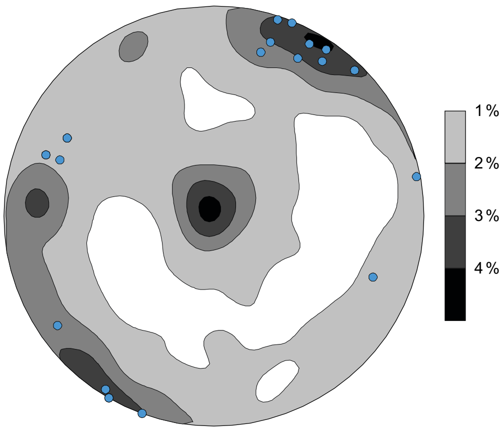

Figure A2e-1. *Contoured fracture orientations (n=2 919) in investigated tunnel sections*, Äspö. ●=fracture correlated with GPR-reflector (n=21).*

* Tunnel sections investigated by borehole radar are also included.

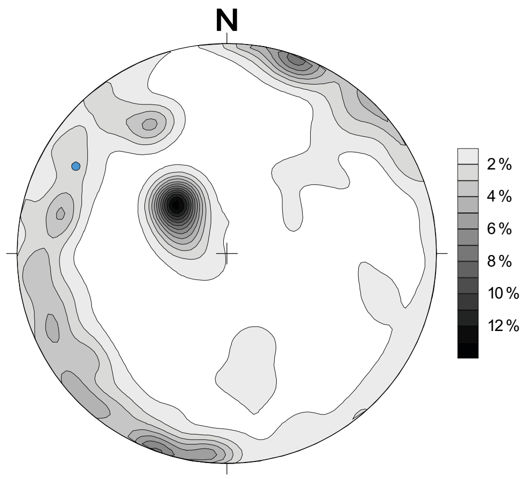

Figure A2e-2. *Contoured zone orientations (n=228) in investigated tunnel sections*. ●=fracture zone correlated with GPR-reflector (n=1). Only one fracture zone exists in the tunnel sections measured with GPR.*

* Tunnel sections investigated by borehole radar are also included.

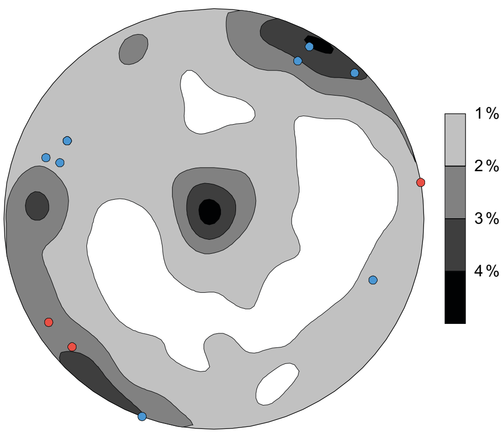

Figure A2e-3. *Contoured fracture orientations (n=2 919) in investigated tunnel sections*, Äspö. ●=FPI-fracture** correlated with GPR-reflector (n=9). ●=FPI-fracture** which has not been correlated with GPR-reflector (n=3).*

* Tunnel sections investigated by borehole radar are also included.

** FPI-fracture = Full Perimeter Intersection fracture, which means it crosscut's the tunnel wall.

NOTE! Orientation data is missing for most rock contacts in the TMS-database in the investigated tunnel section and therefore no stereographic plots of correlated rock contacts were created.

Appendix 3a

Mineralogy in fractures and crushes with oriented extensive radar reflectors relative to background presented in diagrams

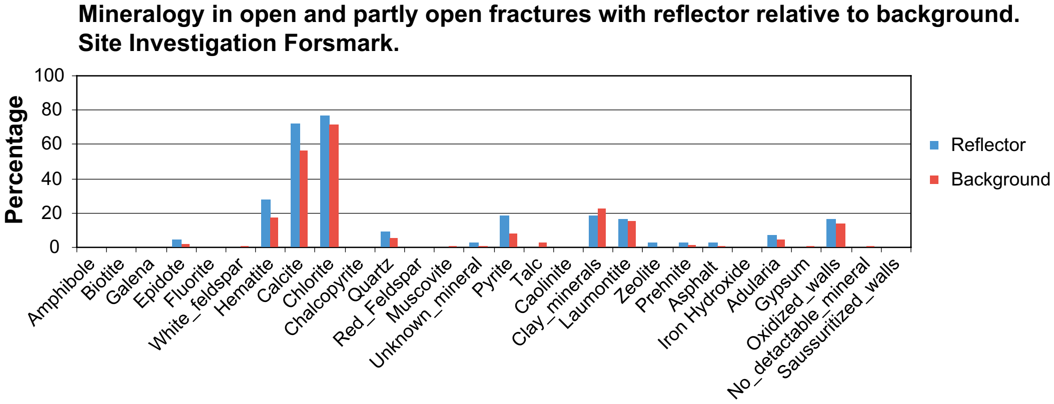

Figure A3a-1. *Mineralogy in open and partly open fractures with extensive oriented radar reflector (n=43) relative to background (n=13 160), displayed as % of all fractures with the mineral in question. Non-weighted data.*

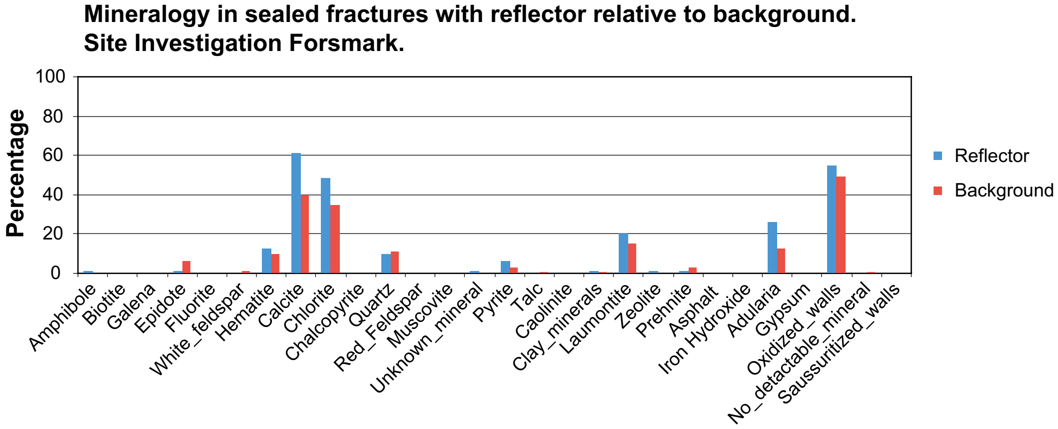

Figure A3a-2. *Mineralogy in sealed fractures with extensive oriented radar reflector (n=80) relative to background (n=41 732), displayed as % of all fractures with the mineral in question. Non-weighted data.*

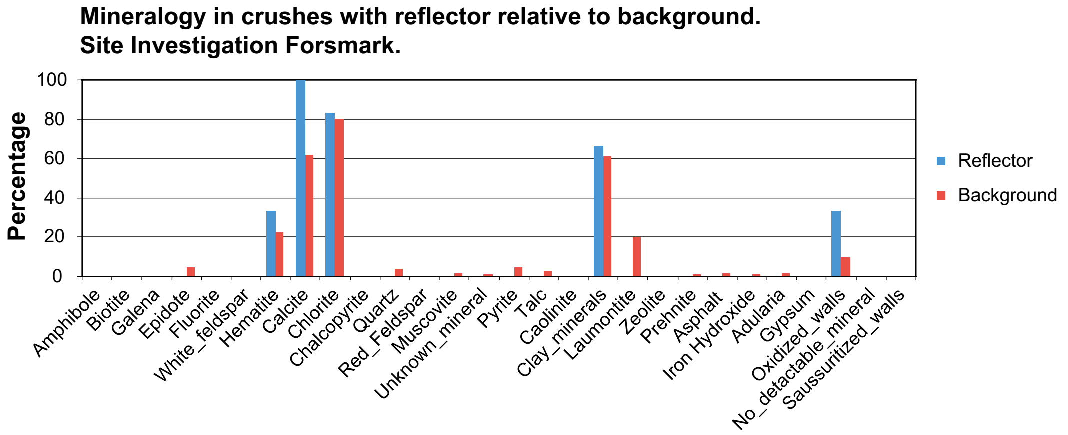

Figure A3a-3. *Mineralogy in crushes with extensive oriented radar reflector (n=6) relative to background (n=103), displayed as % of all fractures with the mineral in question. Note the very few crushes with reflector. Non-weighted data.*

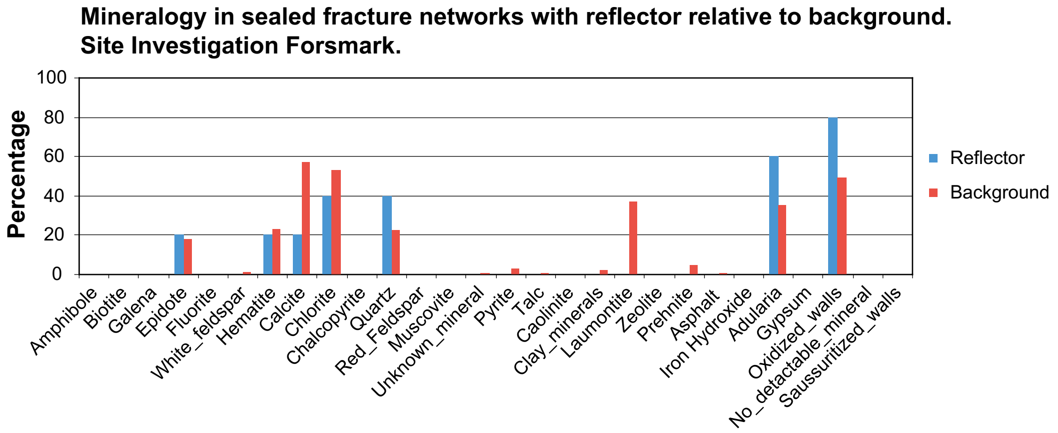

Figure A3a-4. *Mineralogy in sealed networks with extensive oriented radar reflector (n=5) relative to background (n=1 818), displayed as % of all fractures with the mineral in question. Note the very few sealed networks with reflector. Non-weighted data.*

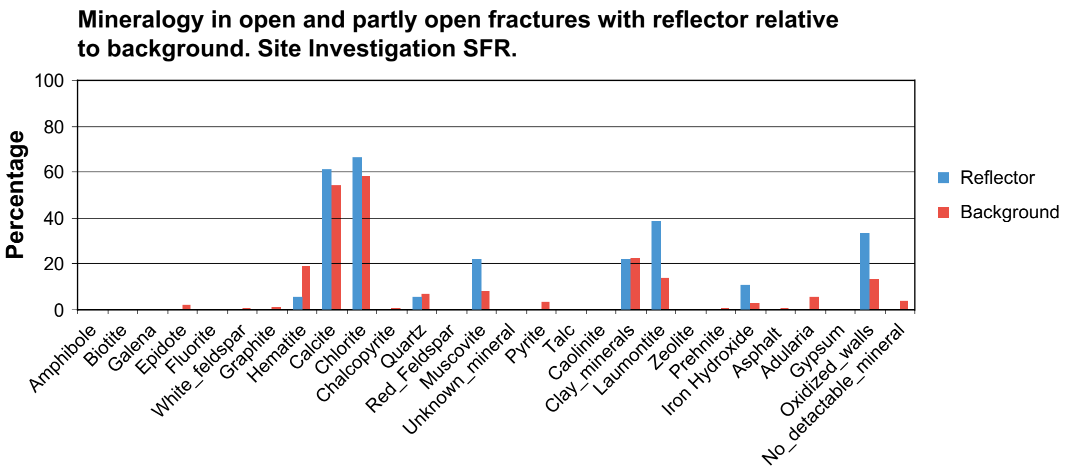

Figure A3a-5. *Mineralogy in open and partly open fractures with extensive oriented radar reflector (n=18) relative to background (n=6 909), displayed as % of all fractures with the mineral in question. Non-weighted data.*

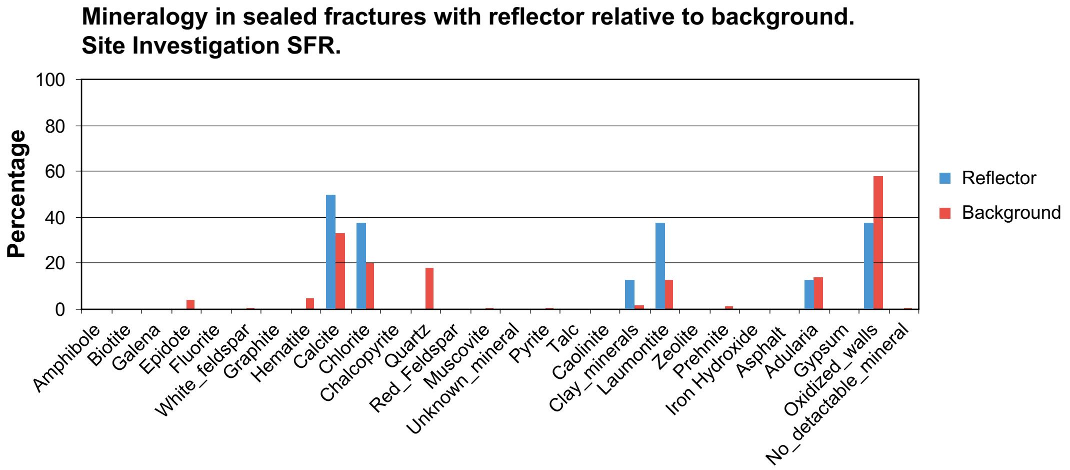

Figure A3a-6. *Mineralogy in sealed fractures with extensive oriented radar reflector (n=8) relative to background (n=11 605), displayed as % of all fractures with the mineral in question. Non-weighted data.*

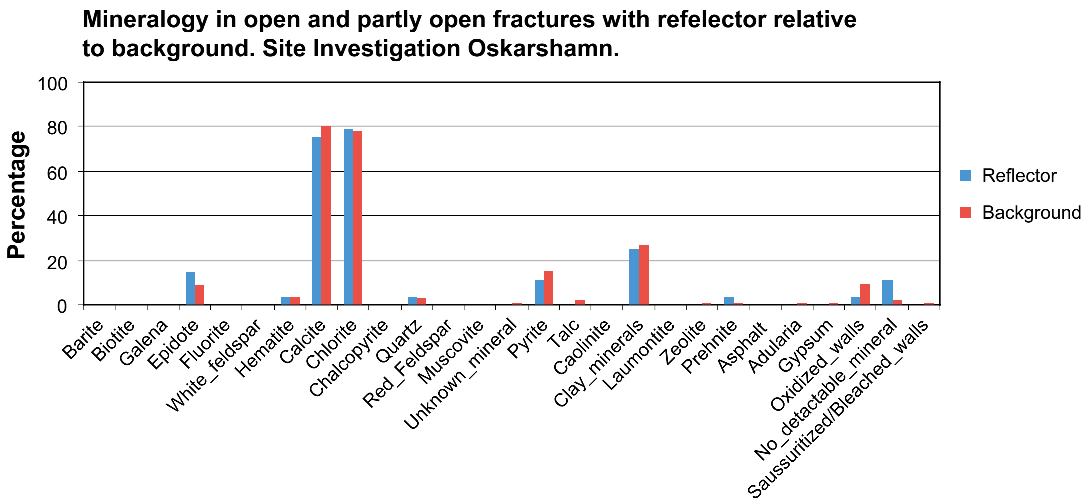

Figure A3a-7. *Mineralogy in open and partly open fractures with extensive oriented radar reflector (n=28) relative to background (n=4 211), displayed as % of all fractures with the mineral in question. Non-weighted data.*

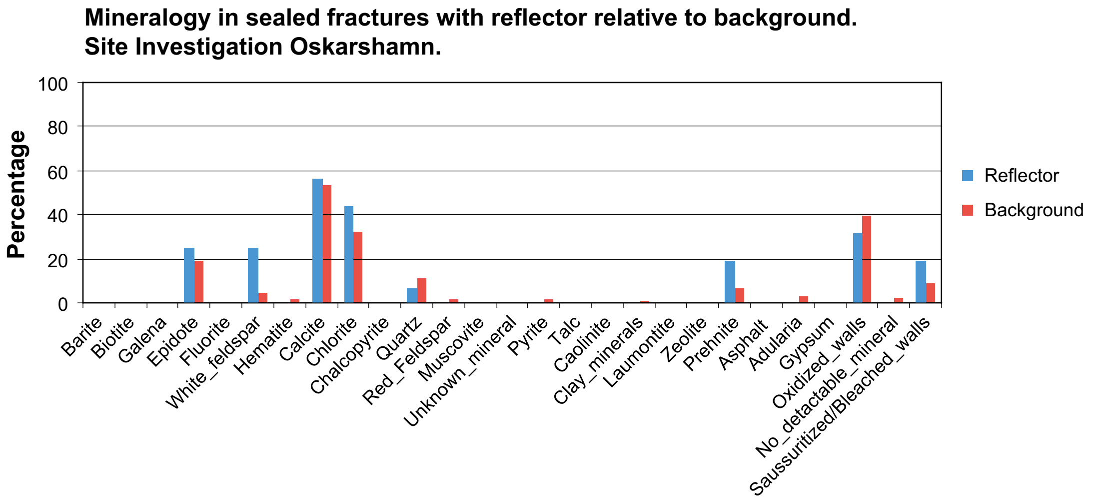

Figure A3a-8. *Mineralogy in sealed fractures with extensive oriented radar reflector (n=16) relative to background (n=7 759), displayed as % of all fractures with the mineral in question. Non-weighted data.*

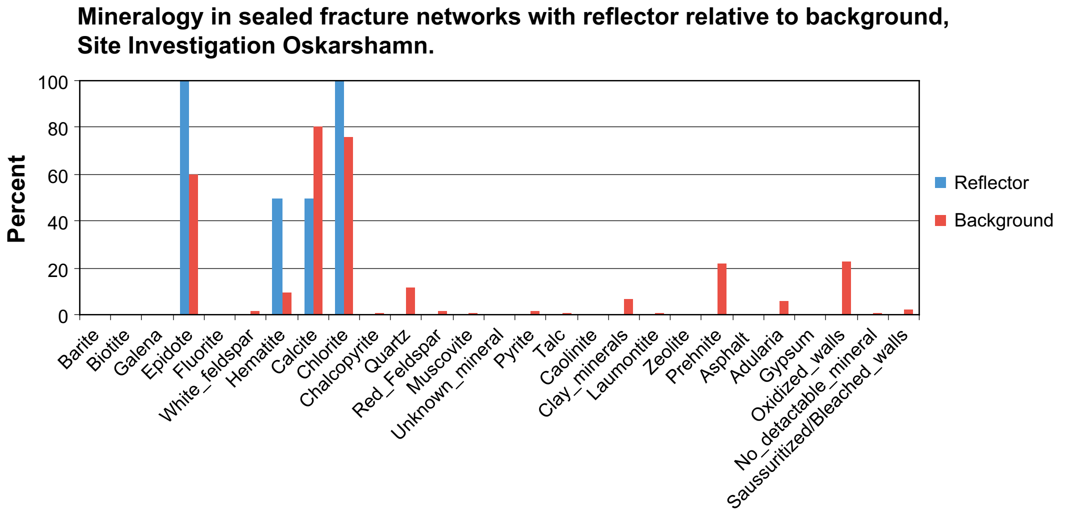

Figure A3a-9. *Mineralogy in sealed fracture networks with extensive oriented radar reflector (n=2) relative to background (n=258), displayed as % of all fractures with the mineral in question. Note the very few amount of reflectors. Non-weighted data.*

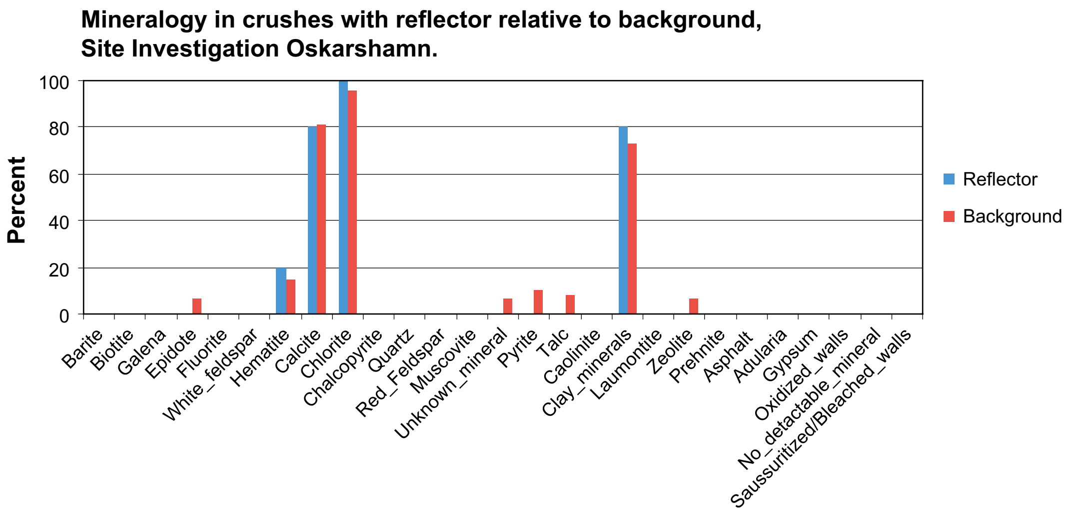

Figure A3a-10. *Mineralogy in crushes with extensive oriented radar reflector (n=5) relative to background (n=48), displayed as % of all fractures with the mineral in question. Note the very few amount of reflectors. Non-weighted data.*

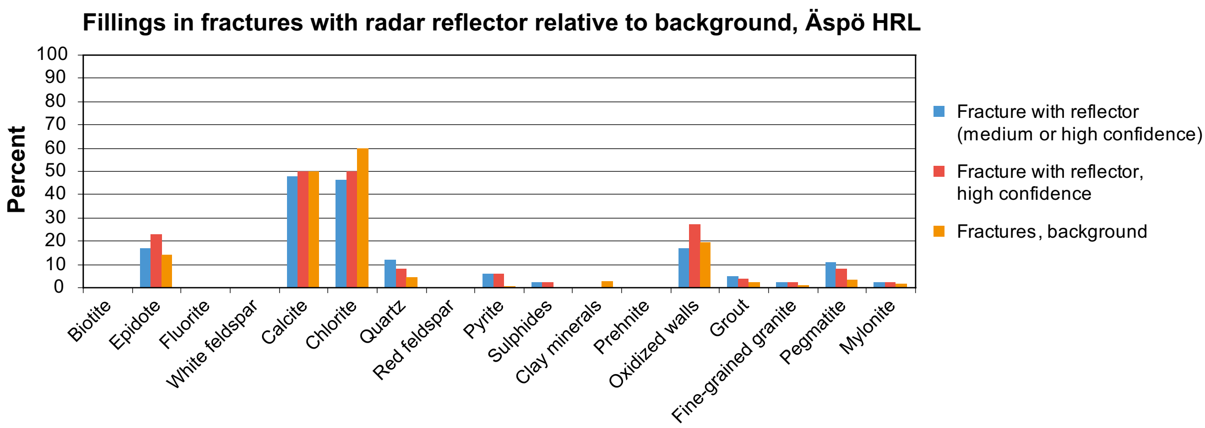

Figure A3a-11. *Fillings in fractures with radar reflector relative to background, Äspö Hard Rock Laboratory. Number of data: ■=105, ■=48, ■=2 403. Non-weighted data.*

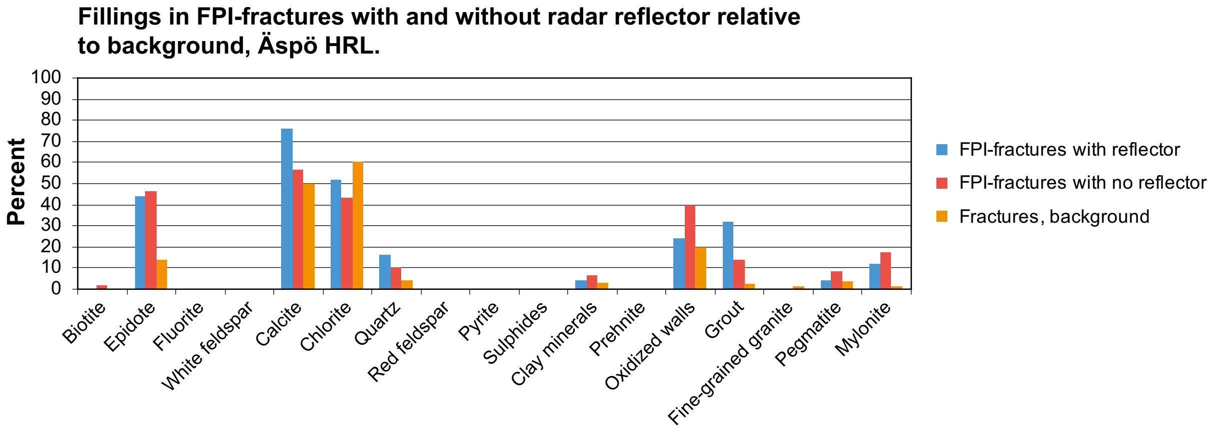

Figure A3a-12. *Fillings in FPI fractures with radar reflector relative to background (all mapped fractures within the investigated tunnel sections). Äspö Hard Rock Laboratory. Number of data: ■=25 ■=58 ■=2 403. Non-weighted data.*

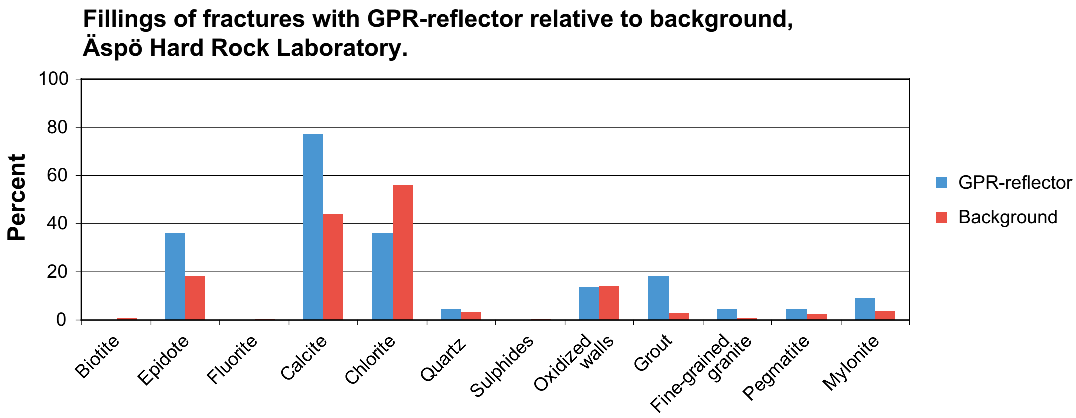

Figure A3a-13. *Fillings of fractures with GPR-reflector (n=22) relative to background (n=228), Äspö Hard Rock Laboratory. Non-weighted data.*

Mineralogy in fractures with oriented extensive radar reflector relative to background presented in tables

Table A3b-1. Mineral occurrences in fractures with extensive radar reflector relative to background, Site investigation Forsmark (%). Non-weighted data.

Forsmark	All	Open and partly open		Sealed		Sealed fracture networks			Crush
Mineral	Reflector (n=134)	Reflector (n=43)	Background (n=13160)	Reflector (n=80)	Background (n=41732)	Reflector (n=5)	Background (n=1818)	Reflector (n=6)	Background (n=103)
Amphibole	1	0	0	1	0	0	0	0	0
Biotite	0	0	0	0	0	0	0	0	0
Galena	0	0	0	0	0	0	0	0	0
Epidote	3	5	2	1	6	20	18	0	5
Fluorite	0	0	0	0	0	0	0	0	0
White_feldspar	0	0	1	0	1	0	1	0	0
Hematite	19	28	17	13	10	20	23	33	22
Calcite	65	72	56	61	40	20	57	100	62
Chlorite	59	77	72	49	35	40	53	83	81
Chalcopyrite	0	0	0	0	0	0	0	0	0
Quartz	10	9	6	10	11	40	22	0	4
Red_Feldspar	0	0	0	0	0	0	0	0	0
Muscovite	0	0	1	0	0	0	0	0	2
Unknown_mineral	1	2	1	1	0	0	0	0	1
Pyrite	10	19	8	6	3	0	3	0	5
Talc	0	0	3	0	0	0	0	0	3
Caolinite	0	0	0	0	0	0	0	0	0
Clay_minerals	10	19	23	1	1	0	2	67	61
Laumontite	17	16	15	20	15	0	37	0	20
Zeolite	1	2	0	1	0	0	0	0	0
Prehnite	1	2	1	1	3	0	5	0	1
Asphalt	1	2	1	0	0	0	0	0	2
Iron Hydroxide	0	0	0	0	0	0	0	0	1
Adularia	20	7	5	26	13	60	35	0	2
Gypsum	0	0	1	0	0	0	0	0	0
Oxidized_walls	43	16	14	55	49	80	49	33	10
No_detactable_mineral	0	0	0	0	0	0	0	0	0
Saussuritized_walls	0	0	0	0	0	0	0	0	0

Table A3b-2. Mineral occurrences in fractures with extensive radar reflector relative to background, Site investigation SFR (%). Non-weighted data.

SFR	All	Open and partly open		Sealed		Sealed fracture networks		Crush	
Mineral	Reflector (n=26)	Reflector (n=18)	Background (n=6909)	Reflector (n=8)	Background (n=11605)	Reflector (n=0)	Background (n=412)	Reflector (n=1)	Background (n=47)
Amphibole	0	0	0	0	0	0		–	0
Biotite	0	0	0	0	0	0		–	0
Galena	0	0	0	0	0	0		–	0
Epidote	0	0	2	0	4	–17		–	4
Fluorite	0	0	0	0	0	0		–	0
White_feldspar	0	0	0	0	0	–3		–	2
Graphite	0	0	1	0	0	0			2
Hematite	4	6	19	0	5	–19		–	32
Calcite	58	61	54	50	33	–59		–	34
Chlorite	58	67	58	38	20	–43		–	70
Chalcopyrite	0	0	0	0	0	0		–	0
Quartz	4	6	7	0	18	–29		–	13
Red_Feldspar	0	0	0	0	0	0		–	0
Muscovite	15	22	8	0	1			–	9
Unknown_mineral	0	0	0	0	0	0		–	0
Pyrite	0	0	4	0	0	0		–	0
Talc	0	0	0	0	0	0		–	0
Caolinite	0	0	0	0	0	0		–	0
Clay_minerals	19	22	22	13	2	–6		–	64
Laumontite	38	39	14	38	13	–39		–	15
Zeolite	0	0	0	0	0	0		–	0
Prehnite	0	0	0	0	1	–2		–	0
Iron Hydroxide	8	11	3	0	0	0		–	9
Asphalt	0	0	1	0	0	0		–	0
Adularia	4	0	6	13	14	–31		–	11
Gypsum	0	0	0	0	0	0		–	0
Oxidized_walls	35	33	13	38	58	–35		–	6
No_detactable_mineral	0	0	4	0	1	0		100	2

Table A3b-3. Mineral occurrences in fractures with extensive radar reflector relative to background, Site Investigation Oskarshamn (%).Non-weighted data.

Oskarshamn	All	Open and partly open		Seale		Sealed fracture networks		Crush	
	Reflector	Reflector	Background	Reflector	Background	Reflector	Background	Reflector	Background
Mineral	(n=51)	(n=28)	(n=4211)	(n=16)	(n=7759)	(n=2)	(n=258)	(n=5)	(n=48)
Barite	0.0	0.0	0.0	0.0	0.0	0	0.0	0	0.0
Biotite	0.0	0.0	0.0	0.0	0.1	0	0.0	0	0.0
Galena	0.0	0.0	0.1	0.0	0.0	0	0.0	0	0.0
Epidote	19.6	14.3	8.8	25.0	18.9	100	60.1	0	6.3
Fluorite	0.0	0.0	0.0	0.0	0.0	0	0.0	0	0.0
White_feldspar	7.8	0.0	0.2	25.0	4.0	0	1.2	0	0.0
Hematite	5.9	3.6	3.7	0.0	1.6	50	9.7	20	14.6
Calcite	68.6	75.0	80.4	56.3	53.0	50	80.6	80	81.3
Chlorite	70.6	78.6	78.3	43.8	32.4	100	75.6	100	95.8
Chalcopyrite	0.0	0.0	0.2	0.0	0.0	0	0.4	0	0.0
Quartz	3.9	3.6	3.1	6.3	10.8	0	11.6	0	0.0
Red_Feldspar	0.0	0.0	0.1	0.0	1.2	0	1.6	0	0.0
Muscovite	0.0	0.0	0.0	0.0	0.0	0	0.4	0	0.0
Unknown_mineral	0.0	0.0	0.6	0.0	0.0	0	0.0	0	6.3
Pyrite	5.9	10.7	15.2	0.0	1.2	0	1.6	0	10.4
Talc	0.0	0.0	2.0	0.0	0.1	0	0.4	0	8.3
Caolinite	0.0	0.0	0.1	0.0	0.0	0	0.0	0	0.0
Clay_minerals	21.6	25.0	26.7	0.0	0.8	0	6.6	80	72.9
Laumontite	0.0	0.0	0.1	0.0	0.1	0	0.4	0	0.0
Zeolite	0.0	0.0	0.8	0.0	0.0	0	0.0	0	6.3
Prehnite	7.8	3.6	1.0	18.8	6.9	0	21.7	0	0.0
Asphalt	0.0	0.0	0.0	0.0	0.0	0	0.0	0	0.0
Adularia	0.0	0.0	0.5	0.0	3.1	0	6.2	0	0.0
Gypsum	0.0	0.0	0.6	0.0	0.0	0	0.0	0	0.0
Oxidized_walls	11.8	3.6	9.2	31.3	39.5	0	22.5	0	0.0
No_detactable_miner	5.9	10.7	2.5	0.0	2.0	0	0.4	0	0.0
Saussuritized/Bleache	5.9	0.0	0.6	18.8	8.9	0	2.3	0	0.0

Table A3b-4. Fillings in fractures with extensive radar reflector relative to background, Äspö HRL (%). Non-weighted data.

Äspö HRL	Reflector, medium & high confidence	Reflector, high confidence	FPI, reflector	FPI, no reflector	Background
TOT	105	48	25	58	2403
Biotite	0	0	0	2	0
Epidote	17	23	44	47	14
Fluorite	0	0	0	0	0
White feldspar	0	0	0	0	0
Calcite	48	50	76	57	50
Chlorite	46	50	52	43	60
Quartz	12	8	16	10	4
Red feldspar	0	0	0	0	0
Pyrite	6	6	0	0	0
Sulphides	2	2	0	0	0
Clay minerals	0	0	4	7	3
Prehnite	0	0	0	0	0
Oxidized walls*	17	27	24	40	20
Grout*	5	4	32	14	2
Fine-grained granite*	2	2	0	0	1
Pegmatite*	11	8	4	9	3
Mylonite*	2	2	12	17	1

* Fracture fillings/alterations that are not minerals.

Table A3b-5. Fillings in fractures with GPR reflector relative to background, Äspö HRL (%). Non-weighted data.

Mineral	Reflector	Background
TOT no	22	228
Biotite	0.0	0.9
Epidote	36.4	18.0
Fluorite	0.0	0.4
Calcite	77.3	43.9
Chlorite	36.4	56.1
Quartz	4.5	3.5
Sulphides	0.0	0.4
Oxidized walls*	13.6	14.5
Grout*	18.2	3.1
Fine-grained granite*	4.5	0.9
Pegmatite*	4.5	2.2
Mylonite*	9.1	3.9

* Fracture fillings/alterations that are not minerals.

Alteration of fractures with oriented extensive radar reflector relative to background

Table A4-1. Alteration of fractures with extensive radar reflector relative to background, non-weighted data. Site Investigation Forsmark.

Fracture alteration	Open fracture, reflector	Open fracture, background	Partly open fracture, reflector	Partly open fracture, background	Sealed fracture, reflector	Sealed fracture, background
TOT no	38	12189	5	971	80	41732
Fresh*	16	23	60	65	99	93
Slightly altered*	82	71	40	34	1	7
Moderately altered*	3	5	0	1	0	0
> Moderately altered*	0	1	0	0	0	0
J_a MEDIAN	1	1.5				
J_a MAX	4	10				
J_a MIN	1	0.75				

* Expressed as percentage of all.

Table A4-2. Alteration of fractures with extensive radar reflector relative to background, non-weighted data. Site Investigation SFR.

Fracture alteration	Open fracture, reflector	Open fracture, background	Partly open fracture, reflector	Partly open fracture, background	Sealed fracture, reflector	Sealed fracture, background
TOT no	17	6282	1	627	8	11605
Fresh*	6	14	100	55	88	94
Slightly altered*	83	84	0	44	13	6
Moderately altered*	6	2	0	0	0	0
> Moderately altered*	0	0	0	0	0	0
J_a MEDIAN	2	1				
J_a MAX	3	14				
J_a MIN	0.75	0.75				

* Expressed as percentage.of all.

Table A4-3. Alteration of fractures with extensive borehole radar reflector relative to background, non-weighted data. Site Investigation Oskarshamn.

Fracture alteration	Open fracture, reflector	Open fracture, background	Partly open fracture, reflector	Partly open fracture, background	Sealed fracture, reflector	Sealed fracture, background
TOT no	28	4169	0	42	16	7759
Fresh*	18	13	–	52	25	25
Slightly altered*	82	86	–	48	75	75
Moderately altered*	0	0	–	0	0	0
> Moderately altered*	0	0	–	0	0	0
J_a MEDIAN	2	1.5				
J_a MAX	2	8				
J_a MIN	1	1				

* Expressed as percentage.of all.

Appendix 5

Roughness of fractures with oriented extensive radar reflector relative to background

Table A5-1. Roughness of fractures with extensive radar reflector relative to background, non-weighted data. Site Investigation Forsmark.

Site	TOT no	Roughness Planar*	Undulating*	Stepped*	Irregular*	Surface Rough*	Smooth*	Slickensided*
Forsmark, reflector	38	58	11	26	5	71	24	5
Forsmark, background	12 189	46	21	8	25	66	31	3

* Expressed as percentage of all.

Table A5-2. Roughness of fractures with extensive radar reflector relative to background, non-weighted data. Site Investigation SFR.

Site	TOT no	Roughness Planar*	Undulating*	Stepped*	Irregular*	Surface Rough*	Smooth*	Slickensided*
SFR, reflector SFR,	17	29	53	12	6	29	65	6
Background	6 282	33	41	5	20	52	44	2

* Expressed as percentage of all.

Table A5-3. Roughness of fractures with extensive radar reflector relative to background, non-weighted data. Site Investigation Oskarshamn.

Site	TOT no	Roughness Planar*	Undulating*	Stepped*	Irregular*	Surface Rough*	Smooth*	Slickensided*
Oskarshamn, reflector	28	46	54	0	0	79	21	0
Oskarshamn, Background	4 169	25	68	3	4	85	7	8

* Expressed as percentage of all.

Table A5-4. Roughness of fractures captured by borehole radar relative to background, with emphasis on FPI-fractures. Äspö HRL. Non-weighted data.

Fracture type	TOT	Roughness Planar*	Undulating*	Arched*	Stepped*	Surface Rough*	Smooth*	Slicken-sided*	Undefined*	Water*
Fracture with radar reflector, weighted	51	79	21	0	0	65	35	0	0	26
Fracture with radar reflector, non-weighted	104	80	19	1	0	54	46	0	0	30
FPI fracture with radar	25	64	36	0	0	80	20	0	0	52
FPI fracture, no radar	58	74	26	0	0	62	38	0	0	40
Fractures, background	2 403	83	14	3	0	44	56	0	0	9

* Expressed as percentage of all.

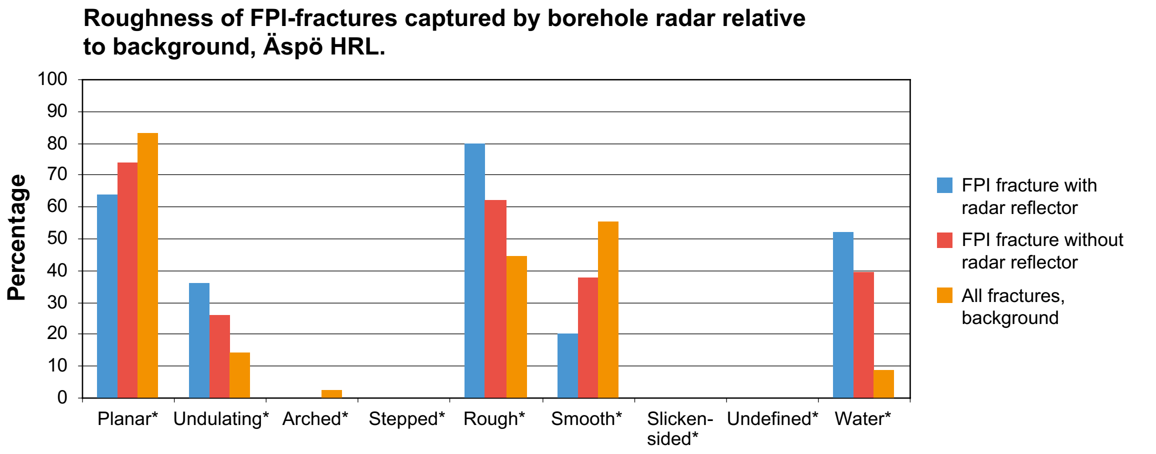

Figure A5-1. *Roughness of FPI-fractures captured by borehole radar relative to background, Äspö HRL (data taken from Table A5-4). Non-weighted data.*

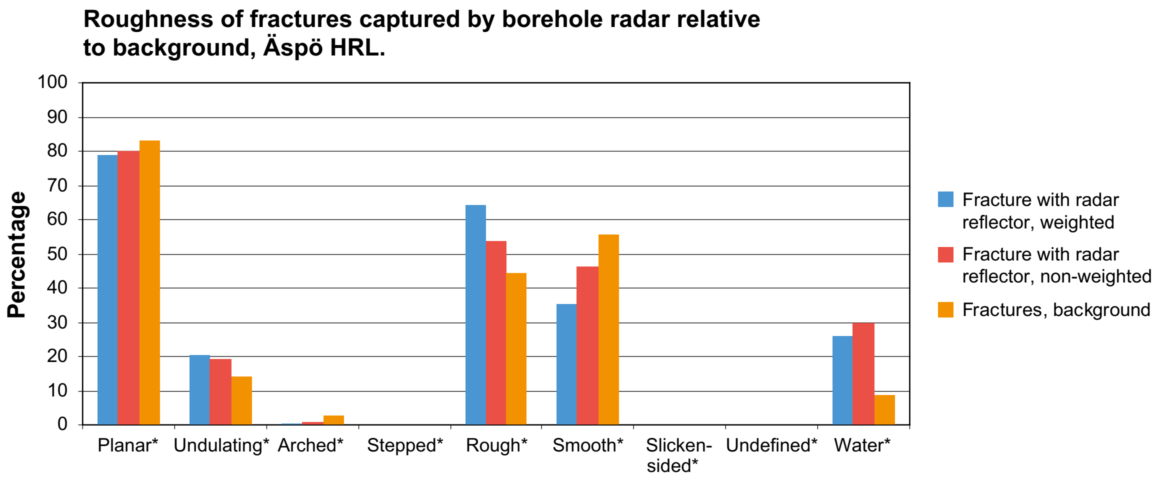

Figure A5-2. *Roughness of fractures captured by borehole radar relative to background, Äspö HRL (data taken from Table A5-4). Non-weighted data.*

Table A5-5. Roughness of fractures captured by GPR and FPI-fractures not captured by GPR relative to background. Values as percentages. Non-weighted data. Äspö HRL.

Fracture type	TOT	Roughness Planar	Undulating	Arched	Stepped	Surface Rough	Smooth	Slicken-sided	Undefined	Water
Fracture with GPR reflector	24	79	21	0	0	54	46	0	0	50
FPI without GPR reflector	3	100	0	0	0	33	67	0	0	0
Fractures, background	228	79	20	0	0	54	46	0	0	12

Background TASZ-data (Section ID 64–81 m) and TASA (Section ID 3 191–3 240 m), Mappings Part P and T only.

Table A5-6. Width and apertures of fractures correlated with extended borehole radar reflectors. Background values in parenthesis. Non-weighted data.

		Width Median	Max	Min	Aperture Median	Max	Min
Forsmark	Open	0.5 (0.5)	11 (20)	0.5 (0.5)	0.5 (0.5)	10 (13)	0.5 (0.5)
	Partly open	1 (0.5)	2 (80)	0.5 (0.5)	0.5 (0.5)	2 (11)	0.5 (0.5
	Sealed	0.5 (0.5)	8 (45)	0.5 (0)	0 (0)	0 (0)	0 (0)
SFR	Open	0.5 (0.5)	1.5 (40)	0.5 (0.5)	0.5 (0.5)	0.5 (17)	0.5 (0.5)
	Partly open	0.5 (0.5)	0.5 (4)	0.5 (0.5)	0.5 (0.5)	0.5 (2)	0.5 (0.5)
	Sealed	0.5 (0.5)	0.5 (54)	0.5 (0.5)	0 (0)	0 (0)	0 (0)
Oskarshamn	Open	1 (0.5)	10 (20)	0.5 (0.5)	0.5 (0.5)	10 (10)	0.5 (0.5)
	Partly open	– (0.5)	– (4)	– (0.5)	– (0.5)	– (2)	– (0.5)
	Sealed	0.5 (0.5)	4 (20)	0.5 (0)	0 (0)	0 (0)	0 (0)

Properties of crushes with no radar reflector

Mineralogy in crushes with no reflector relative to background Forsmark site investigation

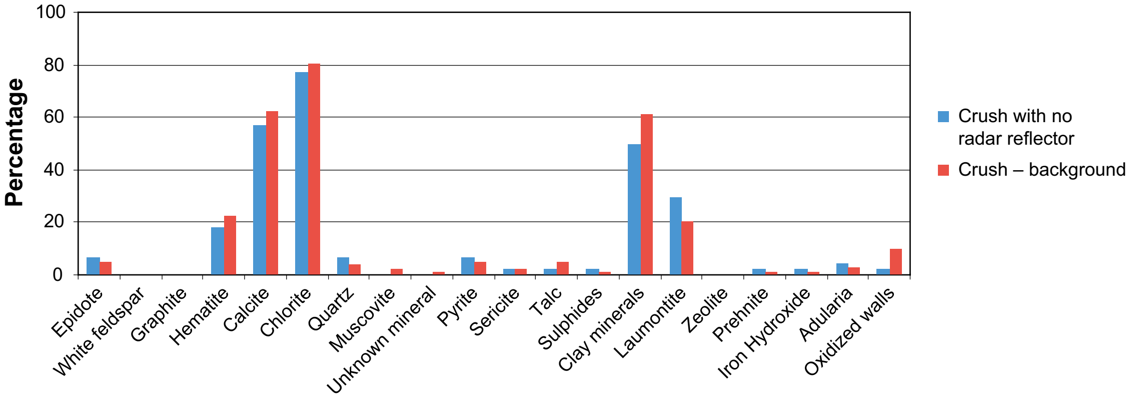

Figure A6-1. *Mineralogy of crushes with no reflector (n=44) relative to background (n=103), Forsmark site investigation.*

Mineralogy in crushes with no reflector relative to background SFR site investigation

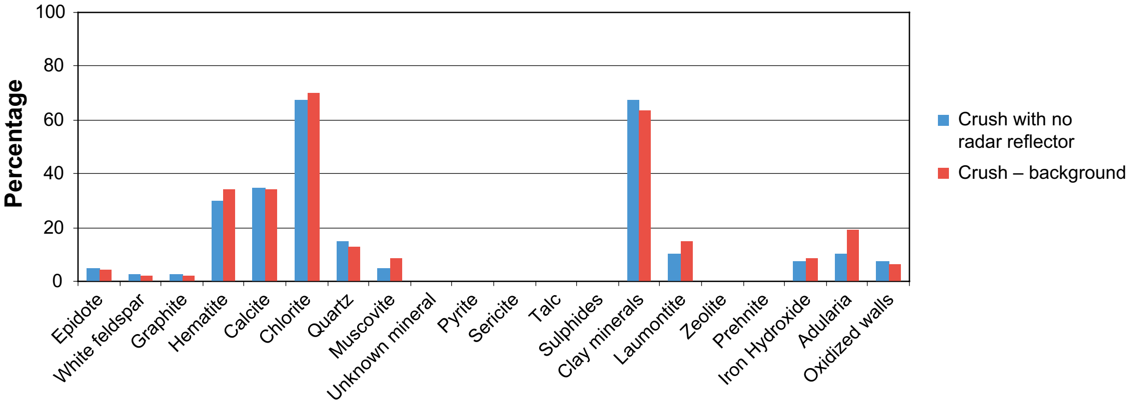

Figure A6-2. *Mineralogy of crushes with no reflector (n=40) relative to background (n=47), SFR site investigation.*

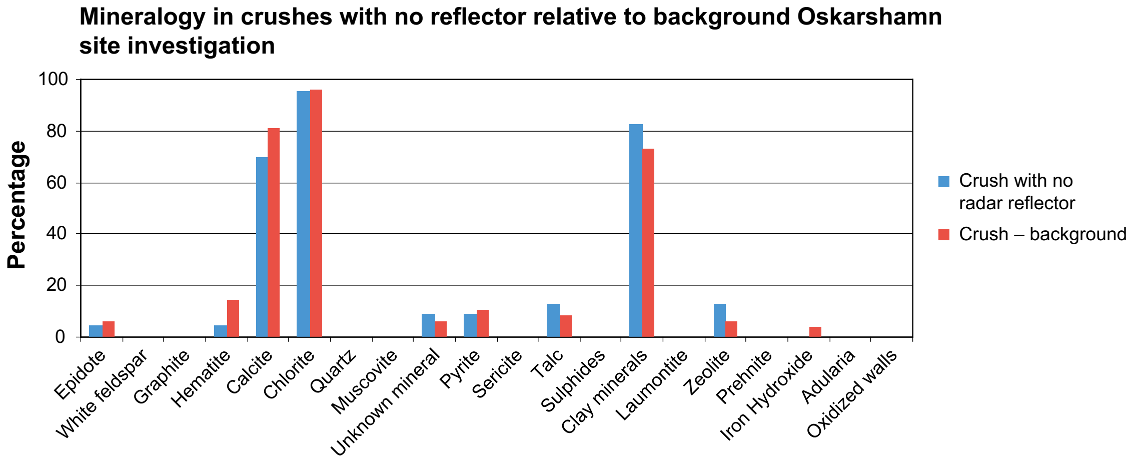

Figure A6-3. *Mineralogy of crushes with no reflector (n=23) relative to background (n=48), Oskarshamn site investigation.*

Table A6-1. Mineralogy of crushes with no reflector relative to background*.

Mineral	Forsmark No radar (n=44)	Forsmark Background (n=103)	SFR No radar (n=40)	SFR Background (n=47)	Oskarshamn No radar (n=23)	Oskarshamn Background (n=48)
Epidote	6.8	4.9	5.0	4.3	4.3	6.3
White feldspar	0.0	0.0	2.5	2.1	0.0	0.0
Graphite	0.0	0.0	2.5	2.0	0.0	0.0
Hematite	18.2	22.3	30.0	34.0	4.3	14.6
Calcite	56.8	62.1	35.0	34.0	69.6	81.3
Chlorite	77.3	80.6	67.5	70.2	95.7	95.8
Quartz	6.8	3.9	15.0	12.8	0.0	0.0
Muscovite	0.0	1.9	5.0	8.5	0.0	0.0
Unknown mineral	0.0	1.0	0.0	0.0	8.7	6.3
Pyrite	6.8	4.9	0.0	0.0	8.7	10.4
Sericite	2.3	1.9	0.0	0.0	0.0	0.0
Talc	2.3	4.9	0.0	0.0	13.0	8.3
Sulphides	2.3	1.0	0.0	0.0	0.0	0.0
Clay minerals	50.0	61.2	67.5	63.8	82.6	72.9
Laumontite	29.5	20.4	10.0	14.9	0.0	0.0
Zeolite	0.0	0.0	0.0	0.0	13.0	6.3
Prehnite	2.3	1.0	0.0	0.0	0.0	0.0
Iron Hydroxide	2.3	1.0	7.5	8.5	0.0	4.2
Adularia	4.5	2.9	10.0	19.1	0.0	0.0
Oxidized walls	2.3	9.7	7.5	6.4	0.0	0.0

* Numbers are percentages of crushes with the mineral in question.

Table A6-2 Alteration of crushes with extensive radar reflector relative to crushes with no reflector. Values are percentages and non-weighted. Note the very small amount of crushes with extensive radar reflectors.

Alteration	Forsmark Reflector	Forsmark No reflector	SFR Reflector	SFR No reflector	Oskarshamn Reflector	Oskarshamn No reflector
TOT no	6	44	1	40	6	23
Slightly altered	67	55	100	78	100	96
Moderately altered	33	18	–	13	–	4
Highly altered	–	2	–	3	–	–
Completely altered	–	–	–	3	–	–
Gouge	–	–	–	3	–	–
Fresh	–	25	–	3	–	–

Table A6-3. Width* of crushes with extensive radar reflector compared to crushes with no reflector. Non-weighted data.

Width	Forsmark Reflector	Forsmark No reflector	SFR Reflector	SFR No reflector	Oskarshamn Reflector	Oskarshamn No reflector
TOT no	6	44	1	40	6	23
MEDIAN	6	6	4	5	9	11
MAX	11	209	4	125	37	235
MIN	4	1	4	1	2	2

* Width is expressed as cm along borehole. NOTE! Not as true widths.

Table A6-4. Number of mapped crushes with no radar reflector divided into real crushes and fracture zones/single fractures.

Forsmark Crush	Forsmark Fractures mapped as crush*	SFR Crush	SFR Fractures mapped as crush*	Oskarshamn Crush	Oskarshamn Fractures mapped as crush*
8	37	21	19	9	14
TOT 45		**TOT 40**		**TOT 23**	

* A single thick fracture or a small fracture zone.

Table A6-5. Relation of upper and lower contact in crushes with extensive radar reflector relative to crushes with no radar reflector. Non-weighted data.

Crush with or without reflector	Forsmark Parallel or subparallel contacts	Forsmark Non-parallel contacts	SFR Parallel or subparallel contacts	SFR Non-parallel contacts	Oskarshamn Parallel or subparallel contacts	Oskarshamn Non-parallel contacts
No reflector, %	77	23	68	33	50	50
TOT no, no reflector	44		40		14	
Reflector	67	33	100	0	67	33
TOT no, reflector	6		1		6	

Appendix 7a

Possible deformation zones without extensive radar reflectors, Forsmark, SFR and Oskarshamn site investigations

ACTIVITY ID	SITE	ACTIVITY TYPE	PROJECT	IDCODE	FROM LENGTH	TO LENGTH	POSSIBLE DEFORMATION ZONE	CONFIDENCE	DESCRIPT_SHI_STAGE1
13019487	FORSMARK	GE300	PLU	KFM04A	169,00	176,00	DZ1	2	Slightly increased frequency of both sealed and open, steeply dipping fractures. Generally weak oxidation. Predominant fracture fillings are calcite, chlorite, hematite and prehnite. Clearly decreased electric resistivity and slightly decreased P-wave velocity. One oriented radar reflector occurs at 170.9 m with the orientation 326/32 and one non-oriented at 168.6 m with the angle 55 degrees to borehole axis. Confidence level = 2.
13019487	FORSMARK	GE300	PLU	KFM04A	202,00	213,00	DZ2	3	Marked increased frequency of flat lying, open fractures and steeply dipping, sealed fractures. Fracture apertures range up to 7 mm in width. Generally faint to weak oxidation. Predominant fracture minerals are calcite, hematite and chlorite. Also a few fractures with epidote and laumontite. Clearly decreased electric resistivity and slightly decreased P-wave velocity. Two radar reflectors occur at 205.9 m (128/73) and at 210.9 m (316/11) and one non-oriented radar reflector at 208.6 m with an intersection angle to the borehole of 48 degrees. Confidence level = 3.
13050560	FORSMARK	GE300	PLU	KFM05A	102,00	114,00	DZ1	3	Marked increase of flat-lying, open fractures, with apertures ranging up to more than 1 cm. Two crush zones. Mostly clay minerals, calcite and some fractures filled with fine-grained, clay-dominated material, inferred to be a clastic sedimentary rock. Faint oxidation throughout the interval. Low resistivity, which is apparent down to 125 m. No indication in the sonic and susceptibility data. One oriented radar reflector at 111.3 m with the orientation 192/53 or 100/20 and one non-oriented at 103.4 m with the angle 37 degrees to the borehole axis. Confidence level = 3.
13050560	FORSMARK	GE300	PLU	KFM05A	416,00	436,00	DZ2	3	Increased frequency of mostly sealed, steeply dipping fractures. Apertures generally less than 0.5 mm. Predominant fracture minerals are calcite, prehnite, chlorite, epidote and laumontite. Faint to medium oxidation. Low resistivity. No indication in the sonic and susceptibility data. Four oriented radar reflectors at 417.3 m (011/80), 424.2 m (151/88), 424.7 m (166/72 or 299/9) and at 427.6 m (092/24 or 200/65). Two non-oriented radar reflectors occur at 427.5 m and 431.1 m with the angle to borehole axis 35 and 53 degrees, respectively. Confidence level = 3.
13050560	FORSMARK	GE300	PLU	KFM05A	892,00	916,00	DZ4	2	Increased frequency of mostly sealed, steeply dipping fractures. Open fractures with apertures less than 1 mm and faint to weak oxidation are concentrated in the lower part of the interval. Predominant fracture minerals are laumontite, calcite and chlorite. Moderate resistivity anomalies. Susceptibility and sonic velocity seem to be unaffected. Two oriented radar reflectors at 903.2 m (086/48) and 909.3 m (041/26). Six non-oriented radar reflectors with angle in the interval 8-41 degrees to borehole axis. Confidence level = 2.
13050560	FORSMARK	GE300	PLU	KFM05A	936,00	950,00	DZ5	2	Increased frequency of both open and sealed, steeply dipping fractures. Part of the interval shows faint to weak oxidation. Predominant fracture minerals are laumontite, calcite and chlorite. Apertures less than 1 mm. Moderate resistivity anomalies. Susceptibility and sonic velocity seem to be unaffected. Two oriented radar reflectors at 932.9 m (001/33 or 005/75) and 946.1 m (258/65). Confidence level = 2.
13072271	FORSMARK	GE300	PLU	KFM06A	652,00	656,00	DZ6	2	Increased frequency of steeply dipping sealed fractures with chlorite and calcite as the main infilling minerals. Apertures up to 2 mm. In part faint to weak oxidation. One radar reflector with the orientation 047/88 (656.2 m). Low resistivity along the entire interval. No indications in the P-wave velocity or caliper data. Confidence level = 2.
13072271	FORSMARK	GE300	PLU	KFM06A	788,00	810,00	DZ8	3	Increased frequency of steeply dipping sealed and open fractures with chlorite and calcite as the main infilling minerals. Quartz and laumontite are subordinate minerals. Fractures with a NE strike dominate. Gently dipping fractures are also present. Apertures up to 1 mm. Four non-oriented radar reflectors with angle to borehole axis in the interval 44-72 degrees. Several low resistivity anomalies along the section. Only minor indications in the P-wave velocity and caliper data. Confidence level = 3.
13072271	FORSMARK	GE300	PLU	KFM06A	950,00	990,00	DZ11	3	Increased frequency of steeply dipping sealed fractures and in the upper half even gently dipping sealed fractures. The steeply dipping fractures strike NE. Chlorite, hematite, laumontite, calcite and quartz as the main infilling minerals. Locally faint oxidation. Six non-oriented and one oriented radar reflector occur. The orientation is 062/10 or 062/66 (962.5 m). Minor low resistivity anomalies occur along the entire interval. No indication in the P-wave velocity or caliper data. Confidence level = 3.
13094674	FORSMARK	GE300	PLU	KFM06C	502,00	555,00	DZ4	3	Incr. freq. of sealed fract., sealed fract. networks and, in the central part (534-540 m), open fract. and crush zones (3, 3, 5 and 40 cm wide). Fract. apertures are typically less than 1 mm, with some up to 3 mm. Most open/partly open fract. strike ESE and dip moderately to the SSW. However, fract. that strike NNE and are steeply dipping, that strike NW and dip steeply to the NE and that are gently dipping are also present. A similar pattern for the orientation of sealed fract. is apparent. However, the fract. within the diff. orientation sets are more evenly distr. The most freq. fract. filling minerals in the order of decr. abundance incl. calcite, chlorite, adularia and hematite. There is a large number of distinct low res. anomalies along the entire section. The interval c. 531-540 m is charact. by a major decr. in the bulk res., a large decr. in P-wave vel. and several dist. caliper anomalies. Five oriented radar refl. occur at 507.4 m (340/89 or 014/37), 509.8 m (150/56 or 085/29), 533.8 m (171/38 or 097/51), 537.3 m (223/88) and at 540.2 m (090/62). Sixteen non-oriented refl. are identified. One persistent non-oriented refl. inters. at 538 m, can be traced at least 40 m from the borehole. Decr. radar ampl. at the interval 530-540 m. Loc. faint to weak oxid. DZ4 consists of aplitic metagranite (10105
13074946	FORSMARK	GE300	PLU	KFM07A	196,00	205,00	DZ2	3	Increased frequency of open and sealed fractures. Gently dipping fractures dominate. Steeply dipping fractures that strike ENE are also present. Fracture apertures up to 2 mm and the predominant fracture filling minerals are chlorite and calcite. Faint to medium oxidation. One oriented radar reflector at 203.0 m (343/87) and one non-oriented at 198.2 m with the angle 39 degrees to borehole axis. General decrease in the resistivity and a minor decrease in the P-wave velocity. No caliper anomalies. Confidence level = 3.
13074946	FORSMARK	GE300	PLU	KFM07A	417,00	422,00	DZ3	3	Increased frequency of open and especially steeply dipping, sealed fractures. This zone occurs at the top of the borehole section in RU1 that was distinguished on the basis of a somewhat increased frequency of sealed fractures (418.84–506.68 m). The steeply dipping fractures strike NS. Gently dipping fractures are also present. Fracture apertures up to 2 mm and the predominant fracture filling minerals are chlorite and calcite. Faint to medium oxidation. One oriented radar reflector at 419.9 m (175/89) and one non-oriented at 418.7 m with the angle 48 degrees to borehole axis. Distinct low resistivity anomaly and low P-wave velocity. Minor indication in the caliper log. Confidence level = 3.
13074946	FORSMARK	GE300	PLU	KFM07A	803,00	999,22	DZ4	3	Increased frequency of steeply dipping open and especially sealed fractures, except in two shorter intervals at 843–857 m and 900–920 m. The steeply dipping sealed fractures show a variable strike between NNW and ENE. The steeply dipping open/partly open fractures strike predominantly NNW. Gently dipping fractures are also present. Fracture apertures are typically less than 1 mm, a few range up to 4 mm and one is over 10 mm. The most frequent fracture filling minerals in order of decreasing abundance include chlorite, calcite, laumontite, adularia and hematite. Also some minor intervals of adularia sealed breccia in the lower part of the zone. Two crush zones at 882.80–882.84 m and 989.51–989.55 m. Locally faint to medium oxidation. Thirty-nine radar reflectors of which one oriented at 827.1 m (208/85). Numerous low resistivity and caliper anomalies, as well as intervals with low P-wave velocity. The geophysical anomalies are mainly concentrated along the sections 873–900 m and 932–977 m. Confidence level = 3.

ACTIVITY ID	SITE	ACTIVITY TYPE	PROJECT	IDCODE	FROM LENGTH	TO LENGTH	POSSIBLE DEFORMATION ZONE	CONFIDENCE	DESCRIPT_SHI_STAGE1
13091306	FORSMARK	GE300	PLU	KFM08A	528,00	557,00	DZ3	2	Increased frequency of sealed fractures and sealed fracture networks. Fracture orientations are variable. A few low resistivity anomalies and one distinct low P-wave velocity anomaly at 557 m. 13 radar reflectors identified, three of them are oriented, 50/111 (530,2 m), 65/102 (535,1 m) and 42/098 (543,1 m). Locally faint to medium oxidation. The most frequent fracture filling minerals in the order of decreasing abundance include chlorite, calcite, hematite and quartz. Confidence level = 2.
13091306	FORSMARK	GE300	PLU	KFM08A	775,00	840,00	DZ5	2	Increased frequency of sealed fractures, sealed fracture networks and open fractures. Sealed fractures dominate. Three sets of steeply dipping fractures are present as well as one gently dipping set. The steeply dipping fractures strike NE, WNW and NNW. A minor group of fractures that strikes NW and dips steeply to the SW is also present. The section 775-805 m is characterised by a general decrease in the bulk resistivity and partly decreased magnetic susceptibility. 15 radar reflectors identified, three of them are oriented, 84/149 (807,3 m), 50/127 (810,4 m) and 29/059 (812,5 m). Locally faint to medium oxidation. The most frequent fracture filling minerals in the order of decreasing abundance include chlorite, calcite, hematite, adularia and laumontite. Confidence level = 2.
13091306	FORSMARK	GE300	PLU	KFM08A	915,00	946,00	DZ6	3	Increased frequency of sealed fractures, sealed fracture networks and open fractures, especially in the upper part (915-930 m). Sealed fractures dominate. Moderately to steeply dipping fractures that strike EW and dip to the S dominate. Steeply dipping fractures that strike WNW and dip to the NNE and strike NNE and dip WNW are also present. One 43 cm wide crush zone at 918.8-919.3 m. Distinct low resistivity, caliper and low P-wave velocity anomalies at 915-929 m. 8 non-oriented radar reflectors identified, intersection angle to borehole axis between 63 and 89 degrees. Locally faint oxidation. Fracture apertures are typically less than 1 mm, with one that is 2 mm at the base of the section. The most frequent fracture filling minerals in the order of decreasing abundance include chlorite, calcite, laumontite, adularia and clay minerals. Laumontite and clay minerals are more frequent in the upper part of the section. Confidence level = 3.
13091306	FORSMARK	GE300	PLU	KFM08A	967,00	976,00	DZ7	2	Increased frequency of open and especially sealed fractures. Two ductile shear zones occur in the section. A few individual low resistivity anomalies. 4 non-oriented radar reflectors identified, intersection angle to borehole axis between 55 and 90 degrees. One very clear reflector, identified in all three dipole antenna frequencies at a depth of 972 m. Fracture apertures are typically less than 1 mm, with one that is 2 mm. The most frequent fracture filling minerals include chlorite and clay minerals (probably illite). Confidence level = 2.
13121552	FORSMARK	GE300	PLU	KFM08C	946,00	949,00	DZ5	2	Increased frequency of sealed fractures predominantly as a sealed fracture network. Fractures are variable in orientation. Fractures that strike in the NW/SE quadrants with variable dip are prominent. Faint to weak oxidation throughout the interval. Low resistivity. Two radar reflectors intersecting the borehole axis with 28° and 29°. The most frequent fracture filling minerals in order of decreasing abundance include adularia, chlorite and calcite. Zone situated in medium-grained metagranite-granodiorite with subordinate occurrences of pegmatitic granite. Confidence level = 2.
13106409	FORSMARK	GE300	PLU	KFM09A	723,00	754,00	DZ4	3	Increased frequency of open fractures, sealed fractures and sealed fracture networks. No apertures in open fractures exceed 1 mm. Fractures show variable orientation. A conspicuous set strikes NW and dips steeply. Predominant fracture minerals are calcite, chlorite, laumontite, hematite, pyrite and clay minerals. Locally faint to medium oxidation. Geophysical anomaly with decreased resistivity (730-750 m) and caliper anomalies. Low magnetic susceptibility between 743-746 m. Five radar reflectors of which one is oriented at 730 m (360/07). The zone consists of medium-grained metagranite-granodiorite (101057), with subordinate pegmatitic granite (101061), amphibolite (102017), quartz- bearing metadiorite (101033), fine- to medium-grained metagranitoid (101051), metatonalite-granodiorite (101054) and felsic to intermediate metavolcanic rock (103076). Confidence level = 3
13106409	FORSMARK	GE300	PLU	KFM09A	770,00	790,00	DZ5	3	Increased frequency of sealed fractures and sealed fracture networks. No apertures in open fractures exceed 1 mm. Fractures show variable orientation. Conspicuous sets are gently dipping to subhorizontal and strike NW and are steeply dipping. Predominant fracture minerals are calcite, chlorite, quartz, laumontite, adularia and clay minerals. Locally faint to weak oxidation. Geophysical anomaly with decreased resistivity (778-788 m). Four radar reflectors of which one has an uncertain orientation at 784 m (313/84 or 044/14). Dominating rock type is felsic to intermediate metavolcanic rock (103076). Subordinate rock types are amphibolite (102017), metagranodiorite (101056) and fine- to medium-grained metagranitoid (101051). Confidence level = 3
13114934	FORSMARK	GE300	PLU	KFM09B	363,00	413,00	DZ3	3	Increased frequency of sealed and open fractures and sealed fracture networks. Steeply dipping fractures with NE strike as well as gently dipping fractures with variable strike dominate. Apertures are typically less than 1 mm, with a few ranging up to 5 mm. Locally faint to weak oxidation. Low resistivity and low P-wave velocity in the interval 379-411 m. Caliper anomaly at 390 m. 20 radar reflectors of which one is confidently oriented (154/65). Weak radar wave attenuation in the interval 380-390 m. The most frequent fracture filling minerals in the order of decreasing abundance include calcite, chlorite and laumontite. Zone situated in medium-grained metagranite-granodiorite with minor occurrences of pegmatitic granite and amphibolite. Confidence level = 3
13114934	FORSMARK	GE300	PLU	KFM09B	561,00	574,00	DZ5	3	Increased frequency of sealed and open fractures. Steeply dipping fractures dominate. One group strikes WSW and dips steeply northwards. A second group varies in strike from NNE to ENE. Fracture apertures are 1.5 mm or less. Faint to weak oxidation. Quartz dissolution occurs in the interval 569-573 m (see RU4b). Low resistivity, magnetic susceptibility and P-wave velocity in the whole zone. Two identified radar reflectors. Prominent radar wave attenuation in the interval (566-573 m). The most frequent fracture filling minerals in the order of decreasing abundance include chlorite, calcite and clay minerals. Zone situated in medium-grained metagranite-granodiorite with subordinate pegmatitic granite. Confidence level = 3
13165198	FORSMARK	GE300	PLU	KFM12A	125,00	158,00	DZ1	3	Increased frequency of sealed fractures, sealed fracture networks and, to some extent, open fractures. Fractures predominantly dip gently to the SE or steeply to the SW. One crush zone at 128.08-128.10 m. Apertures generally 1 mm or less, with a few ranging up to 7 mm. Locally faint to medium oxidation. Sixteen identified radar reflectors with intersection angles 22 to 83° to the borehole axis. Low resistivity, P-wave velocity and magnetic susceptibility. The possible zone is situated on both sides of the contact between porphyritic (RU1) and more equigranular (RU2) metagranodiorite. Subordinate fine- to medium-grained granite (111058), metagabbro/diorite (101033), amphibolite (102017), fine- to medium-grained metagranitoid (101051) and aplitic metagranite (101058). Confidence level = 3.
13165198	FORSMARK	GE300	PLU	KFM12A	513,00	523,00	DZ3	3	Increased frequency of sealed and open fractures. Open fractures show a concentration with moderate dip to the S. Sealed fractures show a highly variable orientation. One crush zone in the upper part at 514.35-514.38 m. Apertures 2 mm or less. Generally faint oxidation. Four identified radar reflectors with intersection angles 51 to 73° to the borehole axis. Low magnetic susceptibility, resistivity and P-wave velocity. The possible deformation zone is situated in fine- to medium-grained granite (111058) and metagranodiorite (101056). Confidence level = 3.

ACTIVITY ID	SITE	ACTIVITY TYPE	PROJECT	IDCODE	FROM LENGTH	TO LENGTH	POSSIBLE DEFORMATION ZONE	CONFIDENCE	DESCRIPT_SHI_STAGE1
13205154	FORSMARK -	GE300	SFR-utbyggnad	KFR101	13,72	88,00	DZ1	3	Increased frequency of open fractures, sealed fracture networks and especially sealed fractures. Occasional slickensides. Fractures aperture up to 1.5 mm. Locally faint to medium oxidation. Several minor intervals (< 1 dm) of breccias, cataclasites, mylonite and brittle-ductile shear zones. Predominant minerals in sealed fractures are calcite, laumontite, chlorite, quartz and epidote, and in open fractures are calcite, chlorite, clay minerals, laumontite and pyrite. Decreased resistivity in the section c. 30–50 m and one distinct caliper anomaly at c. 33 m. The magnetic susceptibility is increased along the entire interval defining the deformation zone. Moderately foliated metagranite-granodiorite (101057), amphibolite (102017), pegmatitic granite (101061) and felsic to intermediate metavolcanic rock (103076).
13205154	FORSMARK -	GE300	SFR-utbyggnad	KFR101	197,00	213,00	DZ4	2	Increased frequency of sealed fractures and sealed fracture networks. Occasional slickensides. Fractures aperture 0.5 mm or less. Locally weak to medium oxidation. Predominant minerals in sealed fractures are calcite, chlorite, adularia, laumontite and quartz. No significant anomalies in the geophysical logging data. Moderately foliated metagranite-granodiorite (101057), felsic to intermediate metavolcanic rock (103076), fine- to medium-grained granite (111058), amphibolite (102017) and pegmatitic granite (101061).
13217112	FORSMARK -	GE300	SFR-utbyggnad	KFR102A	302,00	325,00	DZ2	3	Increased frequency of open and sealed fractures. Fractures aperture generally less than 0.5mm. Locally faint to medium oxidation. Predominant minerals in open fractures are chlorite, calcite, hematite, clay minerals and laumontite and in sealed fractures calcite, laumontite, chlorite and adularia. The possible deformation zone core 308–310 m is characterized by two fractures with five mm aperture, three minor crushes, argillisation and clay minerals as predominant mineral in open fractures. Two radar reflectors without orientation at 302 and 311 m, and one oriented reflector at 325 m (033°/83° or 213°/32°). The magnetic susceptibility is decreased along the entire section. In the section 307–310 m the resistivity is significantly decreased and there is also a distinct caliper anomaly. There is another clear low resistivity anomaly in the interval 322–325 m. In the section 312–318 m there is a fluid temperature anomaly indicating the occurrence of a water bearing fracture. Metagranite-granodiorite (101057), fine- to medium-grained granite (111058) and pegmatitic granite (101061).
13217112	FORSMARK -	GE300	SFR-utbyggnad	KFR102A	422,00	503,00	DZ3	3	Increased frequency of open and sealed fractures in the intervals 422–444 and 461–503 m. Eight crushes with the most extensive at 434.65–435.90 m. Two slickensides. Fracture apertures generally up to 0.5 mm with a few ranging up to 2 mm and a local maximum up to 10 mm. Locally weak to strong oxidation, rarely argillisation, laumontitisation and carbonatitisation. Five interval with quarts dissolution at 440.39–440.91, 441.64–441.76, 448.85–458.65, 473.15–474.14 and 478.35–478.42 m. Ductile deformation recorded at 466.46–466.09 m (019°/81°) and brittle ductile deformation recorded at 488.86–489.10 m (320°/41°). Predominant minerals in open fractures are chlorite, calcite, hematite, clay minerals, in sealed fractures calcite, quarts, adularia and chlorite and in sealed fracture networks calcite, quartz, chlorite and clay minerals. The entire possible deformation zone is characterised by poor radar penetration. The entire interval 422–503 m is characterized by significantly decreased bulk resistivity, several distinct caliper anomalies and decreased magnetic susceptibility. The most prominent low resistivity anomalies occur in the intervals 434–443, 451–458 and 471–475 m. In the section 450–457 m the density is significantly decreased, c. 2,570 kg/m3. Starting at 427 m the fluid ten
13215254	FORSMARK -	GE300	SFR-utbyggnad	KFR104	30,00	45,50	DZ1	1	Increased frequency of sealed fracture networks. Faint oxidation in the lower half of the interval and quarts dissolution at 38.30–40.75 m where vugs are filled with calcite. Fracture apertures up to 1 mm with a single aperture at 3 mm. Predominant minerals in sealed fracture networks are chlorite, adularia and hematite. Low electric resistivity. Pegmatitic granite (101061) and metagranite-granodiorite (101057).
13215254	FORSMARK -	GE300	SFR-utbyggnad	KFR104	149,00	154,00	DZ2	3	Increased frequency of open and sealed fractures. Fractures aperture up to 1 mm. A few moderately altered open fractures. Minor intervals of brecciation at 150.96–151.38 and 153.64–153.80 m. Locally weak to moderate argillization. Predominant minerals in sealed fractures are calcite, chlorite and laumontite and in open fractures are chlorite, calcite and hematite. Low electric resistivity. One distinct radar reflector at the lower end of the interval oriented 105°/15°. Pegmatitic granite (101061), metagranite-granodiorite (101057) and amphibolite (102017).
13215254	FORSMARK -	GE300	SFR-utbyggnad	KFR104	396,00	405,00	DZ5	3	Increased frequency of open fractures. One minor cataclasite along the lower limit of the possible zone at 400.39–400.41 m. Fracture apertures up to 2 mm. Several moderately altered open fractures. Varying degrees of argillization and epidotization in the lower half of the interval. Predominant minerals in open fractures are clay minerals, chlorite and calcite. Low electric resistivity and one minor caliper anomaly. Pegmatitic granite (101061) and amphibolite (102017).
13215254	FORSMARK -	GE300	SFR-utbyggnad	KFR104	447,00	454,57	DZ6	3	Increased frequency of sealed fractures and sealed fracture network in the upper half of the interval. One brecciated interval at 452.97–453.05 m. Locally faint to strong oxidation and laumontization. No BIPS image of the interval. Predominant minerals in sealed fractures are laumontite, calcite and chlorite. Low electric resistivity and one major caliper anomaly. Fine to medium grained granite (111058), pegmatitic granite (101061) and metagranite-granodiorite (101057).
13215255	FORSMARK -	GE300	SFR-utbyggnad	KFR27	108,00	120,00	DZ1	1	Increased frequency of sealed fractures and sealed fracture networks. Locally weak to moderate oxidation. No core available. Moderate resistivity anomalies. One distinct radar reflector at approximately 118 m. Pegmatitic granite (101061), metagranite-granodiorite (101057) and felsic to intermediate metavolcanic rock (103076).
13215255	FORSMARK -	GE300	SFR-utbyggnad	KFR27	323,00	379,50	DZ2	3	Several shorter intervals with increased frequency of open and sealed fractures and a more extensive interval in the lower most part of the possible deformation zone. Thirteen crush sections throughout the interval and one minor breccia at 338.51–338.52 m. Fracture aperture up to 1mm. Locally faint to moderate oxidation and faint to weak argillization. Predominant minerals in open fractures are calcite, chlorite, clay minerals and hematite. Low electric resistivity especially in the lower part of the section. A minor deflection in the temperature gradient. Two radar reflectors (352°/01° or 332°/11° and 334°/65° or 154°/53°). Fine- to medium-grained granite (111058), metagranite-granodiorite (101057), pegmatitic granite (101061) and amphibolite (102017).
13215255	FORSMARK -	GE300	SFR-utbyggnad	KFR27	389,00	401,00	DZ3	2	Increased frequency of sealed and open fractures and sealed fracture networks. One crush at the interval 394.71–394.75 m. Fracture aperture up to 0.5 mm and one single aperture at 3 mm. Generally weak to moderate oxidation. Predominant minerals in open fractures are chlorite, laumontite and clay minerals, in sealed fractures calcite, laumontite and quartz and in the crushed interval chlorite and clay minerals. Moderate resistivity anomalies. Metagranite-granodiorite (101057), pegmatitic granite (101061) and amphibolite (102017).

ACTIVITY ID	SITE	ACTIVITY TYPE	PROJECT	IDCODE	FROM LENGTH	TO LENGTH	POSSIBLE DEFORMATION ZONE	CONFIDENCE	DESCRIPT_SHI_STAGE1
13215255	FORSMARK -	GE300	SFR-utbyggnad	KFR27	421,00	469,00	DZ4	3	The possible deformation zone can be divided in to three different characteristic intervals. The uppermost interval, extending down to c.442 m, is characterized by increased frequency of sealed and especially open fractures. Six crushed sections with a concentration between 431.4–433.5 m. Fracture aperture up to 3 mm Generally faint to moderate oxidation and faint to strong quarts dissolution. Predominant minerals in open fractures are hematite, calcite, clay minerals and adularia, in sealed fractures adularia, epidote, calcite and quartz and in crushed intervals clay minerals and adularia. Very low resistivity especially in the central part. Several calliper anomalies and a moderate deflection in the temperature gradient. The central sub interval extends from c. 442 m to c. 463 m, is characterized by strong brittle-ductile deformation and intense alteration that includes oxidation, quarts dissolution, argillization, chloritization and epidotization. Three crushes at 446.86–446.91, 448.12–448.14 and 458.30–458.33 m. Several moderately altered open fractures. Apertures ranging up to 2 mm. Predominant mineral in open fractures are clay minerals. The lower most interval, from c.463m, is characterized by increased frequency of sealed and open fractures. A few moderately to s
13150801	LAXEMAR	GE300	PLU	KLX14A	10,11	10,61	DZ1	3	Low-grade ductile shear zone associated with fine-grained diorite-gabbro (505102). Increased frequency of sealed fractures. Decreased magnetic susceptibility and resistivity (no sonic or caliper data available). Confidence level = 3.
13150801	LAXEMAR	GE300	PLU	KLX14A	42,07	43,35	DZ3	3	Brittle-ductile deformation zone characterized by increased frequency of open and sealed fractures and crush (0.3 m). Decreased magnetic susceptibility and resistivity, and slightly decreased P-wave velocity (no caliper data available). One non-oriented radar reflector occurs at 43.1 m with the angle 55° to borehole axis. The host rock is totally dominated by quartz monzodiorite (501036) with subordinate pegmatite (501061). Confidence level = 3.
13150801	LAXEMAR	GE300	PLU	KLX14A	74,67	125,35	DZ4	3	Inhomogeneous low-grade ductile shear zone overprinted by brittle deformation, characterized by locally increased frequency of open and sealed fractures, four minor core losses, eight crush zones, slickensides, marked increase in apertures, frequent breccias and mylonites. The zone covers the majority of RU2 and is associated with minor sections of dolerite. A c. 5 m wide mylonite occurs at the base of the zone. The upper part of the zone is faintly saussuritized. Throughout the zone there are narrow sections that exhibit weak to medium red staining and weak epidotization. The most intensely deformed sections (cores) are 74.67-82.20, 89.25-93.35, 102.95-119.50 and 125.05-125.35 m. There is a large decrease in resistivity, magnetic susceptibility and P-wave velocity along a major part of the section. There are also several distinct caliper anomalies. The most significant geophysical anomalies occur in the intervals c 74.7-82.2 m, 92.0-93.5 m, 105.0-107.0 m and 112.5-115.5 m. There is a major decrease in fluid water resistivity at c. 88 m. One oriented and ten non-oriented radar reflectors occur within DZ4. The oriented reflector occurs at 75.8 m with the orientation 144/87. The reflector is strong and can be observed to a distance of 12 m outside the borehole. The non-oriented reflector
13150801	LAXEMAR	GE300	PLU	KLX14A	138,10	138,90	DZ5	3	Brittle deformation zone characterized by increased frequency of sealed fractures and a moderate increase in open fractures, slickensides, weak red staining and epidotiztion. The section is characterized by decreased magnetic susceptibility, resistivity and P-wave velocity. The host rock is dominated by quartz monzodiorite with very sparse occurrence of fine-grained granite (511058). Confidence level = 3.
13150801	LAXEMAR	GE300	PLU	KLX14A	162,07	163,82	DZ6	3	Low-grade ductile shear zone associated with foliated fine-grained granite (511058). The section is characterized by decreased magnetic susceptibility and slightly decreased resistivity. Two non-oriented radar reflectors occur at 162.1 m and 164.9 m with the angle 30° and 36° to borehole axis, respectively. The reflectors are strong and constitute different parts of the same structure. They can be observed to a distance of 25 m outside the borehole. Low radar amplitude occurs in the interval 163-165 m, i.e. partly below DZ6. The host rock is dominated by quartz monzodiorite (501036). Confidence level = 3.
13167655	LAXEMAR	GE300	PLU	KLX15A	253,69	254,37	DZ3	3	Minor brittle-ductile shear zone characterized by slightly increased frequency of open and sealed fractures. Significantly decreased resistivity and magnetic susceptibility and partly decreased P-wave velocity. One oriented radar reflector occurs at 253.6 m with the orientation 339/38 or 250/59. The reflector is prominent and can be observed to a distance of 15 m outside the borehole. The host rock is dominated by quartz monzodiorite (501036). Subordinate rock type comprises fine-grained granite (511058). Confidence level = 3.
13167655	LAXEMAR	GE300	PLU	KLX15A	350,16	350,34	DZ6	3	Minor ductile shear zone in composite intrusion. One slickenside and faint saussuritization. There is a minor decrease in magnetic susceptibility and resistivity. The host rock is dominated by quartz monzodiorite (501036). Subordinate rock type comprises fine-grained diorite-gabbro (505102). Confidence level = 3.
13167655	LAXEMAR	GE300	PLU	KLX15A	362,75	362,95	DZ7	3	Minor deformation zone characterized by brecciation. Partly decreased magnetic susceptibility and resistivity. The host rock is dominated Ävrö granite (501044). Confidence level = 3.
13167655	LAXEMAR	GE300	PLU	KLX15A	377,84	386,00	DZ8	3	Inhomogeneous brittle-ductile shear zone. Increased frequency of sealed fractures, slight increase in open fractures, sealed network, cataclasites, breccias, weak to strong red staining and partly weak epidotization. Significant decrease in bulk resistivity and bulk magnetic susceptibility and a minor decrease in P-wave velocity. Three non-oriented radar reflectors occur at 379.5 m, 383.1 m and 385.9 m with the angle 36°, 10° and 34° to borehole axis, respectively. Low radar amplitude occurs in the section 376-383 m. The host rock is dominated by quartz monzodiorite (501036). Subordinate rock types comprise pegmatite (501061) and fine-grained granite. Confidence level = 3.
13167655	LAXEMAR	GE300	PLU	KLX15A	602,24	608,72	DZ11	3	Brittle deformation zone characterized by increased frequency of sealed fractures, weak to strong red staining, partly faint epidotization, one cataclasite (2 cm) and one breccia (20 cm). Significant decrease in resistivity and magnetic susceptibility and a minor decrease in P-wave velocity. Three non-oriented radar reflectors occur at 603.0 m, 604.8 m and 605.4 m with the angle 58°, 34° and 50° to borehole axis, respectively. Low radar amplitude occurs in the section 602-608 m. The host rock is dominated by quartz monzodiorite (501036). Subordinate rock types are granite (501058) and pegmatite (501061). Confidence level = 3.
13167655	LAXEMAR	GE300	PLU	KLX15A	658,91	659,80	DZ13	3	Brittle-ductile deformation zone. Faint red staining. There is a minor decrease in magnetic susceptibility and resistivity. One non-oriented radar reflector occurs at 658.9 m with the angle 38° to borehole axis. The host rock is dominated by Ävrö granite (501044) (501036). Subordinate rock types comprise quartz monzodiorite (501036) and very sparse occurrence of granite (501058). Confidence level = 3.
13167655	LAXEMAR	GE300	PLU	KLX15A	675,05	682,68	DZ14	3	Brittle deformation zone characterized by increased frequency of sealed fractures and sealed network. Three slickensides, faint to strong red staining and partly faint epidotization. Significantly decreased resistivity and magnetic susceptibility at the two section coordinates 675.5 m and 682.0 m. One strong radar reflector occurs at 681.2 m with the orientation 278/89 or 066/07. The reflector can be observed to a distance of 20 m outside the borehole. Low radar amplitude occurs in the section 680-683 m. The host rock is dominated by Ävrö granite (501044). Subordinate rock types comprise pegmatite (501061), fine-grained granite (511058) and quartz monzodiorite (501036). Confidence level = 3.
13167655	LAXEMAR	GE300	PLU	KLX15A	688,00	688,50	DZ15	3	Minor brittle-ductile shear zone. Moderate increase in sealed fractures. Significantly decreased magnetic susceptibility. The host rock is dominated by quartz monzodiorite (501036). Subordinate rock type comprises pegmatite (501061). Confidence level = 3.

ACTIVITY ID	SITE	ACTIVITY TYPE	PROJECT	IDCODE	FROM LENGTH	TO LENGTH	POSSIBLE DEFORMATION ZONE	CONFIDENCE	DESCRIPT_SHI_STAGE1
13167655	LAXEMAR	GE300	PLU	KLX15A	711,36	743,76	DZ16	3	Inhomogeneous deformation zone characterized by brittle and brittle-ductile deformation. Increased frequency of sealed fractures, sealed fracture network and slight increase in open fractures, eight slickensides, partly weak to medium red staining. The most intensely deformed sections (cores) are: 711.36-711.60 m, 714.08-714.23 m, 717.85-718.60 m, 731.68-732.55 m and 743.10-743.76 m. Significant decrease in magnetic susceptibility along the major part of the section. Decreased resistivity at the section coordinates 711.7 m, 714.2 m, 716.4 m, 718.5 m, 725.5-726.5 m, 732.0 m, 734.2 m and 738.0-747.0 m. There is also decreased P-wave velocity in the section 717.5-719.0 m. Four oriented and sixteen non-oriented radar reflectors occur within DZ16. The oriented reflectors occur at 718.1 m (256/65 or 333/31), at 714.9 m (248/76 or 358/34), at 737.8 m (247/62 or 337/40) and at 743.4 m (225/75). The non-oriented reflectors occur with angles between 3° and 63° to borehole axis. Low radar amplitude occurs in the section 711-719 m. The host rock is dominated by quartz monzodiorite (501036). Subordinate rock types comprise pegmatite (501061), granite (501058), fine-grained granite (511058) and fine-grained diorite-gabbro (505102). Confidence level = 3.
13167655	LAXEMAR	GE300	PLU	KLX15A	821,63	821,94	DZ18	3	Brittle-ductile shear zone. Increased frequency of sealed fractures and sealed network, and slight increase of open fractures and faint epidotization. Significantly decreased resistivity and magnetic susceptibility and partly decreased P-wave velocity. One non-oriented radar reflector occurs at 822.0 m with the angle 69° to borehole axis. The host rock is dominated by quartz monzodiorite (501036). Confidence level = 3.
13167655	LAXEMAR	GE300	PLU	KLX15A	917,75	918,46	DZ19	3	Ductile shear zone in composite intrusion. Increased frequency of sealed fractures and sealed fracture network and one slickenside. Significantly decreased resistivity and magnetic susceptibility and partly decreased P-wave velocity. One of the most prominent radar reflectors in the borehole (reflector 209) occurs at 921.5 m, which is immediately below DZ19. The orientation of the reflector is 088/68 or 077/29, and the reflector can be observed to a distance of 30 m outside the borehole. Parts of the reflector (reflector 209x at 915.6 m, reflector 209xx at 918.9 m and reflector 209xxx at 911.7 m) have been interpreted to intersect close to DZ19. Low radar amplitude occurs in the section 915-920 m, which is partly above and partly below the deformation zone. The host rock is dominated by quartz monzodiorite (501036). Subordinate rock type comprises fine-grained diorite-gabbro (505102). Confidence level = 3.
13167655	LAXEMAR	GE300	PLU	KLX15A	978,43	1000,43	DZ20	3	Inhomogeneous deformation zone characterized by brittle and brittle-ductile deformation. Increased frequency of sealed fractures and sealed fracture network and slight increase in open fractures, faint to strong red staining and partly faint to weak saussuritization, one core loss and ten slickensides. The most intensely deformed sections (cores) are: 994.71-997.50 m (brittle-ductile deformation) and 997.50-1000.43 m (brittle deformation; some fractures subparallel to core). No geophysical data. The geophysical logging was interrupted at c 978 m. Two non-orinted radar reflectors occur at 980.4 m and 987.5 m, both with the angle 52° to borehole axis. The host rock is dominated by quartz monzodiorite (501036). Subordinate rock types comprise pegmatite (501061) and fine-grained granite (511058). Confidence level = 3.
13131040	LAXEMAR	GE300	PLU	KLX20A	261,00	265,90	DZ2	3	Inhomogeneous ductile deformation zone. Faint to weak red staining, silicification, saussuritization and epidotization. Crush zone (7 cm). High frequency of sealed fractures. Moderate frequency of open fractures. Decreased magnetic susceptibility and partly decreased resistivity. Three non-oriented radar reflectors occur at 262.0 m, 262.7 m and 264.3 m with the angle 63°, 21° and 32° to borehole axis, respectively. One oriented reflector occurs at 265.8 m with the orientation 053/87 or 271/48. The host rock is dominated by quartz monzodiorite (501036). Confidence level = 3.
13131040	LAXEMAR	GE300	PLU	KLX20A	410,10	416,40	DZ4	2	Inhomogeneous brittle deformation zone. Breccia (8 mm). Faint to medium red staining, epidotization and saussuritization. High frequency of sealed fractures. Slickenside is observed. Decreased bulk resistivity and magnetic susceptibility, and partly decreased P-wave velocity. One non-oriented radar reflector occurs at 410.5 m with the angle 50° to borehole axis. The host rock is dominated by quartz monzodiorite (501036). Confidence level = 2.
13181338	LAXEMAR	GE300	PLU	KLX27A	105,90	109,80	DZ1	3	Minor brittle deformation zone in composite intrusion with increased frequency of sealed fractures, sealed network, breccia, faint to weak red staining, one slickenside, one crush and faint saussuritization. The resistivity and magnetic susceptibility are significantly decreased, whereas the P-wave velocity is partly decreased. The host rock is dominated by fine-grained diorite-gabbro (505102) and fine-grained granite (511058) in the upper part.
13181338	LAXEMAR	GE300	PLU	KLX27A	167,90	176,45	DZ2	3	Brittle deformation zone characterized by increased frequency of sealed fractures, sealed network, slight increase in open fractures, cataclasites, thin brittle-ductile shear zones, sparse brecciation, partly weak to strong red staining, sparse weak to strong epidotization and one slickenside. The magnetic susceptibility is significantly decreased; the resistivity and P-wave velocity only show minor anomalies. The host rock is dominated by quartz monzodiorite (501036) and fine-grained granite (511058) in the lower part.
13181338	LAXEMAR	GE300	PLU	KLX27A	208,50	255,00	DZ3	3	Brittle deformation zone characterized by increased frequency of sealed and, partly, also open fractures, sealed network, six crush zones, cataclasites, gouge, core loss, weak to medium red staining and two slickensides. Brittle-ductile and ductile shear zones, overprinted by the brittle deformation, also occur. The most intensely deformed sections (cores) are 221.20-221.50 m, 225.17-229.90 m and 241.40-242.50 m. There are major anomalies in all geophysical logs. The most significant geophysical anomalies occur in the sections c. 225-230 m and 240-245 m. The host rock is dominated by quartz monzodiorite (501036). Subordinate rock types comprise fine-grained diorite-gabbro (505102), fine-grained granite (511058) and very sparse occurrence of granite (501058).
13181338	LAXEMAR	GE300	PLU	KLX27A	337,45	339,30	DZ4	3	Minor brittle deformation zone characterized by increased frequency of sealed and open fractures, sealed network, breccia and slickenside. The resistivity and magnetic susceptibility are significantly decreased, and there is also a distinct caliper anomaly. The P-wave velocity is partly decreased. The host rock is dominated by fine-grained diorite-gabbro (505102). Subordinate rock type comprises quartz monzodiorite (501036).
13181338	LAXEMAR	GE300	PLU	KLX27A	343,65	345,05	DZ5	3	Minor brittle deformation zone characterized by increased frequency of sealed and open fractures, faint and strong red staining. Slickenside, breccia and a thin brittle-ductile shear zone occur also. The resistivity and magnetic susceptibility are significantly decreased. The P-wave velocity is partly decreased. The host rock is totally dominated by quartz monzodiorite (501036).
13181338	LAXEMAR	GE300	PLU	KLX27A	595,01	596,54	DZ8	3	Minor ductile shear zone in composite intrusion which is dominated by fine-grained diorite-gabbro (505102). Overprinting sealed fractures and sealed network. The magnetic susceptibility is significantly decreased, but there are only minor anomalies in the other geophysical logs.
13181338	LAXEMAR	GE300	PLU	KLX27A	643,91	644,80	DZ9	3	Minor brittle deformation zone characterized by sealed fractures, sealed network and a slight increase in open fractures, strong red staining and thin brittle-ductile shear zones. The resistivity, magnetic susceptibility and P-wave are significantly decreased. The host rock is dominated by quartz monzodiorite (501036) and fine-grained granite (511058).

Appendix 7b

Possible deformation zones with no radar reflector, Forsmark, SFR and Oskarshamn site investigations

ACTIVITY ID	SITE	ACTIVITY TYPE	PROJECT	IDCODE	START DATE	FROM LENGTH	TO LENGTH	POSSIBLE DEFORMATION ZONE	CONFIDENCE	DESCRIPTION SHI STAGE1	DESCRIPT_SHI_HYDROGEO
13205154	FORSMARK - SFR	GE300	SFR-utbyggnad	KFR101	2008-10-07 09:00:00	13,72	88,00	DZ1	3	Increased frequency of open fractures, sealed fracture networks and especially sealed fractures. Occasional slickensides. Fractures aperture up to 1.5 mm. Locally faint to medium oxidation. Several minor intervals (< 1 dm) of breccias, cataclasites, mylonite and brittle-ductile shear zones. Predominant minerals in sealed fractures are calcite, laumontite, chlorite, quartz and epidote, and in open fractures are calcite, chlorite, clay minerals, laumontite and pyrite. Decreased resistivity in the section c. 30–50 m and one distinct caliper anomaly at c. 33 m. The magnetic susceptibility is increased along the entire interval defining the deformation zone. Moderately foliated metagranite-granodiorite (101057), amphibolite (102017), pegmatitic granite (101061) and felsic to intermediate metavolcanic rock (103076).	Increased frequency of flow anomalies in the section 14–65 m but no flow anomalies below 65 m. The total transmissivity of the interval is quite high (about 5E–6 m^2/s if the dominating flow at the lower edge of the casing is removed). The caliper anomaly at c. 33 m corresponds to a single high-transmissive flow anomaly.
13205154	FORSMARK - SFR	GE300	SFR-utbyggnad	KFR101	2008-10-07 09:00:00	197,00	213,00	DZ4	2	Increased frequency of sealed fractures and sealed fracture networks. Occasional slickensides. Fractures aperture 0.5 mm or less. Locally weak to medium oxidation. Predominant minerals in sealed fractures are calcite, chlorite, adularia, laumontite and quartz. No significant anomalies in the geophysical logging data. Moderately foliated metagranite-granodiorite (101057), felsic to intermediate metavolcanic rock (103076), fine- to medium-grained granite (111058), amphibolite (102017) and pegmatitic granite (101061).	No flow anomalies and transmissivity below the measurement limit in this interval.
13217112	FORSMARK - SFR	GE300	SFR-utbyggnad	KFR102A	2009-06-03 09:00:00	422,00	503,00	DZ3	3	Increased frequency of open and sealed fractures in the intervals 422–444 and 461–503 m. Eight crushes with the most extensive at 434.65–435.90 m. Two slickensides. Fracture apertures generally up to 0.5 mm with a few ranging up to 2 mm and a local maximum up to 10 mm. Locally weak to strong oxidation, rarely argillisation, laumontitisation and carbonatitisation. Five interval with quarts dissolution at 440.39–440.91, 441.64–441.76, 448.85–458.65, 473.15–474.14 and 478.35–478.42 m. Ductile deformation recorded at 466.46–466.09 m (019°/81°) and brittle ductile deformation recorded at 488.86–489.10 m (320°/41°). Predominant minerals in open fractures are chlorite, calcite, hematite, clay minerals, in sealed fractures calcite, quarts, adularia and chlorite and in sealed fracture networks calcite, quartz, chlorite and clay minerals. The entire possible deformation zone is characterised by poor radar penetration. The entire interval 422–503 m is characterized by significantly decreased bulk resistivity, several distinct caliper anomalies and decreased magnetic susceptibility. The most prominent low resistivity anomalies occur in the intervals 434	No flow anomalies above 427 m. Increased frequency of flow anomalies in the interval 427–458 m. No flow anomalies below 458 apart from one single flow anomaly at 474 m. The total transmissivity of the section is 2E–6 m^2/s, where the transmissivity is dominated by one single flow anomaly at 427 m (T = 1E–6 m^2/s) and a number of flow anomalies at the section 435–441 m (T = 8E–7 m^2/s). The character of the inflow indicates porous rock at 451–458 m.
13215254	FORSMARK - SFR	GE300	SFR-utbyggnad	KFR104	2009-02-24 09:00:00	30,00	45,50	DZ1	1	Increased frequency of sealed fracture networks. Faint oxidation in the lower half of the interval and quarts dissolution at 38.30–40.75 m where vugs are filled with calcite. Fracture apertures up to 1 mm with a single aperture at 3 mm. Predominant minerals in sealed fracture networks are chlorite, adularia and hematite. Low electric resistivity. Pegmatitic granite (101061) and metagranite-granodiorite (101057).	Rather high, but not anomalous, transmissivity of the interval (2E–7 m^2/s).
13215254	FORSMARK - SFR	GE300	SFR-utbyggnad	KFR104	2009-02-24 09:00:00	396,00	405,00	DZ5	3	Increased frequency of open fractures. One minor cataclasite along the lower limit of the possible zone at 400.39–400.41 m. Fracture apertures up to 2 mm. Several moderately altered open fractures. Varying degrees of argillization and epidotization in the lower half of the interval. Predominant minerals in open fractures are clay minerals, chlorite and calcite. Low electric resistivity and one minor caliper anomaly. Pegmatitic granite (101061) and amphibolite (102017).	One single flow anomaly (T = 1E–8 m^2/s) at 405 m. This is the only flow anomaly in the borehole below 350 m.
13215254	FORSMARK - SFR	GE300	SFR-utbyggnad	KFR104	2009-02-24 09:00:00	447,00	454,57	DZ6	3	Increased frequency of sealed fractures and sealed fracture network in the upper half of the interval. One brecciated interval at 452.97–453.05 m. Locally faint to strong oxidation and laumontization. No BIPS image of the interval. Predominant minerals in sealed fractures are laumontite, calcite and chlorite. Low electric resistivity and one major caliper anomaly. Fine to medium grained granite (111058), pegmatitic granite (101061) and metagranite-granodiorite (101057).	No hydraulic data from this interval.

ACTIVITY ID	SITE	ACTIVITY TYPE	PROJECT	IDCODE	START DATE	FROM LENGTH	TO LENGTH	POSSIBLE DEFORMATION ZONE	CONFIDENCE	DESCRIPTION SHI STAGE1	DESCRIPT_SHI_HYDROGEO
13215255	FORSMARK - SFR	GE300	SFR-utbyggnad	KFR27	2009-02-24 09:00:00	389,00	401,00	DZ3	2	Increased frequency of sealed and open fractures and sealed fracture networks. One crush at the interval 394.71–394.75 m. Fracture aperture up to 0.5 mm and one single aperture at 3 mm. Generally weak to moderate oxidation. Predominant minerals in open fractures are chlorite, laumontite and clay minerals, in sealed fractures calcite, laumontite and quartz and in the crushed interval chlorite and clay minerals. Moderate resistivity anomalies. Metagranite-granodiorite (101057), pegmatitic granite (101061) and amphibolite (102017).	One single low-transmissive (T = 1E–9 m^2/s) flow anomaly at 392.1 m.
13215255	FORSMARK - SFR	GE300	SFR-utbyggnad	KFR27	2009-02-24 09:00:00	421,00	469,00	DZ4	3	The possible deformation zone can be divided in to three different characteristic intervals. The uppermost interval, extending down to c.442 m, is characterized by increased frequency of sealed and especially open fractures. Six crushed sections with a concentration between 431.4–433.5 m. Fracture aperture up to 3 mm Generally faint to moderate oxidation and faint to strong quarts dissolution. Predominant minerals in open fractures are hematite, calcite, clay minerals and adularia, in sealed fractures adularia, epidote, calcite and quartz and in crushed intervals clay minerals and adularia. Very low resistivity especially in the central part. Several calliper anomalies and a moderate deflection in the temperature gradient. The central sub interval extends from c. 442 m to c. 463 m, is characterized by strong brittle-ductile deformation and intense alteration that includes oxidation, quarts dissolution, argillization, chloritization and epidotization. Three crushes at 446.86–446.91, 448.12–448.14 and 458.30–458.33 m. Several moderately altered open fractures. Apertures ranging up to 2 mm. Predominant mineral in open fractures are clay minerals. The lower most interval, from c.463m,	A cluster of flow anomalies at 410–436 m. The transmissivity is concentrated to the section 423–429 m. No flow anomaly below 436 m. The total transmissivity of the interval is 4E–6 m^2/s.
13150801	LAXEMAR	GE300	PLU	KLX14A	2006-12-18 09:30:00	10,11	10,61	DZ1	3	Low-grade ductile shear zone associated with fine-grained diorite-gabbro (505102). Increased frequency of sealed fractures. Decreased magnetic susceptibility and resistivity (no sonic or caliper data available). Confidence level = 3.	
13150801	LAXEMAR	GE300	PLU	KLX14A	2006-12-18 09:30:00	138,10	138,90	DZ5	3	Brittle deformation zone characterized by increased frequency of sealed fractures and a moderate increase in open fractures, slickensides, weak red staining and epidotiztion. The section is characterized by decreased magnetic susceptibility, resistivity and P-wave velocity. The host rock is dominated by quartz monzodiorite with very sparse occurrence of fine-grained granite (511058). Confidence level = 3.	

Appendix 8

Properties of fractures correlated with radar reflectors (TMS data)

Table A8-1. Properties of fractures correlated with oriented borehole radar reflectors. Äspö HRL. Non-weighted data.

	Confidence 2+3 No	Confidence 2+3 %	Confidence 3 No	Confidence 3 %
Fractures correlated with borehole radar	105		48	
One fracture	97	92	43	90
Two fractures	3	3	1	2
Three fractures	4	4	3	6
Four fractures	1	1	1	2
Quartz	13	12	4	8
Calcite	50	48	24	50
Chlorite	48	46	24	50
Epidote	18	17	11	23
Pyrite	6	6	3	6
Sulphides	2	2	1	2
Oxidized walls	18	17	13	27
Mylonite	2	2	1	2
Pegmatitet	12	11	4	8
Aplite	2	2	1	2
Grout	5	5	2	4
Unknown (HB)	2	2	1	2
Planar fractures	84	80	41	85
Undulating fractures	20	19	7	15
Arched fractures	1	1	0	0
Stepped fractures	0	0	0	0
Rough fracture surface	57	54	27	56
Smoth fracture surface	48	46	21	44
Slickensided fracture surface	0	0	0	0
Undefined fracture surface	0	0	0	0
Open fractures	0	0	0	0
Tight/reopened fractures	96	91	47	98
Observed displacement	0	0	0	0
Waterbearing fractures	31	30	18	38
Length, median (m)	4.8	N/A	4.7	N/A
Length, max (m)	11	N/A	10	N/A
Length, min (m)	0.9	N/A	0.9	N/A
Fracture end1 – outside cell	42	40	14	29
Fracture end1 – free	48	46	25	52
Fracture end1 – against structure	15	14	9	19
Fracture end1 – divided	0	0	0	0
Fracture end2 – outside cell	36	34	17	35
Fracture end1 – free	46	44	20	42
Fracture end1 – against structure	23	22	11	23
Fracture end1 – divided	0	0	0	0

Table A8-2. Properties of fractures correlated with GPR reflector. Äspö HRL. Non-weighted data.

	Investigated tunnel sections	TASA From 3174.3 No	 To 3245 %	TASZ From 25.2 No	 To 76.2 %	SUM No	 %
	Fractures coupled with GPR reflector	17	47	5	33	22	43
	Host rock Äspö diorite	17	100	5	100	22	100
	One fracture	14	82	2	40	16	73
	Two fractures	1	6	0	0	1	5
	Three fractures	2	12	3	60	5	23
Fracture filling	Quartz	1	6	0	0	1	5
	Calcite	12	71	5	100	17	77
	Chlorite	6	35	2	40	8	36
	Epidote	6	35	2	40	8	36
	Ox idized walls	1	6	2	40	3	14
	Mylonite	1	6	1	20	2	9
	Pegmatite	1	6	0	0	1	5
	Aplite	1	6	0	0	1	5
	Grout	2	12	2	40	4	18
Fracture roughness	Planar fractures	13	76	4	80	17	77
	Undulating fractures	4	24	1	20	5	23
	Arched fractures	0	0	0	0	0	0
	Stepped fractures	0	0	0	0	0	0
	Rough fracture surface	9	53	3	60	12	55
	Smooth fracture surface	8	47	2	40	10	45
	Slickensided fracture surface	0	0	0	0	0	0
	Undefined fracture surface	0	0	0	0	0	0
Tightness and wear	Open fractures	0	0	0	0	0	0
	Tight/reopened fractures	17	100	5	100	22	100
	Observed displacement	0	0	0	0	0	0
	Waterbearing fractures	8	47	4	80	12	55
Fracture length	Length, median (m)	5.0		5.4		5.2	
	Length, max (m)	11.5		5.9		11.5	
	Length, min (m)	3.2		5.1		3.2	
	Fracture end1 – outside cell	4	24	4	80	8	36
	Fracture end1 – free	10	59	1	20	11	50
	Fracture end1 – against structure	3	18	0	0	3	14
	Fracture end1 – divided	0	0	0	0	0	0
	Fracture end2 – outside cell	6	35	4	80	10	45
	Fracture end2 – free	6	35	1	20	7	32
	Fracture end2 – against structure	5	29	0	0	5	23

Grey marked columns are percentages of all reflectors.